

Go to: [General](#) [Description](#) [References](#) [Additional](#) [Cross-references](#) [Sequence](#)

General Information

Primary Accession # U02310
 Accession # U02310
 Entry Name EMBL:HS02310
 Molecule Type mRNA
 Sequence Length 3421
 Entry Division HUM
 Sequence Version U02310.1
 Creation Date 28-DEC-1993
 Modification Date 04-MAR-2000

Description

Description Human fork head domain protein (FKHR) mRNA, complete cds.

Keywords .

Organism Homo sapiens (human)

Organism Classification Eukaryota; Metazoa; Chordata; Craniata; Vertebrata; Euteleostomi; Mammalia; Eutheria; Primates; Catarrhini; Hominidae; Homo. ;

References

1. Galili,N. ;
Fusion of a fork head domain to PAX-3 in the solid tumor alveolar rhabdomyosarcoma
 Nat. Genet. 5(3):230-235 (1993)
 Medline 94100975
 Pubmed 8275086
 Position 1-3421
2. Galili,N. ; Davis,R.J. ; Fredericks,W.J. ; Mukhopadhyay,S. ; Rauscher,F.J. III ; Emanuel,B.S. ; Rovera,G. ; Barr,F.G. ;
 Submitted (01-OCT-1993) to the EMBL/GenBank/DBJ databases. Naomi Galili, Wistar Institute, 3606 Spruce Street, Philadelphia, PA 19104 USA
 Position 1-3421

Database Cross-references

BEST AVAILABLE COPY

Exhibit 1

GDB [GDB:266367](#).
[GDB:266368](#).
[GDB:266370](#).
[GDB:277137](#).
[GDB:588453](#).

Additional Information

Features

Key	Location	Qualifier	Value
<u>source</u>	1..3421	<u>db_xref</u>	<u>taxon:9606</u>
		<u>mol_type</u>	mRNA
		<u>organism</u>	Homo sapiens
		<u>codon_start</u>	1
<u>cds</u>	7..1974	<u>db_xref</u>	<u>GOA:Q12778</u>
		<u>db_xref</u>	<u>Genew:3819</u>
		<u>db_xref</u>	<u>HSSP:P98177</u>
		<u>db_xref</u>	<u>UniProt/Swiss-Prot:Q12778</u>
		<u>gene</u>	FKHR
		<u>product</u>	fork head domain protein
		<u>protein_id</u>	<u>AAA03629.1</u>
		<u>translation</u>	>AAA03629 MAEAPQVVEIDPDFEPLPRPRCTWPLPRPEFSQNSATS ASAAVSADEMSNLSLLESEDFQAPGSVAAAVAAAAA APPQPPPGPVSQHPVPVPAAGPLAQPRKSSSSRRNAW LTLSQIYEWVKSVPYFKDKGDSNSSAGWKNSIRHNLSLH

Sequence

Characteristics **Length:** 3421 BP, **A Count:**852, **C Count:**859, **G Count:**805, **T Count:**905, **Others Count:**0

Sequence

```

>embl|U02310|HS02310 Human fork head domain protein (FKHR) mRNA, complete
gtcaccatggccgagcgccctcaggtggtagagatcgaccc ggacttcgagcgcgtgccc
cgccgcgctcgtcacctggcgcgtgccagggcggagtt tagccagtcacaactcgccc
acctccagcccgccgctcgggcagcggcgtgccaaacc cgacgcgcggcgggcctg
ccctcgccctcgctgccgctgtcagcgcgacttcattgag caacctgagcttgctggag
gagagcaggacttccgcagcgcccgcccgctccgtggcggc ggcggtggcgggcgggcc
gccgcccgcacccgggggctgtgcggggacttccaaggg cccggaggcgggctgcctg
caccagcgccacgcagccccgcgcgcgcggcccgctgtc gcagcaccgcgcggtgccc
ccgcgcgcgctggccgctcgcggggcagccgcgcgcaagag cagctcgtcccgccgcgaac
gcgtggggcaacctgtcctacgcgacctcagagtggtggtcaa gacgtgccctacttcaag
aagcggctcacgctgtcgagatctacgagtggtggtcaa gacgtgccctacttcaag
gataaggtgacagcaacagctcgcgggctggaagaattc aattcgtcataatctgtcc
ctacacagcaagtctcgtgtgcagaatgaaggaactgg aaaaagtcttgggtggatg
ctcaatccagaggtggcaagagcgggaaatctcctaggag aagagctgcacccatggac
aacaacagtaaatgtcaagagccgaagccgagctgccaa gaagaaagcatctctccag
tctggccaggggtgctgggacagccctggatcacagt ttccaaatggcctgcaagc
cctggctcacagcaatgacttgataactggagttac attcgcctcgaactagc
tcaaatgctagtactatagtggaacttccaccattat gaccgaacaggatgatctt
ggagaagggtgtgcatctctatgggtgtaaccgacctctgc cgaaagatggccttact
ttaccagctgtctgagataagcaatccgaaaaacatgga aaatcttttggataatctc
aaccttctctcatcacaacatcattaaactgtttcgaccca gtctcacctggcaccatg
atgcagcagacgcgtgctactcgtttgcccacccaacac cagtttgaattcaccacg
ccaaactacaaaaatatacatatggccaatccagcatgag cccttggccccagatgcct
atacaaacacttcaggacaataagtcgagttatggaggtat gagtcagataaactgtgcg
cctggactcttgaggagttgctgacttctgactctctcc ccataatgacattatgaca
ccagttgatcctgggtagccagcccaacagccgggttct gggccagaacgtcatgatg
ggccctaattcgtcatgtcaacctatggcagccaggcatc tcatacaaaaatgatgaat
cccagctcccataccacccctggacatgctcagcagacatc tgcagtcaacgggcgtccc
ctgccccacacggttaagcaccatgccccacacctcggtat gaaccgctgacccaagtg
aagacacctgtacaagtgcctctgccccaccccatgcagat gagtgcctggggggtac
tcctccgtgagcagctgcaatggctatggcagaatggcct tctccaccaggagaagctc
ccaagtgacttggatggcatgttcattgagcgcttagactg tgacatggaatccatcatt
cggaatgacctcatggatggagatacatggattttaactt tgacaatgtgtgccccaac
caaaactccacacagtgtaagacaacgacacatagctg ggtgtcaggtgaggggtta
gtgagcaggttaacctaaaagtacttcagattgtctgaca gcaggaaactgagagaagca
gtccaaaagatgtcttccacaaactcccttttagtttcttg gttaaaaaaaacaaaaa
aaaaaaacccctcttttcccttctcgtcagacttggcagca aagacatttttccctgtaca
ggatgttgccaaatgtgtgcaggttatgtgctgtgtaga taaggactgtgccatbga
aatttcattacaatgaagtgcacaaactcactacaccatata attgcagaaaaagatttca
gatcctgggtgtgcttcaagttttgtatataagcagtagat acagattgtatttgtgtg
gttttgggttttctaaaatataccaattgggtccaagaaagt ttatactctttttgtaata
ctgtgatgggctcatgtctgataagttaaacttttgtt gtactacctgttttctgcg
gaactgacggatcacaaagaactgaatctccattctgcac tccattgaacagccttgga
cctgttcacgttgccacagaattcacatgagaaccaagtag cctgttatcaatctgctaa

```

Go to: [General](#) [Description](#) [References](#) [Additional](#) [Cross-references](#) [Sequence](#)

Exhibit 2A

[Home](#) > [Databases](#) > [UniProt](#)

hosted by

[Text Search UniProt Knowledgebase](#)[Home](#)[About UniProt](#)[Getting Started](#)[Searches/Tools](#)[Databases](#)[Support/Documentation](#)

UniProt Entry

[PIR View](#)[Niceprot View](#) | [SRS View](#)UniProt Entry: **P98177**

ENTRY INFORMATION	
ENTRY NAME	FOXO4_HUMAN
ACCESSION NUMBERS	P98177; O43821; Q13720; Q8TDK9
CREATED	Release 34, 01-OCT-1996
SEQUENCE UPDATE	Release 41, 28-FEB-2003
ANNOTATION UPDATE	Release 46, 01-FEB-2005
NAME AND ORIGIN OF THE PROTEIN	
PROTEIN NAME	Putative fork head domain transcription factor AFX1
DESCRIPTION	Forkhead box protein O4
GENE NAME	MLLT7; AFX; AFX1; FOXO4
SOURCE ORGANISM	Homo sapiens
TAXONOMY ID	9606 [NCBI , NEWT]
LINEAGE	Eukaryota; Metazoa; Chordata; Craniata; Vertebrata; Euteleostomi; Mammalia; Eutheria; Primates; Catarrhini; Hominidae; Homo
REFERENCES	
[1]	Peters U; Haberhausen G; Kostrzewa M; Nolte D; Mueller U. AFX1 and p54nrb: fine mapping, genomic structure, and exclusion as candidate genes of X-linked dystonia parkinsonism. 1997, <i>Hum. Genet.</i> , 100, 569-572. <i>Position:</i> NUCLEOTIDE SEQUENCE (ISOFORM 1).. <i>Comments:</i> tissue=Blood. PubMed: 9341872 ; Medline: 98001080 .
[2]	Borkhardt A; Repp R; Haas OA; Leis T; Harbott J; Kreuder J et al. View all. Cloning and characterization of AFX, the gene that fuses to MLL in acute leukemias with a t(X;11)(q13;q23). 1997, <i>Oncogene</i> , 14, 195-202. <i>Position:</i> NUCLEOTIDE SEQUENCE (ISOFORM 1)..

	PubMed: 9010221 ; Medline: 97163401 .
[3]	<p>Yang Z; Whelan J; Babb R; Bowen BR. An mRNA splice variant of the AFX gene with altered transcriptional activity. 2002, <i>J. Biol. Chem.</i>, 277, 8068-8075. <i>Position</i>: NUCLEOTIDE SEQUENCE (ISOFORM ZETA).. PubMed: 11779849; Medline: 21864263.</p>
[4]	<p>Parry P; Wei Y; Evans G. Cloning and characterization of the t(X;11) breakpoint from a leukemic cell line identify a new member of the forkhead gene family. 1994, <i>Genes Chromosomes Cancer</i>, 11, 79-84. <i>Position</i>: CHROMOSOMAL TRANSLOCATION.. <i>Comments</i>: tissue=Bone marrow. PubMed: 7529552; Medline: 95118921.</p>
COMMENTS	
FUNCTION	Plays a role in the insulin signaling pathway.
SUBCELLULAR LOCATION	Nuclear (Potential).
ALTERNATIVE PRODUCTS	<p>;;</p> <p>IsoID=P98177-1 Name=1 Name=FOXO4a Sequence=displayed</p> <p>IsoID=P98177-2 Name=Zeta Name=AFXzeta Name=FOXO4b Sequence=described Ref=VSP_001552</p>
TISSUE SPECIFICITY	Heart, brain, placenta, lung, liver, skeletal muscle, kidney and pancreas. Isoform zeta is most abundant in the liver, kidney, and pancreas.
DISEASE	Involved in acute leukemias by a chromosomal translocation t(X;11)(q13;q23) that involves MLLT7 and MLL/HRX. The result is a rogue activator protein.
SIMILARITY	Contains 1 fork-head domain.
ONLINE INFORMATION	Atlas Genet. Cytogenet. Oncol. Haematol.; Contains 1 fork-head domain.
DATABASE CROSS-REFERENCES	
EMBL	<p>Y11284,CAA72156.1. [GenBank, DDBJ] Y11285,CAA72156.1,JOINED. [GenBank, DDBJ] Y11286,CAA72156.1,JOINED. [GenBank, DDBJ] X93996,CAA63819.1. [GenBank, DDBJ] U10072,AAA82171.1,ALT_SEQ. [GenBank, DDBJ]</p>

	AF384029,AAL85197.1. [GenBank, DDBJ]
ENSEMBL	ENSG00000184481,Homo sapiens.
GENEW	HGNC:7139,MLLT7.
GO	GO:0005634,C:nucleus,TAS. GO:0003677,F:DNA binding,TAS. GO:0007050,P:cell cycle arrest,TAS. GO:0008285,P:negative regulation of cell proliferation,TAS. GO:0006366,P:transcription from Pol II promoter,TAS. QuickGO
INTERPRO	IPR001766,TF_Fork_head. IPR009058,Wing_hlx_DNA_bnd.
MIM	300033.
PDB	1E17,NMR,A=61-210.
PFAM	PF00250,Fork_head,1.
PRINTS	PR00053,FORKHEAD.
PRODOM	PD000425,TF_Fork_head,1.
PROSITE	PS00657,FORK_HEAD_1,FALSE_NEG. PS00658,FORK_HEAD_2,1. PS50039,FORK_HEAD_3,1.
SMART	SM00339,FH,1.
TRANSFAC	T03403.
UniRef	View cluster of proteins with at least 50% / 90% identity.
KEYWORDS	
3D-structure; Alternative splicing; Chromosomal translocation; DNA-binding; Nuclear protein; Proto-oncogene; Transcription regulation	

FEATURES				
Feature	Description	Begin Position	End Position	Length
<u>DNA-BINDING REGION</u>	Fork-head	100	188	89
<u>SPLICE VARIANT</u>	(in isoform Zeta) /FTId=VSP_001552	58	112	55
<u>SEQUENCE CONFLICT</u>	MDPGNENSATE -> MRIQPQK (in Ref. 2)	1	11	11
<u>SEQUENCE CONFLICT</u>	QSRPRSCTWP -> RAVPLLHLA (in Ref. 1)	25	34	10
<u>SEQUENCE CONFLICT</u>	P -> S (in Ref. 2)	74	74	1
<u>SEQUENCE</u>	A -> G (in Ref. 2)	79	79	1

<u>CONFLICT</u>				
<u>SEQUENCE CONFLICT</u>	L -> F (in Ref. 2)	109	109	1
<u>SEQUENCE CONFLICT</u>	R -> P (in Ref. 1)	422	422	1
<u>TURN</u>		100	101	2
<u>HELIX</u>		106	116	11
<u>STRAND</u>		122	123	2
<u>HELIX</u>		124	134	11
<u>HELIX</u>		136	138	3
<u>HELIX</u>		139	142	4
<u>TURN</u>		143	143	1
<u>TURN</u>		145	146	2
<u>HELIX</u>		147	159	13
<u>TURN</u>		162	163	2
<u>STRAND</u>		164	167	4
<u>TURN</u>		170	172	3
<u>STRAND</u>		177	180	4
<u>TURN</u>		182	183	2

Feature sequence (Put the mouse on the feature above to see the sequence below):

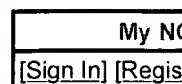
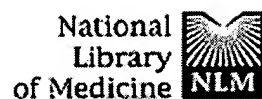
SEQUENCE	
LENGTH	505 aa
MOLECULAR WEIGHT	53758 Da
CRC64 CHECKSUM	809CED90E6EFCA8B
SEQUENCE	<pre> -----+-----+-----+-----+-----+ MDPGNENSAT EAAAIIDLDP DFEPQSRPRS CTWPLPRPEI ANQPSEPPEV 50 EPDLGEKVHT EGRSEPILLP SRLPEPAGAP QPGILGAVTG PRKGGSRRNA 100 WGNQSYAELI SQAIESAPEK RLTLAQIYEW MVRTVPYFKD KGDSNSSAGW 150 KNSIRHNLST HSKFIKVHNE ATGKSSWWML NPEGGKSGKA PRRRAASMDS 200 SSKLLRGRSK APKKKPSVLP APPEGATPTS PVGHFAKWSG SPCSRNREEA 250 DMWTTFRPRS SSNASSVSTR LSPLRPESEV LAEEIPASVS SYAGGVPPTL 300 NEGLELLDGL NLTSSHSLLS RSGLSGFSLQ HPGVTGPLHT YSSSLFSPA 350 GPLSAGEGCF SSSQALEALL TSDTPPPPAD VLMTQVDPIL SQAPTLALLG 400 GLPSSSKLAT GVGLCPKPLE ARGPSSLVPT LSMIAPPPVM ASAPIPKALG 450 TPVLTPTPEA ASQDRMPQDL DLDMYMENLE CDMDNIISDL MDEGEGLDFN 500 FEPDP 505 </pre>

ADDITIONAL INFORMATION FROM iProClass		Go to iProClass
GENE ONTOLOGY	<i>Molecular Function</i>	
	GO:0003677: DNA binding [SPKW ; evidence: IEA] [PMID:9010221 ; evidence: TAS]	
	GO:0003700: transcription factor activity [INTERPRO ; evidence: IEA]	
	<i>Biological Process</i>	
	GO:0006355: regulation of transcription, DNA-dependent [INTERPRO ; evidence: IEA] [SPKW ; evidence: IEA]	
	GO:0008151: cell growth and/or maintenance [SPKW ; evidence: IEA]	
	GO:0007050: cell cycle arrest [PMID:10783894 ; evidence: TAS]	
	GO:0008285: negative regulation of cell proliferation [PMID:10783894 ; evidence: TAS]	
	GO:0006366: transcription from Pol II promoter [PMID:10783894 ; evidence: TAS]	
	<i>Cellular Component</i>	
	GO:0005634: nucleus [INTERPRO ; evidence: IEA] [SPKW ; evidence: IEA] [PMID:9010221 ; evidence: TAS]	

POWERED BY

[About UniProt](#) [Getting Started](#) [Searches/Tools](#) [Databases](#) [Support/Documentation](#)[HOME](#) | [HELP](#) | [SITE MAP](#)

Copyright ©2002 - 2003, UniProt All rights reserved.



Entrez PubMed Nucleotide Protein Genome Structure OMIM PMC Journals Book

Search PubMed for

Go Clear

Limits Preview/Index History Clipboard Details

Display Abstract Show: 20 Sort Send to Text

All: 1

About Entrez

Text Version

Entrez PubMed

Overview

Help | FAQ

Tutorial

New/Noteworthy

E-Utilities

PubMed Services

Journals Database

MeSH Database

Single Citation Matcher

Batch Citation Matcher

Clinical Queries

LinkOut

My NCBI (Cubby)

Related Resources

Order Documents

NLM Catalog

NLM Gateway

TOXNET

Consumer Health

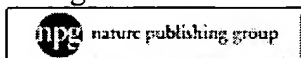
Clinical Alerts

ClinicalTrials.gov

PubMed Central

☐ 1: Oncogene. 1997 Jan 16;14(2):195-202.

Related Articles, L




**Cloning and characterization of AFX, the gene that fuses to MLL in acute leukemias with a t(X;11)(q13;q23).****Borkhardt A, Repp R, Haas OA, Leis T, Harbott J, Kreuder J, Hammermann J, Henn T, Lampert F.**

Department of Pediatrics, University of Giessen, Germany.

We report the cloning and characterization of the entire AFX gene which fuses to MLL in acute leukemias with a t(X;11)(q13;q23). AFX consists of two exons and encodes for a protein of 501 amino acids. We found that normal B- and T cells contain similar levels of AFX mRNA and that both the MLL/AFX as well as the AFX/MLL fusion transcripts are present in the cell line and the ANLL sample with a t(X;11)(q13;q23). The single intron of the AFX gene consists of 3706 nucleotides. It contains five simple sequence repeats with lengths of at least 12 bps, a chi-like octamer sequence (GCA/TGGA/TGG) and several immunoglobulin heptamer-like sequences (GATAGTG) that are distributed throughout the entire AFX intron sequence. In the KARPAS 45 cell line the breakpoints occur at nucleotides 2913/2914 of the AFX intron and at nucleotides 4900/4901 of the breakpoint cluster region of the MLL gene. The AFX protein belongs to the forkhead protein family. It is highly homologous to the human FKHR protein, the gene of which is disrupted by the t(2;13)(q35;q14), a chromosome rearrangement characteristic of alveolar rhabdomyosarcomas. It is noteworthy that the t(X;11)(q13;q23) in the KARPAS 45 cell line and in one acute nonlymphoblastic leukemia (ANLL) disrupts the forkhead domain of the AFX protein exactly at the same amino acids as does the t(2;13)(q35;q14) in case of the FKHR protein. In addition, the 5'-part of the AFX protein contains a conserved hexapeptide motif (QIYEW) that is homologous to the functionally important conserved hexapeptide QIYPWM upstream of the homeobox domain in Hox proteins. This motif mediates the cooperative DNA binding of Pbx family members and Hox proteins and, therefore, plays an important role in physiologic and oncogenic processes. In acute leukemias with a t(X;11)(q13;q23), this hexapeptide motif is separated from the remaining forkhead domain within the AFX protein. The predicted amino acid sequence of AFX differs significantly from the partial AFX prote

sequence published previously (Genes, Chromosomes and Cancer, 1994, 11, 79-84). This discrepancy can be explained by the occurrence of two sequencing errors in the earlier work at nucleotide number 783 and 844 (loss of a cytosine residue or guanosine residue, respectively) that lead to two reading frame shifts.

PMID: 9010221 [PubMed - indexed for MEDLINE]

Display	Abstract		Show: 20		Sort		Send to	Text
---------	----------	---	----------	--	------	---	---------	------

[Write to the Help Desk](#)

[NCBI](#) | [NLM](#) | [NIH](#)

Department of Health & Human Services

[Privacy Statement](#) | [Freedom of Information Act](#) | [Disclaimer](#)

Feb 7 2005 09:57:23

Insulin Inhibition of Transcription Stimulated by the Forkhead Protein Foxo1 Is Not Solely due to Nuclear Exclusion

WEN-CHI TSAI, NISAN BHATTACHARYYA, LI-YING HAN, JOHN A. HANOVER, AND MATTHEW M. RECHLER

Diabetes Branch (W.-C.T., N.B., L.-Y.H., M.M.R.) and Laboratory of Cell Biochemistry and Biology (J.A.H.), National Institute of Diabetes and Digestive and Kidney Diseases, National Institutes of Health, Bethesda, Maryland 20892-1758

The FOXO family of forkhead transcription factors stimulates the transcription of target genes involved in many fundamental cell processes, including cell survival, cell cycle progression, DNA repair, and insulin sensitivity. The activity of FOXO proteins is principally regulated by activation of protein kinase B (PKB)/Akt by insulin and other cytokines. PKB/Akt phosphorylates three consensus sites in FOXO proteins, leading to their export from the nucleus and the inhibition of FOXO-stimulated transcription. It has been widely accepted that the decreased transcription results from reduced abundance of FOXO proteins in the nucleus. In the present study we mutated Leu³⁷⁵ to alanine in the nuclear export signal of Foxo1 (mouse FOXO1), so that it would remain in the nucleus of H4IIE rat hepatoma cells after insulin treatment, and determined whether insulin

could still inhibit transcription stimulated by the Foxo1 mutant. Despite the retention of the Foxo1 mutant in the nucleus, insulin inhibited L375A-Foxo1-stimulated transcription to the same extent as transcription stimulated by wild-type Foxo1. Similar results were obtained using reporter plasmids containing the rat IGF-binding protein-1 promoter or a minimal promoter with three copies of the insulin response element to which FOXO proteins bind. We conclude that insulin can inhibit Foxo1-stimulated transcription even when nuclear export of Foxo1 is prevented, indicating that insulin inhibition can occur by direct mechanisms that do not depend on altering the subcellular distribution of the transcription factor. (*Endocrinology* 144: 5615–5622, 2003)

DECREASED INSULIN inhibition of the transcription of two key enzymes in gluconeogenesis, phosphoenolpyruvate carboxykinase and the catalytic subunit of glucose-6-phosphatase, contributes to the increased hepatic glucose production and hyperglycemia associated with type 2 diabetes (1–3). The promoters of both genes contain a consensus insulin response element (IRE) that confers on minimal promoters the ability to be negatively regulated by insulin (4, 5). A similar IRE is present in the promoter for IGF-binding protein-1 (IGFBP-1) (6–8), a protein that binds IGF-I and IGF-II and regulates their growth-promoting and insulin-like activities. IGFBP-1 transcription is increased in diabetic rat liver and is rapidly normalized by insulin (9, 10).

Insulin inhibition of IGFBP-1 gene expression is mediated by phosphatidylinositol 3-kinase (PI 3-kinase) (11, 12) and its downstream effector, serine/threonine-specific protein kinase B (PKB)/Akt (12). Recognition that a similar insulin signaling pathway in *Caenorhabditis elegans* inhibited the transcription factor Daf16 (13, 14), an ortholog of the FOXO subfamily of forkhead transcription factors (15), suggested that FOXO proteins might mediate insulin inhibition of transcription in mammalian cells. Three human FOXO proteins

(FOXO1, FOXO3a, and FOXO4)¹ and their mouse counterparts (Foxo1, Foxo3, and Foxo4) have been identified and extensively characterized (16–19). They share a conserved central DNA-binding domain (the Fox box, residues 155–255 in the 652-amino acid Foxo1 used in the present study) and have a C-terminal *trans*-activation domain (20). The FOXO proteins bind to an IRE in the proximal promoter (21–23) of target genes involved in insulin sensitivity, cell survival, cell cycle progression, and DNA repair (24–27) and stimulate their transcription.

After being activated by insulin or the closely related growth factor IGF-I, PKB/Akt phosphorylates FOXO proteins at three conserved sites (Thr²⁴, Ser²⁵³, and Ser³¹⁶ in Foxo1) (28–30). Phosphorylation of these sites leads to inhibition of FOXO-stimulated transcription (24, 31–33) and redistribution of the transcription factor from the nucleus to the cytoplasm (24, 34, 35). Brunet *et al.* (24) proposed that the export of FOXO from the nucleus after phosphorylation by PKB/Akt would prevent the transcription factor from activating its target genes. The concept that nuclear exclusion is the principal mechanism of FOXO regulation has been widely accepted and has been extrapolated to other growth factors and cytokines that activate PKB/Akt (36–38).

The present study examines whether insulin also can inhibit Foxo1-stimulated transcription by other mechanisms

Abbreviations: FITC, Fluorescein isothiocyanate; FOXO, forkhead box transcription factor, subfamily O; Foxo1, mouse FOXO1; GFP, green fluorescence protein; IGFBP-1, IGF-binding protein-1; IRE, insulin response element; NES, nuclear export signal; PI 3-kinase, phosphatidylinositol 3-kinase; PKB, protein kinase B.

¹ The human (FOXO) and mouse (Foxo) members of the FOXO subfamily were previously known as FKHR (FOXO1, Foxo1), FKHL1 (FOXO3a, Foxo3), and AFX (FOXO4, Foxo4).

when redistribution of Foxo1 to the cytoplasm has been prevented. Our strategy was based on the demonstration by Biggs et al. (39), subsequently confirmed by other investigators (40–42), that Foxo1 was exported from the nucleus by the Crm1 export transporter that binds to a leucine-rich nuclear export signal (NES) in the presence of Ran-GTP (43–46). Biggs et al. (39) reported that a Foxo1 mutant in which Leu³⁷⁵, a key residue in the NES (47), was mutated to alanine remained in the nucleus of CV1 monkey kidney cells after incubation with insulin (39). In the present study we demonstrate that L375A-Foxo1 is localized predominantly in the nucleus of H4IIE rat hepatoma cells after insulin treatment, and that despite nuclear localization of the mutant transcription factor, insulin inhibits transcription stimulated by L375A-Foxo1 and wild-type Foxo1 to the same extent. We conclude that insulin can inhibit Foxo1-stimulated transcription by additional mechanisms besides simple relocation to the cytoplasm.

Materials and Methods

Materials

The plasmid pCMV5-c-Myc-Foxo1 (henceforth, pCMV5-Foxo1) was provided by J. Nakae and D. Accili (29, 33). p925-GL3 Basic, a luciferase reporter plasmid containing nucleotides –925 to +79 of the rat IGF1R promoter (7, 33), was previously described. pCMV5 empty vector was prepared by *Xba*I digestion of pCMV5-Foxo1 to delete the Foxo1 insert.

The plasmid pGL3-Promoter was obtained from Promega Corp. (Madison, WI); plasmid Bluescript II (KSII⁺) was purchased from Stratagene (La Jolla, CA); DMEM (low glucose) was obtained from Invitrogen (Carlsbad, CA); fetal bovine serum was purchased from HyClone Laboratories (Logan, UT); Humulin U-100 regular insulin was obtained from Eli Lilly & Co. (Indianapolis, IN); anti-c-Myc mouse monoclonal immunoglobulin G (9E-10) was purchased from Santa Cruz Biotechnology, Inc. (Santa Cruz, CA); fluorescein isothiocyanate (FITC)-conjugated AffiniPure donkey antimouse antibody was purchased from Jackson ImmunoResearch Laboratories (West Grove, PA); LY294002, an inhibitor of PI 3-kinase, was obtained from Calbiochem (San Diego, CA); restriction enzymes and QuikChange Site-Directed mutagenesis kit were purchased from Stratagene; Centri-Sep columns were obtained from Princeton Separations (Adelphia, NJ); plasmid purification kits were obtained from Qiagen (Valencia, CA); and DNA sequencing kits were purchased from PE Applied Biosystems (Foster City, CA).

Cell cultivation

H4IIE rat hepatoma cells (48) were grown as monolayer cultures in low glucose DMEM supplemented with 10% fetal bovine serum and were incubated in a humidified 95% air/5% CO₂ atmosphere at 37°C. Cultures were passaged weekly (when they reached confluence) at a ratio of 1:20 using trypsin-EDTA. Fresh stocks were thawed after 8–10 passages.

Construction of L375A-Foxo1 expression vector

Full-length wild-type Foxo1 was excised from pCMV5-Foxo1 using *Xba*I and was ligated into *Xba*I-digested pBluescript vector to generate pBluescript-Foxo1. The L375A mutation was introduced into pBluescript-Foxo1 by overlapping PCR. The 5' fragment was generated by PCR using primers 490-GAC CTC ATC ACC AAG GCC ATC-510 (numbered with respect to ATG = 1) and 1142-GGG GAC GAG AGA AGG TTG GCA TTA TCC AGA AGG TTC-1106 [in which CT has been mutated to GC (underlined)] and contained an internal *Bgl*II site (545-AGA TCT 550). The 3' fragment was generated using primer 1106-GAA CCT TCT GGA TAA TGC CAA CCT TCT CTC GTC CCC-1142 and 1489-GGC CCA TCA TTA CAT TTT GGC CCA GGA C-1462 and contained an internal *Age*I site (1425-ACC GGT-1430). The 5' and 3' fragments were amplified by PCR using the two nonoverlapping primers. The resulting fragment containing the L375A mutation was digested

with *Bgl*II and *Age*I and ligated into pBluescript-Foxo1 that had been digested with *Bgl*II and *Age*I to generate pBluescript-L375A-Foxo1. L375A-Foxo1 was excised with *Xba*I and ligated into the dephosphorylated *Xba*I sites of pCMV5-c-Myc. The orientation and sequence of the insert containing the mutation were confirmed by DNA sequencing.

Construction of pGL3-IRE-3x and pGL3-GC-3x reporter genes

Three tandem copies of the wild-type IRE were inserted into the pGL3-Promoter plasmid (which contains a simian virus 40 promoter upstream from a luciferase reporter gene) to construct pGL3-IRE-3x. The sense strand of IRE-3x contained three copies of the IRE (GCA AAA CAA ACT TAT TTT GAA; the inverted palindrome is underlined). The antisense strand of IRE-3x contained three complementary copies of the IRE plus a *Bgl*II site (GATC) at the 5' end and a *Kpn*I site (GTCA) at the 3' end. Plasmid pGL3-GC-3x containing three copies of an inactive G/C-C/A mutant IRE (49, 50) was constructed similarly using oligonucleotides in which G was substituted for C and C substituted for A (shown in **bold**) in both half-sites of the inverted palindrome (GCA AAA GAA ACT **TCT** **TTT** GAA). The G/C-C/A mutant IRE does not bind FOXO1 (21). Annealed and phosphorylated IRE-3x and GC oligonucleotides were ligated into the pGL3-promoter vector (digested with *Kpn*I and *Bgl*II and dephosphorylated) using a ligation kit (Takara Biomedical, Inc., Berkeley, CA). The sequences of the IRE-3x and GC-3x inserts were confirmed.

Immunofluorescence

H4IIE cells were transiently transfected with wild-type or mutant pCMV5-c-myc-Foxo1 and incubated with or without insulin, and the subcellular distribution of transfected Foxo1 was studied by fluorescence microscopy as previously described (35). In brief, H4IIE cells were plated onto 60-mm dishes at 3–3.75 million cells/dish and incubated overnight in serum-supplemented medium. The cells then were transfected with the indicated plasmids using Lipofectamine and Plus Reagent (Invitrogen) according to the manufacturer's protocol (1 µg DNA/4 µl Plus Reagent/5 µl Lipofectamine). After 24 h the cells were trypsinized, and approximately 20,000 cells/well were seeded into 8-well slide culture chambers (Nalge Nunc International, Naperville, IL). After overnight incubation, the medium was changed to serum-free medium (DMEM containing 0.1% BSA) for 24 h, after which insulin (1 µg/ml, final concentration) was added to half of the wells for 1 h. Cells were fixed using a solution of 2% paraformaldehyde (Electron Microscopy Sciences, Fort Washington, PA) and permeabilized in 0.5% Triton X-100. Myc-tagged Foxo1 was visualized using anti-Myc monoclonal antibody (2 µg/ml, final concentration) and FITC-conjugated AffiniPure donkey antimouse IgG (5 µg/ml, final concentration). Slides were examined using Axiovert TV-100 and TV-200 fluorescence microscopes (Zeiss, New York, NY). Only transfected cells were fluorescent; FITC-stained cells were not observed when primary or secondary antibodies were omitted, and only a small percentage of the cells identified using Sytox nuclear stain were fluorescent.

Digital images of fluorescent cells were taken using the UltraView Confocal Imaging System in conjunction with a Zeiss Axiovert TV-100 microscope. Single cells were analyzed using Open Lab Image Analysis Software (Improvision, Inc., Lexington, MA). Cytoplasmic to nuclear ratios were calculated using the HIS colorspace feature of Open Lab. Pixel intensities were determined at 10 points in the nucleus, 10 points in the cytoplasm, and 10 background points for 5–7 cells in each condition, averaged, and analyzed statistically. In addition, z-axis sections (7- to 10-µm slices, ~10–15 slices/cell) of a representative cell for each condition also were analyzed. Cell and nuclear boundaries were estimated, and the mean intensities were determined in the nuclear and cytoplasmic areas of each section and summed. In addition, the nuclear/cytoplasmic ratio was determined by volume rendering using the Open Lab software.

Transient transfection and luciferase assay

H4IIE cells were transfected as described previously (51). The day before transfection, cells (3–3.75 million/dish) were plated onto 60-mm tissue culture dishes in 3 ml DMEM containing 10% serum and were

typically 70–100% confluent at the time of transfection. Diethylaminoethyl dextran stock solution (2 mg/ml in 0.15 M NaCl; Amersham Pharmacia Biotech, Piscataway, NJ) was diluted with an equal volume of Tris-buffered saline [25 mM Tris (pH 7.5), 137 mM NaCl, 5 mM KCl, 0.7 mM CaCl₂, 0.5 mM MgCl₂, and 0.6 mM Na₂HPO₄]. Plasmid DNA (~5 µg diluted in 100 µl Tris-buffered saline) was mixed with 100 µl diethylaminoethyl dextran-Tris-buffered saline and incubated at room temperature. [Typically, 3 µg pCMV5 expression vector, 2 µg luciferase reporter, and 40 ng pRSV β-galactosidase (33) were used.] After 15 min, 190 µl of the mixture were added to each dish. Fifteen minutes later, 3 ml DMEM containing 10% serum were added, and the incubation was continued overnight. After medium change and a second overnight incubation, the medium was replaced with serum-free DMEM containing 0.1% BSA with or without recombinant human insulin (0.25 µg/ml). After 24 h the cells were washed twice with ice-cold PBS and harvested for luciferase assay. After the addition of 360 µl lysis buffer [100 mM potassium phosphate (pH 7.8) and 0.2% Triton X-100], cells were scraped and centrifuged (4°C, 14,000 rpm, 5 min). Supernatant from each sample was transferred to a fresh tube. Luciferase activities of the supernatants were measured using a Lumat LB 9507 luminometer (EG&G Berthold, Bad Wildbad, Germany) with a Dual Light chemiluminescent reporter gene assay kit (Tropix, PE Applied Biosystems, Bedford, MA) as specified by the manufacturer. Assays were performed in duplicate.

Results

L375A-Foxo1 is retained in the nucleus after insulin treatment

The effect of insulin treatment on the subcellular localization of wild-type and L375A-Foxo1 transfected into H4IIE cells was examined by fluorescence microscopy. In the absence of insulin, wild-type and L375A-Foxo1 were localized predominantly in the nucleus in all fluorescent cells (Fig. 1). After incubation with insulin, wild-type Foxo1 redistributed to the cytoplasm, whereas L375A-Foxo1 remained predominantly in the nucleus. The cells depicted in the upper panel of Fig. 1 are representative of more than 70 cells examined in each condition (tabulated in Fig. 1, lower panel) and show the same predominant localization of wild-type and mutant Foxo1 to the nucleus or cytoplasm.

The relative amounts of nuclear and cytoplasmic Foxo1 in individual cells transfected with wild-type or mutant Foxo1 and incubated with or without insulin were determined by quantifying the levels of nuclear and cytoplasmic fluorescence in whole cells (Fig. 2) and confirmed in sections of digital images of representative cells (Fig. 3). The ratios of average pixel intensities (cytoplasm/nucleus) in whole cells in the absence of insulin were 0.27 for wild-type Foxo1 and 0.31 for L375A-Foxo1 (Fig. 2). After incubation with insulin, wild-type Foxo1 was preferentially localized to the cytoplasm (cytoplasm/nucleus = 5.3), whereas L375A-Foxo1 remained predominantly in the nucleus (cytoplasm/nucleus = 0.19; Fig. 2).

To exclude the possibility that some of the observed nuclear fluorescence might have arisen from overlying or underlying cytoplasm, we also analyzed z-sections of digital images of representative cells (Fig. 3). Analysis of cell sections confirmed that the redistribution of wild-type Foxo1 to the cytoplasm after insulin treatment was much greater than that observed for L375A-Foxo1. In the absence of insulin, greater than 80% of total Foxo1 fluorescence was present in the nucleus with either the wild-type or mutant construct. After insulin treatment, nuclear fluorescence of wild-type Foxo1 decreased by 55%, whereas a much smaller decrease

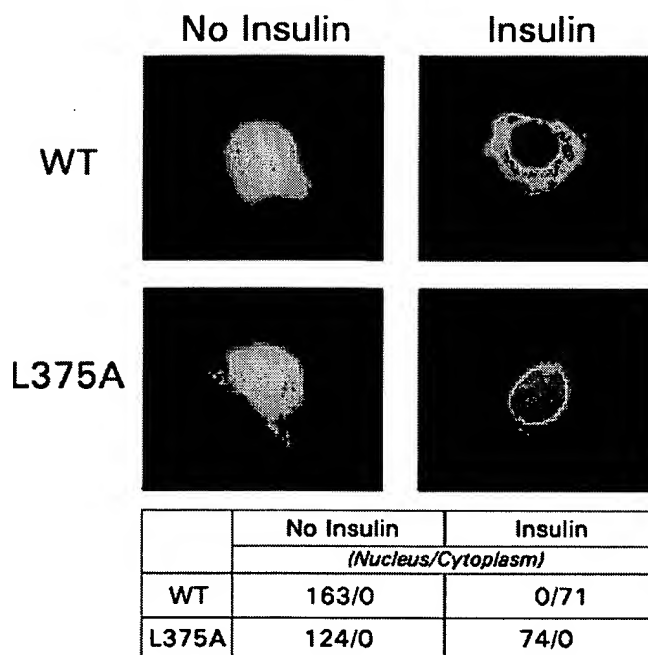


FIG. 1. Fluorescence microscopy of representative cells transfected with wild-type or L375A-Foxo1 and incubated with insulin. *Top panel*, Cells were transfected with wild-type (WT) or L375A-Foxo1, incubated with or without insulin for 1 h, fixed, and incubated with mouse monoclonal antibodies to the c-Myc epitope and fluorescein-labeled second antibody. Photographs of representative cells are shown. *Bottom panel*, The number of fluorescently labeled cells that were more intensely labeled in the nucleus or cytoplasm was determined. The ratio of the total number of cells with predominantly nuclear labeling to the total number of cells with predominantly cytoplasmic labeling from three experiments is shown.

in nuclear fluorescence (14%) was observed with L375A-Foxo1. Although the extent of redistribution of wild-type Foxo1 from nucleus to cytoplasm determined by optical sectioning was less complete than that indicated by analysis of whole cells, nuclear export was decreased by 75% in the L375A-Foxo1 mutant compared with that in wild-type Foxo1. Together these results indicate that insulin treatment of H4IIE cells causes a major redistribution of wild-type Foxo1 from nucleus to cytoplasm that is not seen with the L375A-Foxo1 NES mutant, which is predominantly retained in the nucleus after insulin treatment.

Insulin inhibits transcription stimulated by L375A-Foxo1

The ability of insulin to inhibit transcription stimulated by wild-type or L375A-Foxo1 was examined by transient transfection of H4IIE rat hepatoma cells. A luciferase reporter (pGL3-IRE-3x) that contains three tandem copies of the IRE upstream from a minimal simian virus 40 promoter was used (Fig. 4). Reporter plasmids lacking an IRE insert (pGL3 empty vector) or containing a mutant IRE that could not bind Foxo1 (pGL3-GC-3x) (21, 49, 50) were used as negative controls. Stimulation of transcription was dependent on both Foxo1 and the IRE (Fig. 4, left panel). In the absence of insulin, wild-type and L375A-Foxo1 stimulated pGL3-IRE-3x promoter activity approximately 25-fold relative to pCMV5

FIG. 2. The effect of insulin treatment on cytoplasmic to nuclear ratios of c-Myc-Foxo1 immunofluorescence in H4IIE rat hepatoma cells transfected with wild-type or L375A-Foxo1. Cells were transfected with wild-type Foxo1 (upper panels) or L375A-Foxo1 (lower panels), and treated (right panels) or not treated (left panels) with insulin as described in *Materials and Methods*. The mean \pm SD of fluorescence intensity in five to seven cells examined for each condition is plotted.

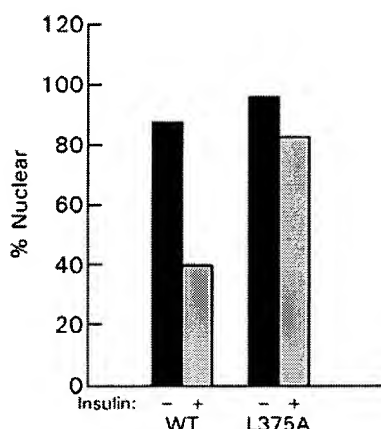
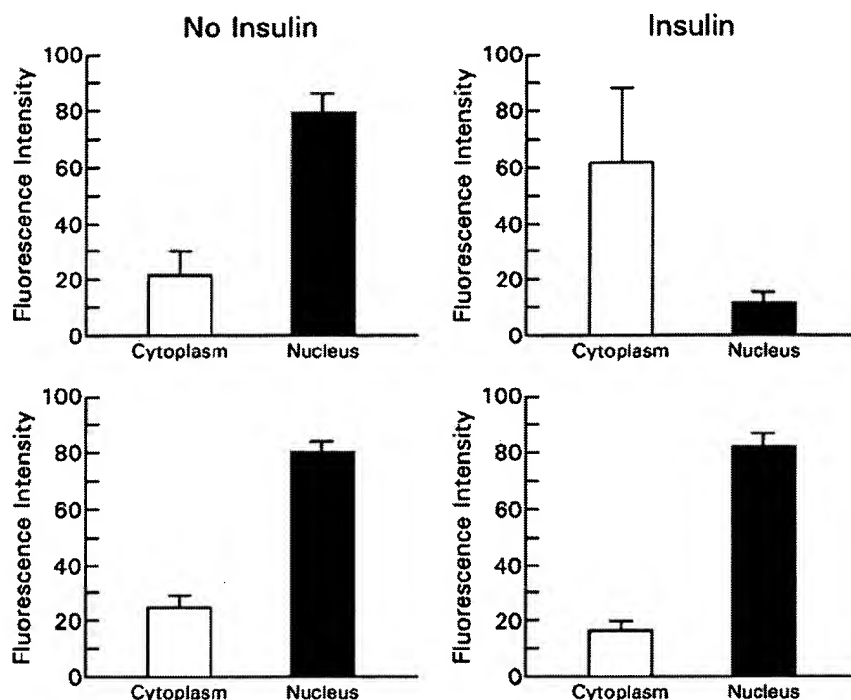


FIG. 3. Quantification of the effect of insulin on the subcellular distribution of wild-type (WT) and L375A-Foxo1 in sections of individual cells. Z-Sections of digital confocal images of representative fluorescent cells transfected with WT or L375A-Foxo1 were analyzed using the Open Lab program. The mean fluorescence intensity in the nucleus and cytoplasm was determined in each of the sections and summed. The percentage of total fluorescence in the nucleus is plotted in the absence of insulin (■) and after insulin treatment (▨). Relative nuclear and cytoplasmic volumes (47%:53%) were estimated from the mean intensity values after incubation with insulin. The cytoplasmic signal in the absence of insulin was too low to allow accurate estimates of cytoplasmic volume.

empty vector; no significant stimulation was seen with pGL3-GC-3x.

Insulin inhibited transcription stimulated by L375A-Foxo1 or wild-type Foxo1 to the same extent (Fig. 4, right panel). In cells transfected with L375A-Foxo1, luciferase activity in the presence of insulin was $31 \pm 6\%$ (mean \pm SE; $n = 6$) of that in cells not treated with insulin compared with $32 \pm 5\%$ (mean \pm SE; $n = 5$) for wild-type Foxo1. Thus, insulin in-

hibited L375A-Foxo1-stimulated transcription in pGL3-IIE-3x to the same extent as transcription stimulated by wild-type Foxo1, even though L375A-Foxo1 remained predominantly in the nucleus after insulin treatment.

Similar results were obtained using a luciferase reporter containing the native rat IGFBP-1 promoter, p925-GL3. In the absence of insulin, wild-type and L375A-Foxo1 stimulated transcription of the p925-GL3 luciferase reporter containing the rIGFBP-1 promoter by 5-fold (Fig. 5). Insulin treatment decreased transcription stimulated by wild-type and L375A-Foxo1 to about 35% of that in cells transfected with the same plasmids that did not receive insulin. Insulin also inhibited promoter activity in cells transfected with the pCMV5 empty vector. Inhibition of basal transcription has been observed previously and attributed to insulin inhibition of endogenous Foxo proteins (33, 52–54). Consistent with this interpretation, H4IIE cells synthesize Foxo3 (53, 55) and Foxo1 (33, 56), and insulin stimulates the phosphorylation of endogenous Foxo3 at two PKB/Akt sites, Thr³² and Ser²⁵³ (53).

PI 3-kinase mediates insulin inhibition of L375A-Foxo1-stimulated transcription

Insulin inhibition of Foxo1-stimulated transcription is mediated by PI 3-kinase (32). Inhibition of PI 3-kinase activity with LY294002 abolished insulin inhibition of IGFBP-1 transcription stimulated by either wild-type or L375A-Foxo1 (Fig. 6). With wild-type Foxo1, abrogation of insulin inhibition of transcription by LY294002 could be secondary to blocking insulin-induced nuclear exclusion of Foxo1 (24, 34, 35) or be a direct effect on transcription. Our results indicate that LY294002 also can block the direct effects of insulin on transcription, because it abolishes insulin inhibition of L375A-Foxo1-stimulated transcription when nuclear export does not occur.

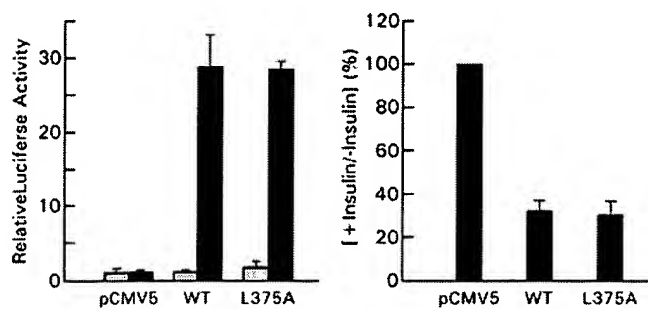


FIG. 4. Stimulation of pGL3-IRES-3x transcription by wild-type and L375A-Foxo1 is IRE dependent and inhibited by insulin. *Left panel*, No insulin. Cells were cotransfected with pCMV5 empty vector, wild-type (WT) Foxo1 or L375A-Foxo1, and pGL3-IRES-3x, pGL3-GC-3x, or pGL3 empty vector luciferase reporter plasmids. Fold stimulation of luciferase activity normalized to pGL3 empty vector is plotted for pGL3-GC-3x (□) and pGL3-IRES-3x (■; mean \pm SE; $n = 4$). *Right panel*, Effect of insulin. Luciferase activity also was determined in the same experiments after insulin treatment. The ratio of luciferase activity in the presence and absence of insulin [(+Insulin)/(-Insulin) \times 100] using the pGL3-IRES-3x reporter for WT or L375A-Foxo1 is expressed relative to the pCMV5 empty vector in the same experiment. The mean \pm SE ($n = 6$) are plotted. Identical results were obtained when the relative luciferase activity (+Insulin/-Insulin) using pGL3-IRES-3x was normalized to the activity observed using pGL3 empty vector or pGL3-GC-3x (results not shown). [With the pCMV5 empty vector, luciferase activity in the presence of insulin was $174 \pm 20\%$ (\pm SE; $n = 6$) of that in the absence of insulin. Similar stimulation was seen with pGL3 empty vector and pGL3-GC-3x, indicating that this is a property of the expression vector-reporter system and not of IRE- and Foxo1-dependent transcription.]

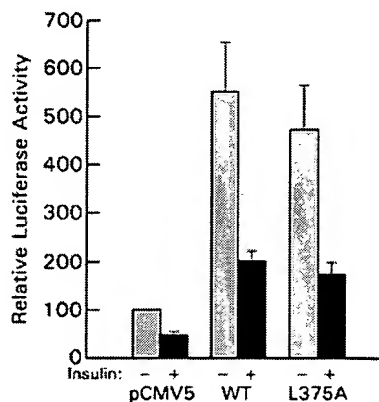


FIG. 5. Insulin inhibits IGF1 promoter activity stimulated by wild-type and mutant Foxo1. H4IIE cells were cotransfected with pCMV5 empty vector, pCMV5-Foxo1 [wild-type (WT)] or pCMV5-L375A-Foxo1, and the p925-GL3 luciferase reporter. The cells were incubated with or without insulin, and luciferase activity was determined. Relative luciferase activity (mean \pm SE from 8–10 experiments) in the absence (□) and presence (■) of insulin is plotted. The activity with pCMV5 empty vector in the absence of insulin is taken as 100.

Discussion

It has been widely accepted that phosphorylation of the three consensus PKB/Akt sites in Foxo1 and other FOXO proteins after incubation with insulin or other cytokines inhibits FOXO-stimulated transcription of target genes by inducing the export of FOXO proteins from the nucleus (24). In the present study we demonstrate that insulin can inhibit

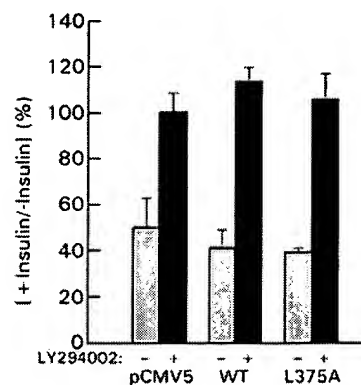


FIG. 6. Insulin inhibition of IGF1 promoter activity stimulated by wild-type (WT) and mutant Foxo1 requires PI 3-kinase. H4IIE cells were cotransfected with pCMV5, pCMV5-Foxo1 (WT), or pCMV5-L375A-Foxo1 expression vectors and the p925-GL3 luciferase reporter. Cells were preincubated for 30 min with (■) or without (□) 50 μ M LY294002, after which half of the cells in each group were treated with insulin. Relative luciferase activity [(+Insulin)/(-Insulin) \times 100; mean \pm SE] in the absence and presence of LY294002 in three to five experiments is plotted. [In the absence of insulin, luciferase activity in the presence of LY294002 compared with its absence was $141 \pm 31\%$ (\pm SE; $n = 3$) for pCMV5 empty vector and $44 \pm 8\%$ ($n = 8$) for WT and L375A-Foxo1.]

Foxo1-stimulated transcription even when export of Foxo1 from the nucleus is prevented by mutation, providing direct evidence that inhibition can occur in intact cells by mechanisms unrelated to subcellular redistribution of the transcription factor.

The C-terminal *trans*-activation domain of Foxo1 contains a leucine-rich NES (39, 47, 57).² Previous studies had shown that leptomycin B, which inhibits binding of the nuclear export transporter Crm1 to the NES (43–46), blocks the export of FOXO proteins from the nucleus (39–41). The effect of leptomycin B on the ability of insulin to inhibit FOXO-stimulated transcription was examined in only one of these studies, however, and the results were inconclusive. Leptomycin B decreased insulin inhibition of FOXO4-stimulated transcription in A14 mouse fibroblasts by only 60%, suggesting that both export-dependent and export-independent mechanisms contributed to inhibition (40).

Because of these uncertainties, we decided to evaluate whether insulin could inhibit IGF1 transcription in H4IIE cells when Crm1-mediated nuclear export of Foxo1 was blocked by mutating Leu³⁷⁵ to alanine in the NES (Fig. 5). Biggs *et al.* (39) had shown that the Leu³⁷⁵Ala mutation abolished nuclear export of an N-terminal Foxo1 fragment (1–380) in CV1 cells. This truncated construct lacks the C-terminal *trans*-activation domain (20, 58, 59), however, so

² FOXO4 contains a single NES (300-LELLDGLNL-308) (40) in a similar location to the Foxo1 NES (368-MENLLDNLNL-377) (39), whereas FOXO3a has two adjacent NES in this location (369-LTDMAGTMNL-378 and 386-LMDDLLDNITL-396 (41). Mutation of both NES sites abolished the export of FOXO3a from the nucleus, but the individual contributions of the two sites was not examined (41). Zhao *et al.* (Program of the 85th Annual Meeting of The Endocrine Society, Philadelphia, PA, June 19–22, Abstract P1-369) identified additional Crm1-independent and Crm1-dependent NES sites in N-terminal fragments of FOXO1 coupled to GFP, but the importance of these sites for export of full-length FOXO1 is unknown.

that its effect on transcription could not be studied. We introduced the Leu³⁷⁵Ala mutation into full-length Foxo1. In contrast to the dramatic redistribution of wild-type Foxo1 to the cytoplasm after incubation with insulin, L375A-Foxo1 remained predominantly in the nucleus of transfected H4IIE cells. This result was quantified by determining the relative intensities of wild-type and mutant Foxo1 in the nucleus and cytoplasm of digital images of representative cells and cell sections. As the nuclear and cytoplasmic volumes of H4IIE cells are comparable, the ratio of nuclear/cytoplasmic fluorescence intensities reflects the relative abundance of Foxo1 in the nucleus. Although the decrease in wild-type Foxo1 in the nucleus after insulin treatment would be sufficient to account for the approximately 65% decrease in Foxo1-stimulated transcription, the minimal decrease in nuclear L375A-Foxo1 after incubation with insulin is too low to account for the decreased transcription.

The ability of insulin to inhibit transcription stimulated by L375A-Foxo1 was examined in reporter constructs in which luciferase was fused to two different insulin-sensitive promoters: a 925-nucleotide rat IGFBP-1 promoter (7) and a minimal promoter containing three copies of the IRE. L375A-Foxo1 stimulated transcription from both promoters in the absence of insulin. With both reporters, insulin inhibited transcription stimulated by wild-type Foxo1 and L375A-Foxo1 to the same extent. These results directly demonstrate that insulin is able to inhibit Foxo1-stimulated transcription when nuclear export of the transcription factor is prevented and indicate that insulin can inhibit transcription by other mechanisms in addition to inducing the subcellular redistribution of Foxo1. We propose that direct regulation of transcription also might contribute to the regulation of FOXO-induced transcription by other growth factors [IGF-I (24), epidermal growth factor (36), nerve growth factor (60), and platelet-derived growth factor (61)] and cytokines [TGF β (62), erythropoietin (37, 63, 64), thrombopoietin (65), IL-3 (38), and IL-2 (66)] that have been reported to activate PKB/Akt and phosphorylate FOXO proteins. Insulin inhibition of L375A-Foxo1-stimulated transcription was abolished when PI 3-kinase was inhibited, indicating that direct transcription regulation as well as nuclear export are dependent on PI 3-kinase. Insulin-induced phosphorylation of the PKB/Akt phosphorylation sites, Thr²⁴ and Ser²⁵³, in L375A-Foxo1 (results not shown) is consistent with the possibility that PKB/Akt mediates PI 3-kinase-dependent regulation of Foxo1-stimulated transcription.

Parallel studies also were performed with a second mutant, Thr²⁴Ala-Foxo1, which had been shown in several studies to be localized to the nucleus (34, 35, 39), but the results were inconclusive. Although T24A-Foxo1 localized predominantly to the nucleus in most H4IIE cells after insulin treatment, nuclear retention was less complete than with L375A-Foxo1 in individual sectioned cells (results not shown). Scheimann *et al.* (67) also observed intermediate levels of nuclear retention in HepG2 cells, but the Thr²⁴Ala mutation did not affect the export of green fluorescent protein (GFP)-FOXO1 to the cytoplasm in HEK293 cells (55). Insulin inhibited IGFBP-1 promoter activity stimulated by wild-type and T24A-Foxo1 to the same extent, but insulin inhibition of IRE-3x-promoter activity stimulated by T24A-Foxo1 was de-

creased by 50% (results not shown). Scheimann *et al.* (67) saw a similar intermediate reduction of insulin inhibition of T24A-FOXO1-stimulated transcription in HepG2 cells, but Guo *et al.* (32) observed no decrease in insulin inhibition. Thus, our findings with T24A-Foxo1 are consistent with those obtained with L375A-Foxo1, but are more difficult to interpret in light of the partial inhibition of redistribution observed with the Thr²⁴Ala mutation.

During the preparation of our manuscript, Zhang *et al.* (42) reported results consistent with our conclusion that inhibition of FOXO-stimulated transcription by insulin does not depend solely on nuclear exclusion. They mutated Ser²⁵⁶, the PKB/Akt site at the C-terminal end of the Fox box in FOXO1, to aspartate. Both FOXO1 T24A/S319A and FOXO1 T24A/S256D/S319A localized to the nucleus of HEK-293 cells in serum-free medium, whereas wild-type FOXO1-GFP was predominantly cytoplasmic. Basal transcription in the absence of insulin was increased by FOXO1 T24A/S319A, but not by FOXO1 T24A/S256D/S319A, suggesting that introduction of the S256D mutation into FOXO1 T24A/S319A to mimic insulin-induced phosphorylation of the PKB/Akt site decreased basal FOXO1-stimulated transcription without affecting nuclear export.

The mechanism by which insulin inhibits FOXO-stimulated transcription in the absence of nuclear export could involve inhibition of DNA binding to the promoter or regulation of *trans*-activation. Two studies have reported inhibition of FOXO binding to the IRE under conditions mimicking insulin stimulation in *in vitro* gel shift assays. Cahill *et al.* (68) showed that dimers of the phosphoserine-phosphothreonine-specific binding protein 14-3-3 (69, 70) bound to Daf16 when the PKB/Akt sites equivalent to T24 and S316 of Foxo1 were phosphorylated and prevented the transcription factor from binding to the IRE. Zhang *et al.* (42) reported that substituting aspartate for Ser²⁵⁶ at the C-terminal end of the Fox box decreased binding of FOXO1 to the IRE by 50%. Insulin-stimulated phosphorylation of Thr²⁴ and Ser²⁵³ in L375A-Foxo1 could decrease binding to the IRE by either of these mechanisms.

Insulin also can regulate Foxo1-stimulated *trans*-activation (33). This was demonstrated in constructs in which the C-terminal *trans*-activation domain of Foxo1 was fused to a heterologous Gal4 DNA-binding domain (71). Insulin inhibited Gal4 promoter activity stimulated by the fusion protein without significantly affecting the nucleocytoplasmic distribution of the fusion constructs (71). IRE-dependent FOXO-stimulated transcription also may be regulated by coactivators that bind to FOXO proteins: CBP/p300 (52), estrogen receptor α (59, 72), androgen receptor (72), Hoxa5 (73), and Hoxa10 (74). Whether any of these coactivator interactions are involved in the inhibition of FOXO-stimulated transcription by insulin is presently unknown.

Multiple mechanisms of regulating transcription such as we have observed for Foxo1 have been described for the yeast transcription factor, Pho4. Phosphorylation of multiple sites that determine nuclear export, nuclear import, and transcription activity contributes to the regulation of Pho4-stimulated transcription and allows adaptation to low and high phosphate environments (75, 76). Under low phosphate conditions, unphosphorylated Pho4 is imported into the nu-

cleus, and its export from the nucleus is inhibited. Nuclear Pho4 binds to Pho2 and stimulates the transcription of genes that help overcome phosphate deprivation. Under high phosphate conditions, Pho4 becomes phosphorylated at two sites that promote nuclear export and a third site that prevents nuclear import. Although Pho4 was retained in the nucleus after mutation of these three sites, mutation of a fourth phosphorylation site was required before Pho4 could form complexes with Pho2 to activate transcription. Given the number of vital cell functions in which genes whose transcription is regulated by FOXO proteins are involved (reviewed in Ref. 27), the ability to directly regulate transcription as well as the nuclear abundance of FOXO proteins makes it possible to achieve tighter control of FOXO-regulated gene expression.

Acknowledgments

We thank Derek LeRoith and Peter Nissley for critical reading of the manuscript.

Received April 16, 2003. Accepted September 5, 2003.

Address all correspondence and requests for reprints to: Dr. M. M. Rechler, Building 10, Room 8D12, 9000 Rockville Pike, Bethesda, Maryland 20892-1758. E-mail: mrechler@helix.nih.gov.

This work was presented in part at the 84th Annual Meeting of The Endocrine Society, San Francisco, CA, June 19–23, 2002.

References

- O'Brien RM, Granner DK 1996 Regulation of gene expression by insulin. *Physiol Rev* 76:1109–1161
- Cherrington AD 1999 Banting Lecture 1997. Control of glucose uptake and release by the liver in vivo. *Diabetes* 48:1198–1214
- Saltiel AR 2001 New perspectives into the molecular pathogenesis and treatment of type 2 diabetes. *Cell* 104:517–529
- O'Brien RM, Lucas PC, Forest CD, Magnuson MA, Granner DK 1990 Identification of a sequence in the PEPCK gene that mediates a negative effect of insulin on transcription. *Science* 249:533–537
- Streeter RS, Svitek CA, Chapman S, Greenbaum LE, Taub R, O'Brien RM 1997 A multicomponent insulin response sequence mediates a strong repression of mouse glucose-6-phosphatase gene transcription by insulin. *J Biol Chem* 272:11698–11701
- Suwanichkul A, Allander SV, Morris SL, Powell DR 1994 Glucocorticoids and insulin regulate expression of the human gene for insulin-like growth factor-binding protein-1 through proximal promoter elements. *J Biol Chem* 269:30835–30841
- Suh DS, Ooi GT, Rechler MM 1994 Identification of cis-elements mediating the stimulation of rat insulin-like growth factor-binding protein-1 promoter activity by dexamethasone, cyclic adenosine 3',5'-monophosphate, and phorbol esters, and inhibition by insulin. *Mol Endocrinol* 8:794–805
- Goswami R, Lacson R, Yang E, Sam R, Unterman T 1994 Functional analysis of glucocorticoid and insulin response sequences in the rat insulin-like growth factor-binding protein-1 promoter. *Endocrinology* 134:736–743
- Ooi GT, Tseng LY, Tran MQ, Rechler MM 1992 Insulin rapidly decreases insulin-like growth factor-binding protein-1 gene transcription in streptozotocin-diabetic rats. *Mol Endocrinol* 6:2219–2228
- Nakae J, Biggs III WH, Kitamura T, Cavenne WK, Wright CV, Arden KC, Accili D 2002 Regulation of insulin action and pancreatic β -cell function by mutated alleles of the gene encoding forkhead transcription factor Foxo1. *Nat Genet* 32:245–253
- Band CJ, Posner BI 1997 Phosphatidylinositol 3'-kinase and p70s6k are required for insulin but not bisphenoxovanadium 1,10-phenanthroline (bpV-phen)) inhibition of insulin-like growth factor binding protein gene expression. Evidence for MEK-independent activation of mitogen-activated protein kinase by bpV(phen). *J Biol Chem* 272:138–145
- Cichy SB, Uddin S, Danilkovich A, Guo S, Klippel A, Unterman TG 1998 Protein kinase B/Akt mediates effects of insulin on hepatic insulin-like growth factor-binding protein-1 gene expression through a conserved insulin response sequence. *J Biol Chem* 273:6482–6487
- Ogg S, Paradis S, Gottlieb S, Patterson GI, Lee L, Tissenbaum HA, Ruvkun G 1997 The Fork head transcription factor DAF-16 transduces insulin-like metabolic and longevity signals in *C. elegans*. *Nature* 389:994–999
- Lin K, Dorman JB, Rodan A, Kenyon C 1997 daf-16: An HNF-3/forkhead family member that can function to double the life-span of *Caenorhabditis elegans*. *Science* 278:1319–1322
- Kaestner KH, Knochel W, Martinez DE 2000 Unified nomenclature for the winged helix/forkhead transcription factors. *Genes Dev* 14:142–146
- Galili N, Davis RJ, Fredericks WJ, Mukhopadhyay S, Rauscher III FJ, Emanuel BS, Rovera G, Barr FG 1993 Fusion of a fork head domain gene to PAX3 in the solid tumour alveolar rhabdomyosarcoma [published erratum appears in *Nat Genet* 1994 Feb;6(2):214]. *Nat Genet* 5:230–235
- Borkhardt A, Repp R, Haas OA, Leis T, Harbott J, Kreuder J, Hammermann J, Henn T, Lampert F 1997 Cloning and characterization of AFX, the gene that fuses to MLL in acute leukemias with a t(X;11)(q13;q23). *Oncogene* 14:195–202
- Anderson MJ, Viars CS, Czekay S, Cavenne WK, Arden KC 1998 Cloning and characterization of three human forkhead genes that comprise an FKHR-like gene subfamily. *Genomics* 47:187–199
- Biggs III WH, Cavenne WK, Arden KC 2001 Identification and characterization of members of the FKHR (FOX O) subclass of winged-helix transcription factors in the mouse. *Mamm Genome* 12:416–425
- Bennicelli JL, Fredericks WJ, Wilson RB, Rauscher III FJ, Barr FG 1995 Wild type PAX3 protein and the PAX3-FKHR fusion protein of alveolar rhabdomyosarcoma contain potent, structurally distinct transcriptional activation domains. *Oncogene* 11:119–130
- Durham SK, Suwanichkul A, Scheimann AO, Yee D, Jackson JG, Barr FG, Powell DR 1999 FKHR binds the insulin response element in the insulin-like growth factor binding protein-1 promoter. *Endocrinology* 140:3140–3146
- Tang ED, Nunez G, Barr FG, Guan KL 1999 Negative regulation of the forkhead transcription factor FKHR by Akt. *J Biol Chem* 274:16741–16746
- Furuyama T, Nakazawa T, Nakano I, Mori N 2000 Identification of the differential distribution patterns of mRNAs and consensus binding sequences for mouse DAF-16 homologues. *Biochem J* 349:629–634
- Brunet A, Bonni A, Zigmond MJ, Lin MZ, Juo P, Hu LS, Anderson MJ, Arden KC, Blenis J, Greenberg ME 1999 Akt promotes cell survival by phosphorylating and inhibiting a Forkhead transcription factor. *Cell* 96:857–868
- Medema RH, Kops GJ, Bos JL, Burgering BM 2000 AFX-like Forkhead transcription factors mediate cell-cycle regulation by Ras and PKB through p27kip1. *Nature* 404:782–787
- Tran H, Brunet A, Grenier JM, Datta SR, Fornace Jr AJ, DiStefano PS, Chiang LW, Greenberg ME 2002 DNA repair pathway stimulated by the forkhead transcription factor FOXO3a through the Gadd45 protein. *Science* 296:530–534
- Birkenkamp KU, Coffey PJ 2003 Regulation of cell survival and proliferation by the FOXO (Forkhead box, class O) subfamily of Forkhead transcription factors. *Biochem Soc Trans* 31:292–297
- Paradis S, Ruvkun G 1998 *Caenorhabditis elegans* Akt/PKB transduces insulin receptor-like signals from AGE-1 PI3 kinase to the DAF-16 transcription factor. *Genes Dev* 12:2488–2498
- Nakae J, Park BC, Accili D 1999 Insulin stimulates phosphorylation of the forkhead transcription factor FKHR on serine 253 through a wortmannin-sensitive pathway. *J Biol Chem* 274:15982–15985
- Rena G, Guo S, Cichy SC, Unterman TG, Cohen P 1999 Phosphorylation of the transcription factor forkhead family member FKHR by protein kinase B. *J Biol Chem* 274:17179–17183
- Kops GJ, de Ruiter ND, De Vries-Smits AM, Powell DR, Bos JL, Burgering BM 1999 Direct control of the Forkhead transcription factor AFX by protein kinase B. *Nature* 398:630–634
- Guo S, Rena G, Cichy S, He X, Cohen P, Unterman T 1999 Phosphorylation of serine 256 by protein kinase B disrupts transactivation by FKHR and mediates effects of insulin on insulin-like growth factor-binding protein-1 promoter activity through a conserved insulin response sequence. *J Biol Chem* 274:17184–17192
- Tomizawa M, Kumar A, Perrot V, Nakae J, Accili D, Rechler MM 2000 Insulin inhibits the activation of transcription by a C-terminal fragment of the forkhead transcription factor FKHR. A mechanism for insulin inhibition of insulin-like growth factor-binding protein-1 transcription. *J Biol Chem* 275:7289–7295
- Takaishi H, Konishi H, Matsuzaki H, Ono Y, Shirai Y, Saito N, Kitamura T, Ogawa W, Kasuga M, Kikkawa U, Nishizuka Y 1999 Regulation of nuclear translocation of forkhead transcription factor AFX by protein kinase B. *Proc Natl Acad Sci USA* 96:11836–11841
- Nakae J, Barr V, Accili D 2000 Differential regulation of gene expression by insulin and IGF-1 receptors correlates with phosphorylation of a single amino acid residue in the forkhead transcription factor FKHR. *EMBO J* 19:989–996
- Jackson JG, Kreisberg JJ, Koterba AP, Yee D, Brattain MG 2000 Phosphorylation and nuclear exclusion of the forkhead transcription factor FKHR after epidermal growth factor treatment in human breast cancer cells. *Oncogene* 19:4574–4581
- Uddin S, Kottagoda S, Stigger D, Plataniotis LC, Wickrema A 2000 Activation of the Akt/FKHL1 pathway mediates the antiapoptotic effects of erythropoietin in primary human erythroid progenitors. *Biochem Biophys Res Commun* 275:16–19
- Dijkers PF, Medema RH, Pals C, Banerji L, Thomas NS, Lam EW, Burgering BM, Raaijmakers JA, Lammers JW, Koenderman L, Coffey PJ 2000 Forkhead transcription factor FKHR-L1 modulates cytokine-dependent transcriptional regulation of p27(KIP1). *Mol Cell Biol* 20:9138–9148
- Biggs III WH, Meisenhelder J, Hunter T, Cavenne WK, Arden KC 1999

- Protein kinase B/Akt-mediated phosphorylation promotes nuclear exclusion of the winged helix transcription factor FKHR1. *Proc Natl Acad Sci USA* 96:7421–7426
40. Brownawell AM, Kops GJ, Macara IG, Burgering BM 2001 Inhibition of nuclear import by protein kinase B (Akt) regulates the subcellular distribution and activity of the forkhead transcription factor AFX. *Mol Cell Biol* 21:3534–3546
 41. Brunet A, Kanai F, Stehn J, Xu J, Sarbassova D, Frangioni JV, Dalal SN, DeCaprio JA, Greenberg ME, Yaffe MB 2002 14-3-3 Transits to the nucleus and participates in dynamic nucleocytoplasmic transport. *J Cell Biol* 156:817–828
 42. Zhang X, Gan L, Pan H, Guo S, He X, Olson ST, Mesecar A, Adam S, Unterman TG 2002 Phosphorylation of serine 256 suppresses transactivation by FKHR (FOXO1) by multiple mechanisms. Direct and indirect effects on nuclear/cytoplasmic shuttling and DNA binding. *J Biol Chem* 277:45276–45284
 43. Fornerod M, Ohno M, Yoshida M, Mattaj JW 1997 CRM1 is an export receptor for leucine-rich nuclear export signals. *Cell* 90:1051–1060
 44. Fukuda M, Asano S, Nakamura T, Adachi M, Yoshida M, Yanagida M, Nishida E 1997 CRM1 is responsible for intracellular transport mediated by the nuclear export signal. *Nature* 390:308–311
 45. Kudo N, Wolff B, Sekimoto T, Schreiner EP, Yoneda Y, Yanagida M, Horinouchi S, Yoshida M 1998 Leptomycin B inhibition of signal-mediated nuclear export by direct binding to CRM1. *Exp Cell Res* 242:540–547
 46. Sekimoto T, Yoneda Y 1998 Nuclear import and export of proteins: the molecular basis for intracellular signaling. *Cytokine Growth Factor Rev* 9:205–211
 47. Kim FJ, Beeche AA, Hunter JJ, Chin DJ, Hope TJ 1996 Characterization of the nuclear export signal of human T-cell lymphotropic virus type 1 Rex reveals that nuclear export is mediated by position-variable hydrophobic interactions. *Mol Cell Biol* 16:5147–5155
 48. Ooi GT, Brown DR, Suh DS, Tseng LY, Rechler MM 1993 Cycloheximide stabilizes insulin-like growth factor-binding protein-1 (IGFBP-1) mRNA and inhibits IGFBP-1 transcription in H4-II-E rat hepatoma cells. *J Biol Chem* 268:16664–16672
 49. O'Brien RM, Noisin EL, Suwanichkul A, Suwanichkul A, Yamasaki T, Lucas PC, Wang JC, Powell DR, Granner DK 1995 Hepatic nuclear factor 3- and hormone-regulated expression of the phosphoenolpyruvate carboxykinase and insulin-like growth factor-binding protein 1 genes. *Mol Cell Biol* 15:1747–1758
 50. Allander SV, Durham SK, Scheimann AO, Wasserman RM, Suwanichkul A, Powell DR 1997 Hepatic nuclear factor 3 and high mobility group I/Y proteins bind the insulin response element of the insulin-like growth factor-binding protein-1 promoter. *Endocrinology* 138:4291–4300
 51. Suh DS, Zhou Y, Ooi GT, Rechler MM 1996 Dexamethasone stimulation of rat insulin-like growth factor binding protein-1 promoter activity involves multiple cis-elements. *Mol Endocrinol* 10:1227–1237
 52. Nasrin N, Ogg S, Cahill CM, Biggs W, Nui S, Dore J, Calvo D, Shi Y, Ruvkun G, Alexander-Bridges MC 2000 DAF-16 recruits the CREB-binding protein coactivator complex to the insulin-like growth factor binding protein 1 promoter in HepG2 cells. *Proc Natl Acad Sci USA* 97:10412–10417
 53. Hall RK, Yamasaki T, Kucera T, Waltner-Law M, O'Brien R, Granner DK 2000 Regulation of phosphoenolpyruvate carboxykinase and insulin-like growth factor-binding protein-1 gene expression by insulin. The role of winged helix/forkhead proteins. *J Biol Chem* 275:30169–30175
 54. Yeagley D, Guo S, Unterman T, Quinn PG 2001 Gene- and activation-specific mechanisms for insulin inhibition of basal and glucocorticoid-induced insulin-like growth factor binding protein-1 and phosphoenolpyruvate carboxykinase transcription. Roles of forkhead and insulin response sequences. *J Biol Chem* 276:33705–33710
 55. Rena G, Prescott AR, Guo S, Cohen P, Unterman TG 2001 Roles of the forkhead in rhabdomyosarcoma (FKHR) phosphorylation sites in regulating 14-3-3 binding, transactivation and nuclear targeting. *Biochem J* 354:605–612
 56. Schmolli D, Walker KS, Alessi DR, Grempler R, Burchell A, Guo S, Walther R, Unterman TG 2000 Regulation of glucose-6-phosphatase gene expression by protein kinase B α and the forkhead transcription factor FKHR. Evidence for insulin response unit-dependent and -independent effects of insulin on promoter activity. *J Biol Chem* 275:36324–36333
 57. Arden KC, Biggs III WH 2002 Regulation of the FoxO family of transcription factors by phosphatidylinositol-3 kinase-activated signaling. *Arch Biochem Biophys* 403:292–298
 58. Sublett JE, Jeon IS, Shapiro DN 1995 The alveolar rhabdomyosarcoma PAX3/FKHR fusion protein is a transcriptional activator. *Oncogene* 11:545–552
 59. Schuur ER, Loktev AV, Sharma M, Sun Z, Roth RA, Weigel RJ 2001 Ligand-dependent interaction of estrogen receptor- α with members of the forkhead transcription factor family. *J Biol Chem* 276:33554–33560
 60. Zheng WH, Kar S, Quirion R 2002 FKHL1 and its homologs are new targets of nerve growth factor Trk receptor signaling. *J Neurochem* 80:1049–1061
 61. Yellaturu CR, Bhanoori M, Neeli I, Rao GN 2002 N-Ethylmaleimide inhibits platelet-derived growth factor BB-stimulated Akt phosphorylation via activation of protein phosphatase 2A. *J Biol Chem* 277:40148–40155
 62. Shin I, Bakin AV, Rodeck U, Brunet A, Arteaga CL 2001 Transforming growth factor β enhances epithelial cell survival via Akt-dependent regulation of FKHL1. *Mol Biol Cell* 12:3328–3339
 63. Kashii Y, Uchida M, Kirito K, Tanaka M, Nishijima K, Toshima M, Ando T, Koizumi K, Endoh T, Sawada K, Momoi M, Miura Y, Ozawa K, Komatsu N 2000 A member of Forkhead family transcription factor, FKHL1, is one of the downstream molecules of phosphatidylinositol 3-kinase-Akt activation pathway in erythropoietin signal transduction. *Blood* 96:941–949
 64. Mahmud DL, M GA, Deb DK, Platanias LC, Uddin S, Wickrema A 2002 Phosphorylation of forkhead transcription factors by erythropoietin and stem cell factor prevents acetylation and their interaction with coactivator p300 in erythroid progenitor cells. *Oncogene* 21:1556–1562
 65. Tanaka M, Kirito K, Kashii Y, Uchida M, Watanabe T, Endo H, Endoh T, Sawada K, Ozawa K, Komatsu N 2001 Forkhead family transcription factor FKHL1 is expressed in human megakaryocytes. Regulation of cell cycling as a downstream molecule of thrombopoietin signaling. *J Biol Chem* 276:15082–15089
 66. Stahl M, Dijkers PF, Kops GJ, Lens SM, Coffey PJ, Burgering BM, Medema RH 2002 The forkhead transcription factor FoxO regulates transcription of p27(Kip1) and Bim in response to IL-2. *J Immunol* 168:5024–5031
 67. Scheimann AO, Durham SK, Suwanichkul A, Snuggs MB, Powell DR 2001 Role of three FKHR phosphorylation sites in insulin inhibition of FKHR action in hepatocytes. *Horm Metab Res* 33:631–638
 68. Cahill CM, Tzivion G, Nasrin N, Ogg S, Dore J, Ruvkun G, Alexander-Bridges M 2001 Phosphatidylinositol 3-kinase signaling inhibits DAF-16 DNA binding and function via 14-3-3-dependent and 14-3-3-independent pathways. *J Biol Chem* 276:13402–13410
 69. Tzivion G, Avruch J 2002 14-3-3 Proteins: active cofactors in cellular regulation by serine/threonine phosphorylation. *J Biol Chem* 277:3061–3064
 70. Yaffe MB 2002 How do 14-3-3 proteins work? Gatekeeper phosphorylation and the molecular anvil hypothesis. *FEBS Lett* 513:53–57
 71. Perrot V, Rechler MM 2003 Characterization of insulin inhibition of transactivation by a C-terminal fragment of the forkhead transcription factor Foxo1 in rat hepatoma cells. *J Biol Chem* 278:26111–26119
 72. Li P, Lee H, Guo S, Unterman TG, Jenster G, Bai W 2003 AKT-independent protection of prostate cancer cells from apoptosis mediated through complex formation between the androgen receptor and FKHR. *Mol Cell Biol* 23:104–118
 73. Foucher I, Volovitch M, Frain M, Kim JJ, Souberbielle JC, Gan L, Unterman TG, Prochiantz A, Trembleau A 2002 Hoxa5 overexpression correlates with IGFBP1 upregulation and postnatal dwarfism: evidence for an interaction between Hoxa5 and forkhead box transcription factors. *Development* 129:4065–4074
 74. Kim JJ, Taylor HS, Akbas GE, Foucher I, Trembleau A, Jaffe RC, Fazleabas AT, Unterman TG 2003 Regulation of insulin-like growth factor binding protein-1 promoter activity by FKHR and HOXA10 in primate endometrial cells. *Biol Reprod* 68:24–30
 75. Komeili A, O'Shea EK 1999 Roles of phosphorylation sites in regulating activity of the transcription factor Pho4. *Science* 284:977–980
 76. Komeili A, O'Shea EK 2000 Nuclear transport and transcription. *Curr Opin Cell Biol* 12:355–360

Phosphatidylinositol 3-Kinase Signaling Inhibits DAF-16 DNA Binding and Function via 14-3-3-dependent and 14-3-3-independent Pathways*

Received for publication, November 3, 2000, and in revised form, December 19, 2000
Published, JBC Papers in Press, December 20, 2000, DOI 10.1074/jbc.M010042200

Catherine M. Cahill^{‡§}, Guri Tzivion^{§¶}, Nargis Nasrin[‡], Scott Ogg[¶], Justin Dore[‡], Gary Ruvkun[¶], and Maria Alexander-Bridges^{‡**}

From the [‡]Diabetes Unit, Massachusetts General Hospital and Department of Medicine, Harvard Medical School, the [¶]Diabetes Research Laboratory, Department of Molecular Biology, Massachusetts General Hospital and Department of Medicine, Harvard Medical School, and the [§]Department of Molecular Biology, Massachusetts General Hospital and Department of Genetics, Harvard Medical School, Boston, Massachusetts 02114

In *Caenorhabditis elegans*, an insulin-like signaling pathway to phosphatidylinositol 3-kinase (PI 3-kinase) and AKT negatively regulates the activity of DAF-16, a Forkhead transcription factor. We show that in mammalian cells, *C. elegans* DAF-16 is a direct target of AKT and that AKT phosphorylation generates 14-3-3 binding sites and regulates the nuclear/cytoplasmic distribution of DAF-16 as previously shown for its mammalian homologs FKHR and FKHRL1. *In vitro*, interaction of AKT-phosphorylated DAF-16 with 14-3-3 prevents DAF-16 binding to its target site in the insulin-like growth factor binding protein-1 gene, the insulin response element. In HepG2 cells, insulin signaling to PI 3-kinase/AKT inhibits the ability of a GAL4 DNA binding domain/DAF-16 fusion protein to activate transcription via the insulin-like growth factor binding protein-1-insulin response element, but not the GAL4 DNA binding site, which suggests that insulin inhibits the interaction of DAF-16 with its cognate DNA site. Elimination of the DAF-16/1433 association by mutation of the AKT/14-3-3 sites in DAF-16, prevents 14-3-3 inhibition of DAF-16 DNA binding and insulin inhibition of DAF-16 function. Similarly, inhibition of the DAF-16/14-3-3 association by exposure of cells to the PI 3-kinase inhibitor LY294002, enhances DAF-16 DNA binding and transcription activity. Surprisingly constitutively nuclear DAF-16 mutants that lack AKT/14-3-3 binding sites also show enhanced DNA binding and transcription activity in response to LY294002, pointing to a 14-3-3-independent mode of regulation. Thus, our results demonstrate at least two mechanisms, one 14-3-3-dependent and the other 14-3-3-independent, whereby PI 3-kinase signaling regulates DAF-16 DNA binding and transcription function.

In *Caenorhabditis elegans*, genetic evidence indicates that an

* This work was supported by National Institutes of Health NCI Grant CA73818-1, by National Institutes of Health Grant DK57200A01, by institutional support from Massachusetts General Hospital, and by National Institutes of Health Training Grant T32 DK07028-24 (to N. N.) and Grants AG05790 (to N. N.) and AG14161 and GM58012 (to S. O. and G. R.). The costs of publication of this article were defrayed in part by the payment of page charges. This article must therefore be hereby marked "advertisement" in accordance with 18 U.S.C. Section 1734 solely to indicate this fact.

§ These authors contributed equally to this work.

** To whom correspondence should be addressed: 306 Wellman, Diabetes Unit, Dept. of Medicine, Massachusetts General Hospital, 50 Blossom St., Boston, MA 02114. Tel.: 617-726-6998; Fax: 617-726-6954; E-mail: alex-bri@helix.mgh.harvard.edu.

insulin-like signaling pathway, which includes an insulin/IGF-1-like receptor (DAF-2), phosphatidylinositol 3-kinase (PI 3-kinase; AGE-1), and protein kinase B (also known as AKT) controls life cycle, metabolism, and longevity (1–5). This pathway negatively regulates the activity of DAF-16, a member of the Forkhead (FKH) family of transcription factors (3, 6–8).

In mammalian cells, insulin/IGF-1 signaling via PI 3-kinase and AKT mediates diverse effects on cell metabolism, growth, and survival (9–11). Biochemical studies to date suggest that PI 3-kinase is important to the metabolic actions of insulin including its effects on gene transcription. A common DNA sequence, referred to as the insulin response element (IRE), binds members of the Forkhead transcription factor family and mediates the negative effect of insulin on transcription of the insulin-like growth factor binding protein-1 (IGFBP-1) and phosphoenolpyruvate carboxykinase (PEPCK) genes (12). In hepatoma cells, insulin inhibition of IRE-directed gene transcription is mediated via a PI 3-kinase-dependent signaling pathway (13). Accordingly, work in several laboratories aimed at identifying the downstream targets of insulin signaling to the nucleus has focused on the role of mammalian homologues of DAF-16, FKHR, FKHRL1, and AFX in mediating the negative effect of insulin/IGF-1 signaling on gene transcription. In the absence of insulin/IGF-1, FKHRL1 (14), AFX (15), and FKHR (16–18) activate gene transcription via the IGFBP-IRE. Insulin/IGF-1 signaling (19–21) or overexpression of AKT (17, 19) stimulates phosphorylation of these factors and inhibits their activating effect (16, 17).

The prevailing view of the mechanism underlying insulin/IGF-1 inhibition of FKHRL1 and other DAF-16 homologs is that phosphorylation of FKHRL1 by AKT at two sites, Thr-32 and Ser-253 promotes retention of these proteins in the cytoplasm (14). AKT preferentially phosphorylates substrates that carry the RXRXXS, which is contained within certain consensus 14-3-3 binding motifs RSXS^PXP, or RXXXS^PXP where S^P represents phosphoserine (22). Hence, AKT phosphorylation of its target proteins may create 14-3-3 binding sites. For example, the AKT site at T32 in FKHRL1 is a 14-3-3 consensus binding sequence; AKT phosphorylation of FKHRL1 at sites Thr-32 and Ser-253 promotes interaction of FKHRL1 with 14-3-3 and cytoplasmic retention of FKHRL1 (14). The 14-3-3

¹ The abbreviations used are: IGF, insulin-like growth factor; FKH, forkhead; PKB, protein kinase B; PI 3-kinase, phosphatidylinositol 3 kinase; IGFBP-1, insulin-like growth factor binding protein-1; IRE, insulin response element; PEPCK, phosphoenolpyruvate carboxykinase; GST, glutathione S-transferase; PAGE, polyacrylamide gel electrophoresis; WT, wild-type.

family of proteins has also been shown to play a role in nuclear export and/or cytoplasmic retention of the yeast protein Cdc25 (23–25). In addition to promoting changes in cellular localization, binding of 14-3-3 to certain of its target proteins directly affects their activity. For example, 14-3-3 can stimulate the catalytic activity of the serine/threonine kinase c-Raf-1 (26, 27), the DNA binding activity of p53 (28), and other targets (29–31).

The Thr-32 and Ser-253 sites are conserved within DAF-16 (Thr-54 and Ser-240/Thr-242), FKHL1 (Thr-32, Ser-253) (14), FKHR (Thr-24, Ser-253) (32), and AFX (Thr-28, Ser-258) (15). Accordingly, regulation of nuclear export by growth factor signaling to PI 3-kinase and AKT has been demonstrated for FKHL1 (32), FKHR (33), and AFX (34). We questioned whether the Thr-54 site in DAF-16 would function as a 14-3-3 binding site and, if so, whether PI 3-kinase signaling would regulate the interaction of *C. elegans* DAF-16 with elements of the mammalian nuclear import/export machinery as is the case for the mammalian homologs of DAF-16.

We therefore examined the effect of AKT phosphorylation and 14-3-3 association on several aspects of DAF-16 function, including its ability to localize to the nucleus, bind DNA and activate transcription. We find evidence for PI 3-kinase-dependent inhibition of DAF-16 DNA binding activity via 14-3-3-dependent and 14-3-3-independent mechanisms. Thus, our observations suggest a more complex mode of DAF-16 regulation than previously anticipated.

EXPERIMENTAL PROCEDURES

Plasmids and Reagents—The DAF-16a1 *HindIII/NheI* insert from pGEM-FLAG-DAF-16a1 was ligated into the *HindIII/XbaI* site of pcDNA3 (+) (Invitrogen) to generate pcDNA3-Flag DAF-16a1. The DAF-16a1 *BstYI* insert from pGEM-FLAG-DAF-16a1 was ligated into the *BamHI* site of pGEX-4T-1 (Amersham Pharmacia Biotech) to generate pGEX-DAF-16a1. Phosphorylation site mutants were prepared using the QuickChange site-directed mutagenesis kit (Stratagene). The DAF-16a1 *BstYI* insert from pGEM-FLAG-DAF-16a1 was ligated into the *BamHI* site of the GAL4 DNA binding domain plasmid to generate GAL4-DAF-16 derivatives. The rat IGF-BP-1 promoter (nucleotides –921 to +79) cloned in PGL3-LUC was a gift from M. Rechler (National Institutes of Health, Bethesda, MD). Preparation of pMT2-Myc-14-3-3, pGEX-GST-14-3-3, and the pGEX-GST-14-3-3 dimerization mutant has been described previously (26, 27). The pEBG-GST-AKT plasmid was a gift from J. R. Woodgett (Toronto, Canada). Specific DAF-16 antibodies were produced in rabbits using the Forkhead DNA binding domain of DAF-16 cloned into GST as the antigen. The competitor 14-3-3 binding phosphopeptide LPKINRSA(Sp)EPLHR (PP, corresponding to c-Raf-1 amino acids 613–627) and the unphosphorylated version (P) were synthesized by QCB (Boston, MA). Anti-phosphopeptide specific antibodies against 14-3-3 binding consensus were a gift from M. Comb (New England Biolabs, Beverly, MA).

Kinase Assay—For experiments to phosphorylate DAF-16 *in vitro*, GST-DAF-16 proteins were purified from bacteria and GST-AKT was expressed in 293 cells and subsequently affinity-purified on GSH beads (Amersham Pharmacia Biotech). Kinase assays were performed using 2 μ g of GST-AKT as the kinase and 2 μ g of GST-DAF-16 or DAF-16 mutant as the substrate in a kinase buffer containing 40 mM Tris-HCl, pH 7.5, 0.1 mM EDTA, 5 mM MgCl₂, 2 mM dithiothreitol, and 100 μ M ATP (cold assay) supplemented with [γ -³²P]ATP (10–20 μ Ci/reaction) (hot assay) at 30 °C for 40 min.

Protein Interaction Assays—Myc epitope-tagged 14-3-3 expressed in 293 cells was absorbed to anti-Myc epitope antibodies (clone 9E10) pre-coupled to protein-A beads and incubated with 2 μ g of AKT-phosphorylated wild-type and mutant GST-DAF-16 for 90 min at 4 °C. Following extensive washes, the associated proteins were separated on SDS-PAGE and phosphorylated DAF-16 was detected by autoradiography. Both wild-type and mutant GST-DAF-16 variants were detected by anti-GST immunoblotting.

Electrophoretic Mobility Shift Assay—Samples containing 2 μ g of GST-DAF-16 or 5–10 μ g of nuclear extracts, treated as indicated in the figure legends were supplemented with 50,000 cpm of ³²P-labeled IGFBP-IRE probe (caaaacaaactattttgaa) or G-C/A-C mutant probe (caaaagaaactttcttgaa) for 15 min at 4 °C in a buffer containing 40 mM Tris-HCl, pH 7.5, 5 mM MgCl₂, 0.1 mM EDTA, 1 mM dithiothreitol, 50 mM

KCl, 10% glycerol, 0.1% bovine serum albumin, and 1 μ g of poly(dG/dC) in each sample. For competition assays, 10 \times cold IRE or mutant IRE was added prior to the addition of ³²P-labeled IRE probe. For supershift assays, the reaction was pre-incubated with 1 μ g of either specific DAF-16 antibody (for detection of GST fusion proteins) or M2 antibody (against the Flag tag for detection of DAF-16 expressed in mammalian cells) for 15 min at 4 °C prior to the addition of ³²P-labeled IRE probe. To demonstrate inhibition of DNA binding by 14-3-3, DAF-16 (2 μ g) was phosphorylated with GST-AKT (2 μ g) for 30 min at 30 °C, followed by addition of 14-3-3 (2 μ g). The reaction was further incubated at 4 °C for 15 min, at which time labeled ³²P-IRE probe was added. Samples were resolved on 4% Tris-glycine PAGE at 100 V for 3 h. Nuclear and cytoplasmic extracts were prepared using the NE-PER kit (Pierce) according to the manufacturer's instructions.

Transfections—For transcriptional analysis, HepG2 cells were transfected using the CaPO₄ method in 30-mm six-well plates with IGFBP-LUC (15 μ g) reporter plasmid and pcDNA3-DAF-16 variants (2 μ g) or pcDNA3 control vector (2 μ g) per 1.5 ml of precipitate. The RSV- β -galactosidase vector (2 μ g) was used to control for transfection efficiency. In the experiments described in Figs. 3 and 5, 2 μ g of GAL4 DNA binding domain control vector or GAL4-DAF-16 fusion protein vector variants cotransfected with either the IGFBP-luciferase reporter gene or a luciferase reporter gene driven by five GAL4 DNA binding sites cloned upstream of the TK109 promoter. Cells were shocked for 1 min with 10% Me₂SO and the incubation continued in the absence of serum. Insulin was added during the last 16 h of the incubation.

For the DAF-16/14-3-3 association experiments, 293 cells were transfected using LipofectAMINE (Life Technologies, Inc.) in 10-cm plates with 2 μ g each of GST-14-3-3 or GST-AKT and 4 μ g of pcDNA3-DAF-16 variants. For the DAF-16 localization and DNA binding experiments, 293 cells were transfected with 5 μ g of the pcDNA3-DAF-16 variants or pcDNA3 alone.

RESULTS

AKT Phosphorylates DAF-16 and Promotes Its Association with 14-3-3—Consistent with the genetic data that positions DAF-16 downstream of the PI 3-kinase-regulated serine/threonine kinase AKT in *C. elegans*, there are four consensus AKT phosphorylation sites in DAF-16 (Fig. 1A). As has been established for the mammalian DAF-16 orthologs FKHL1 (16, 19, 32), FKHL1 (14), and AFX (15, 34), AKT can phosphorylate DAF-16 on at least three of its four potential AKT sites, and these sites serve as the only AKT-phosphorylation sites *in vitro* (Fig. 1B, top). Phosphospecific antibodies generated against 14-3-3-binding consensus sequences can specifically recognize DAF-16 phosphorylated by AKT but not unphosphorylated DAF-16 (Fig. 1B, compare lane 2 to lane 1). This antibody recognizes phosphorylation of DAF-16 at threonine 54 (Fig. 1B, middle, lane 2 versus lane 3). Phosphorylation of recombinant prokaryotic GST-DAF-16 by AKT induces its binding to recombinant mammalian 14-3-3 *in vitro* (Fig. 1C). This association is inhibited by a competitor phosphopeptide corresponding to a 14-3-3 binding site on c-Raf-1 but not by the unphosphorylated form of the peptide (compare lane 2 with lanes 3 and 4). The association with 14-3-3 is also inhibited by mutation of the AKT-phosphorylation sites on DAF-16 (compare lane 2 with lanes 5, 7, and 8). In particular, the AKT-phosphorylation site at threonine 54, a site matching closest to the 14-3-3 binding consensus, represents a site whose phosphorylation is indispensable for 14-3-3 binding *in vitro* (compare lane 2 with lane 5).

14-3-3 Association with Wild-type DAF-16 Inhibits Its DNA Binding Activity—Homologues of DAF-16 bind and activate transcription through the IRE in the IGFBP gene (14, 16). Accordingly we also find that DAF-16 binds specifically to the IRE (Fig. 2A). A DAF-16 derivative L201P, with a leucine to proline substitution in the forkhead DNA binding domain, does not bind to the ³²P-labeled IRE, nor does an amino-terminal fragment (1–69) of DAF-16 that lacks the forkhead DNA binding domain (Fig. 2, compare lane 4 to lanes 6 and 7). A specific antibody raised against DAF-16 supershifts the DAF-16/DNA

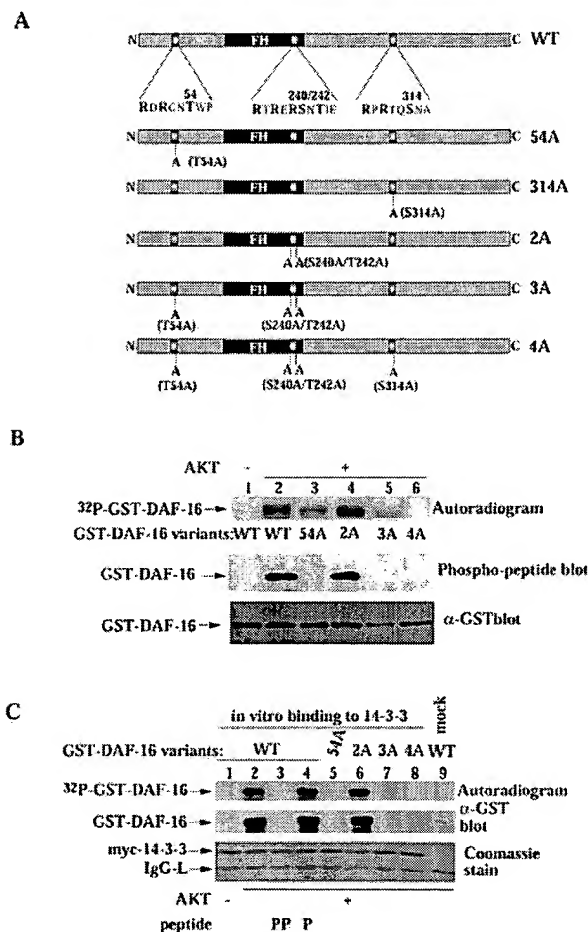


FIG. 1. AKT phosphorylates DAF-16 on four distinct sites and mediates 14-3-3 binding. **A**, linear map of DAF-16 protein showing the amino acid sequence of the putative AKT consensus (RXXRXXS) phosphorylation sites at Thr-54, Ser-240, Thr-242, and Ser-314. The indicated mutants were constructed for expression in both mammalian and bacterial cells: 1A (T54A); 2A (S240A and T242A); 3A (T54A, S240A, and T242A); 4A (all four sites mutated to alanine). **B**, phosphorylation of GST-DAF-16 *in vitro* by AKT. Recombinant prokaryotic GST-fused DAF-16 (lanes 1 and 2) and the indicated mutants (lanes 3–6), 2 μ g each, were incubated in a kinase buffer containing 2 μ g of active recombinant mammalian GST-AKT (lanes 2–6) or vehicle (lane 1) for 40 min at 30 °C. Following SDS-PAGE, the samples were blotted with phosphopeptide antibodies against degenerated 14-3-3 binding consensus (XXXXRXXS(p)XPXXXXX) (a gift from M. Comb). Autoradiogram showing GST-DAF-16 phosphorylation (top) and immunoblot showing reactivity with the phosphospecific antibodies (middle) and an anti-GST immunoblot showing equal protein loading (bottom) are presented. **C**, *in vitro* binding of AKT phosphorylated GST-DAF-16 to 14-3-3. Unphosphorylated GST-DAF-16 (lane 1), AKT-phosphorylated GST-DAF-16 (lanes 2–4 and 9), or the indicated GST-DAF-16 mutants (lanes 5–8) were incubated with immobilized Myc-tagged 14-3-3 (prepared using anti-Myc antibodies and protein A beads) from 293 cells (lanes 1–8) or control beads (lane 9) in the presence of competitor 14-3-3 binding phosphopeptide (PP, 1 mM, lane 3) or unphosphorylated control peptide (P, 1 mM, lane 4) for 2 h at 4 °C. Following washes to remove nonspecific binding, bound proteins retained on the immobilized Myc-tagged 14-3-3 beads were subjected to SDS-PAGE, transferred to a polyvinylidene difluoride membrane, and tested for phospho-GST-DAF-16 by autoradiography (top). Anti-GST immunoblot (middle) was used for the detection of both DAF-16 WT and AKT site mutant DAF-16 derivatives bound to the Myc-14-3-3 column. The DAF-16 mutants 3A and 4A are only partially phosphorylated or not at all and can not be detected by autoradiography. A Coomassie stain of the blot (bottom) is shown to demonstrate equal 14-3-3 input.

complex (Fig. 2A, lane 5). We examined whether AKT phosphorylation and/or subsequent association of DAF-16 with 14-3-3 could alter the ability of DAF-16 to bind its target IRE site.

Phosphorylation of DAF-16 by AKT did not by itself affect DAF-16-DNA binding (Fig. 2B, compare lanes 1 and 3); however, the addition of 14-3-3 to AKT-phosphorylated DAF-16 resulted in an almost complete inhibition of DAF-16 DNA binding activity (Fig. 2B, compare lanes 3 and 4). The addition of 14-3-3 had no effect on DAF-16 DNA binding when AKT was omitted (Fig. 2B, compare lanes 2 and 4), or when ATP was omitted (Fig. 2C, compare lanes 7 and 3) from the kinase reaction. Moreover, the competitor 14-3-3 binding phosphopeptide selectively blocked the ability of 14-3-3 to inhibit DAF-16 DNA binding while the unphosphorylated version had no effect (Fig. 2B, compare lanes 5 and 6) demonstrating the requirement of the 14-3-3-phosphopeptide binding domain for the inhibition. Thus, the ability of 14-3-3 to inhibit DAF-16 DNA binding required the association of 14-3-3 with phospho-DAF-16. The DNA binding activity of DAF-16 mutants impaired in their ability to bind 14-3-3, DAF-16 54A (T54A), and DAF-16 4A (T54A, S240A, T242A, S314A) was unaffected by AKT/14-3-3 (Fig. 2D, compare lanes 1 and 2 with lanes 4 and 5 and lanes 7 and 8). Conversely, the DNA binding activity of the DAF-16 2A (S240A/T242A) mutant that retains the ability to bind 14-3-3 was inhibited (Fig. 2D, lanes 13 and 14). Although the DAF-16 (S314A) mutant retains the ability to bind 14-3-3 following AKT phosphorylation (data not shown), 14-3-3 does not inhibit its ability to bind DNA (Fig. 2D, lanes 10 and 11). The inability of the dimerization-deficient 14-3-3 mutant to inhibit DAF-16 DNA binding (Fig. 2C, compare lane 3 with lane 6), together with the ability of wild-type 14-3-3 to inhibit mutant DAF-16 2A (S240A/T242A), but not mutant DAF-16 (T54A) or (S314A) DNA binding, suggests that dimeric 14-3-3 interacts with DAF-16 at sites Thr-54 and Ser-314. This interaction may, in turn, mask the forkhead DNA binding domain of DAF-16.

Insulin Inhibition of DAF-16 Activity Is Mediated at the Level of DNA Binding—We have shown that AKT phosphorylation of DAF-16 WT allows association of 14-3-3 and that this association inhibits transcription activation by DAF-16 and this effect requires the AKT/14-3-3 sites in DAF-16 (21). If insulin inhibition of DAF-16 activity results from an interaction of DAF-16 with 14-3-3 that inhibits DNA binding, we would not expect to see insulin inhibition of DAF-16 activity if the protein were tethered to the promoter by way of a heterologous DNA binding domain. Therefore, we compared the effect of insulin on the activity of a fusion protein encoding the GAL4 DNA binding domain and DAF-16 using the IRE DNA site in IGFBP-1 or GAL4 DNA (Fig. 3).

In HepG2 cells, DAF-16 expressed in a pcDNA vector activates transcription of the IGFBP promoter by 4-fold (Fig. 3A, compare bars A and D) and this effect is inhibited by insulin (bar E) or by overexpression of constitutively active AKT (bar F). The AKT site mutant DAF-16 4A is resistant to the effect of insulin and AKT on IGFBP gene transcription (compare bar G to bars H and I, respectively). Thus, in HepG2 cells, the inhibitory effect of insulin and AKT on DAF-16 is dependent on its AKT/14-3-3 sites (16, 21).

DAF-16 WT and DAF-16 4A mutant were expressed as fusion proteins with the GAL4 DNA binding domain (Fig. 3, panel B) and their response to insulin was assessed using the IGFBP-IRE (bars A–D) or the GAL4 DNA site (bars E–H) to drive transcription. The GAL4-DAF-16 fusion protein stimulated basal IGFBP gene transcription 4-fold, identical to the DAF-16 derivatives expressed in the pcDNA expression system (data not shown). As expected, when activity was assessed using the IGFBP-1 promoter (containing the IRE), GAL4-DAF-16 activity was inhibited by insulin (Fig. 3, panel B, compare bars A and B), while the activity of GAL4-DAF-16–

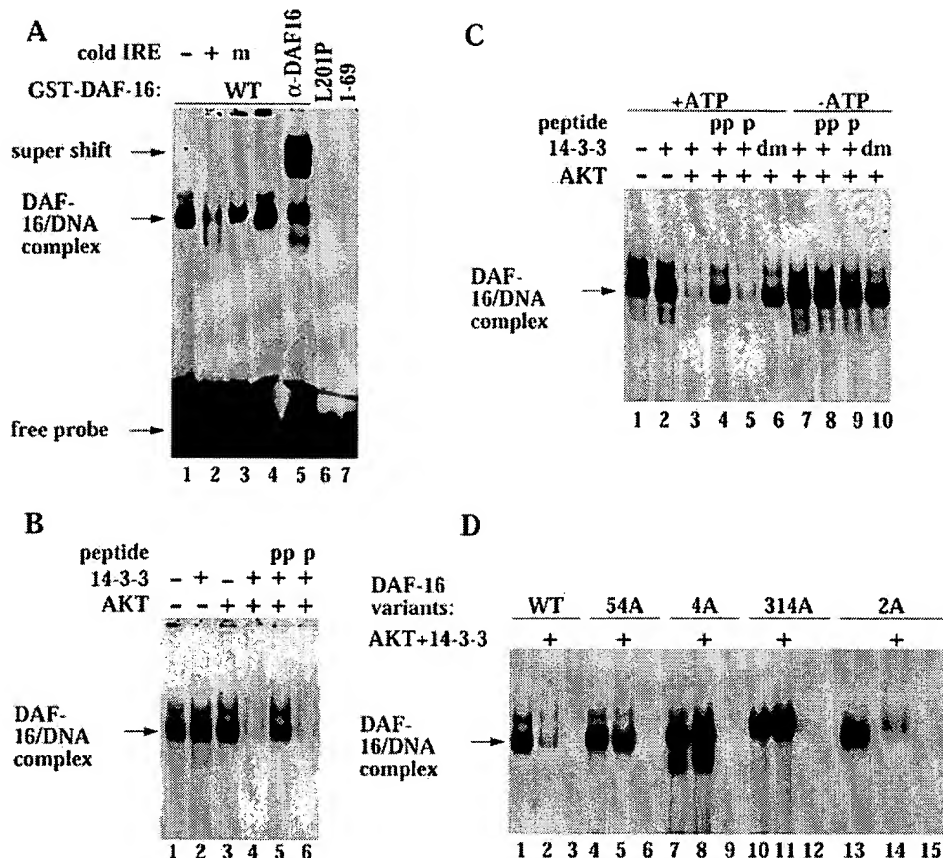


FIG. 2. AKT phosphorylation and subsequent 14-3-3 binding inhibit DAF-16 DNA binding. **A**, DAF-16 binds to IRE DNA. Prokaryotic recombinant GST-DAF-16 (lanes 1–5), GST-DAF-16 (L201P, mutation in the DNA binding domain) (lane 6), and GST-DAF-16 (amino acids 1–69, lane 7), 2 μ g each, were incubated with 32 P-labeled IGFBP IRE (50,000 cpm) in electrophoretic mobility shift assay binding buffer alone (lanes 1, 4, 6, and 7) or in the presence of 10 \times cold competitor wild-type IRE (lane 2) or mutant IRE (lane 3) or in the presence of anti-DAF-16 antibody (lane 5) and resolved on a 4% nondenaturing gel as described under “Experimental Procedures.” An autoradiogram of the gel is presented. The positions of DAF-16/DNA complexes and complexes supershifted with antibody are indicated. **B**, AKT phosphorylation of DAF-16 and 14-3-3 association prevents DAF-16 binding to IRE DNA. GST-DAF-16 (2 μ g) was incubated in a kinase buffer containing 2 μ g of active GST-AKT (lanes 3–6) or vehicle (lane 1 and 2) for 40 min at 30 $^{\circ}$ C, followed by a 30-min incubation with prokaryotic recombinant GST-14-3-3 (lanes 2 and 4–6), or vehicle (lanes 1 and 3). The presence of competitor phosphopeptide (pp, 1 mM, lane 5) or unphosphorylated peptide (p, 1 mM, lane 6) is indicated. **C**, Inhibition of DAF-16 binding to the IRE requires active AKT and an intact 14-3-3 dimer. GST-DAF-16 (2 μ g) was incubated in a kinase buffer containing 2 μ g of active GST-AKT in the presence (lanes 1–6) or absence (lanes 7–10) of ATP, followed by a 30-min incubation with GST-14-3-3 (lanes 2–5 and 7–9), vehicle (lane 1), or a dimerization-deficient GST-14-3-3 (dm, lanes 6 and 10) in the presence of competitor phosphopeptide (pp, 1 mM, lanes 4 and 8) or unphosphorylated peptide (p, 1 mM, lanes 5 and 9). The samples were assayed for DNA binding as in panel A. **D**, inhibition of DAF-16 binding to the IRE by AKT/14-3-3 requires intact AKT sites Thr-54 and Ser-314 on DAF-16. GST-DAF-16 (lanes 1–3), GST-DAF-16(T54A) (lanes 4–6), GST-DAF-16(4A) (lanes 7–9), GST-DAF-16(314A) (lanes 10–12), and GST-DAF-16(2A) (lanes 13–15), 2 μ g each, were incubated in a kinase buffer containing 2 μ g of active GST-AKT (lanes 2, 5, 8, 11, and 14) or vehicle (all others) for 40 min at 30 $^{\circ}$ C followed by 30-min incubation with prokaryotic recombinant GST-14-3-3 (lanes 2, 5, 8, 11, and 14) or vehicle (all others). The samples were assayed for binding to mutant (lanes 3, 6, 9, 12, and 15) or wild type (all others) 32 P-IRE probes as in panel A.

4A, which fails to bind 14-3-3, was not affected by insulin (Fig. 3, panel B, compare bars C and D). By contrast, although the GAL4-DAF-16 and GAL4-DAF-16 4A fusion proteins activated transcription similarly when assessed on the GAL4 DNA binding site (bars E–H), neither wild-type GAL4-DAF-16, nor GAL4-DAF-16–4A were inhibited by insulin (panel B, bars E and F and bars G and H).

The observation that GAL4-DAF-16 responds to insulin when its activity is assessed using an IRE site, but not a GAL 4 site, indicates that the response of this fusion protein is analogous to that of the native DAF-16 protein. If insulin's action to inhibit DAF-16 activity resulted from a direct effect on the intrinsic transcription activity of GAL4-DAF-16 or from nuclear export of GAL4-DAF-16, we would expect to see the negative effect of insulin on both the GAL4 and the IRE DNA binding sites. Inasmuch as we observe the inhibitory effect of insulin on the IRE alone, we conclude that insulin's effect is mediated at the level of DAF-16 DNA binding. Furthermore,

the observation that GAL4-DAF-16 is resistant to insulin signaling when the protein is tethered to the GAL4 DNA target site suggests that 14-3-3 inhibition of DAF-16 DNA binding may be a first step in the negative regulation of DAF-16 activity allowing subsequent changes in DAF-16 subcellular localization to occur.

PI 3-Kinase Signaling Regulates DAF-16/14-3-3 Interaction and Consequent Subcellular Distribution—Our *in vitro* DNA binding results imply that the association of DAF-16 with 14-3-3 plays a crucial role in the negative regulation of DAF-16 DNA binding. As HepG2 cells do not express sufficient DAF-16 to enable detection by DNA binding assay, we were unable to study direct effects of insulin on DAF-16 DNA binding in these cells. However, coexpression studies of GST-tagged 14-3-3 and Flag-tagged DAF-16 proteins in 293 cells demonstrate that 14-3-3 and DAF-16 can associate both in serum-deprived cells and in cells growing exponentially in serum (Fig. 4A, compare lanes 2 and 4). Treatment of serum-starved cells with the PI

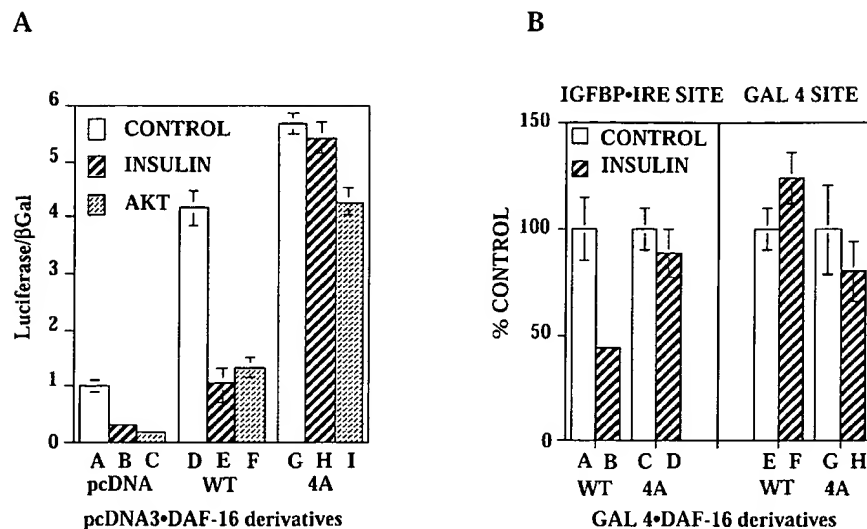


FIG. 3. Insulin inhibition of DAF-16 activity in HepG2 cells is dependent on the AKT sites and is mediated at the level of DNA binding. A, insulin and AKT/PKB inhibits the transcription activity of DAF-16 WT but not AKT site mutant DAF-16 4A. HepG2 cells were transiently cotransfected with the IGF1P-luciferase reporter gene (15 μ g) and the expression vector pcDNA3 (1 μ g/ml) (bars A–C), wild-type pcDNA-DAF-16 (1 μ g/ml) (bars D–F), or a mutant of DAF-16 in which an alanine residue was inserted in place of serine or threonine at the four putative AKT sites, DAF-16 4A (1 μ g/ml) (bars G–I), and constitutively active PKB (2 μ g/ml) (bars C, F, and I). Serum-starved cells were incubated with insulin (1 milliunit/ml) (bars B, E, and H) or vehicle (bars A, C, D, F, G, and I) during the last 16 h of the incubation. Luciferase activity is shown corrected for β -galactosidase gene expression. B, insulin mediates its inhibitory effects on DAF-16 at the level of DNA binding. HepG2 cells were transiently cotransfected with an expression vector encoding wild-type GAL4-DAF-16 (bars A, B, E, and F), or mutant GAL4-DAF-16 derivative 4A (bars C, D, G, and H) and either the IGF1P-luciferase reporter containing the IRE (bars A–D) or the GAL4-LUC reporter gene (bars E–H) (15 μ g) together with the RSV- β -galactosidase reporter gene. Cells were stimulated with vehicle (bars A, C, E, and F) or with insulin (bars B, D, F, and H) as described in panel A. Luciferase activity was corrected for β -galactosidase and plotted as percentage of the unstimulated control.

3-kinase-specific inhibitor LY294002 caused a marked decrease in 14-3-3/DAF-16 association (Fig. 4A, compare lane 2 with 3 and lane 11 with 12). These findings suggested that PI 3-kinase signaling to AKT and phosphorylation of DAF-16 could regulate its association with mammalian 14-3-3 as it does for FKHL1 (14).

Accordingly, we found that the 14-3-3/DAF-16 association depended on the presence of the AKT-phosphorylation site at residue Thr-54 on DAF-16 (Fig. 4A, lanes 13–15) *in vivo*, as is the case *in vitro*. However, the alanine mutations at residues 240/242, which did not prevent association of DAF-16 2A with 14-3-3 *in vitro*, greatly reduced 14-3-3 association *in vivo* (lanes 16–18). Mutation of site Thr-54 and sites Ser-240/Thr-242 in DAF 3A completely prevented DAF-16/14-3-3 association (lanes 19–21).

The ability of DAF-16 derivatives to associate with mammalian 14-3-3 correlated with the subcellular localization of DAF-16. In exponentially growing cells, recombinant DAF-16 was present both in the cytoplasm and in the nucleus (Fig. 4B, lanes 2–4 and 15–17). Mutants of DAF-16 impaired in 14-3-3 binding, DAF-16 T54A, 2A, and 4A were confined strictly to the nucleus (Fig. 4B, compare lanes 2 and 3 with lanes 5 and 6, lanes 8 and 9, and lanes 11 and 12). Thus, DAF-16 can interact with mammalian import/export proteins.

Inhibition of PI 3-kinase signaling with LY294002 caused a shift of DAF-16 to the nucleus and an almost complete disappearance of DAF-16 from the cytoplasm (Fig. 4B, compare lanes 15 and 16 with lanes 18 and 19 and lane 21 and 22). The finding that the *C. elegans* transcription factor DAF-16 can couple to mammalian AKT, 14-3-3, and the mammalian import/export machinery demonstrates it functions in an analogous manner to its mammalian homologs FKRL and FKHL1 (14, 32).

Inhibition of Endogenous PI 3-Kinase Signaling Enhances DAF-16 DNA Binding Activity Independent of DAF-16 AKT Phosphorylation Sites—Having demonstrated that inhibition of PI 3-kinase signaling with LY294002 leads to dissociation of DAF-16/14-3-3 in 293 cells, we examined the effect of

LY294002 on DAF-16 DNA binding activity in these cells. Nuclear extracts were isolated from 293 cells transiently transfected with expression plasmids encoding Flag-tagged DAF-16 (Fig. 5). The identity of DAF-16 overexpressed in HEK 293 cells was demonstrated by supershift experiments using antibodies against the Flag epitope tag on DAF-16 (Fig. 5A, compare lanes 2 and 5).

We detected low DAF-16 DNA binding activity in the nuclear extracts of 293 cells growing exponentially in serum (Fig. 5B, lane 2); inhibition of PI 3-kinase by LY294002 markedly increased DAF-16 DNA binding activity (compare lanes 2 and 3). This increase was not simply a reflection of an increase in DAF-16 protein in the LY294002 treated nuclear extracts due to nuclear translocation, because extracts containing equal amounts of DAF-16 were employed (Fig. 5B, see Western blot (lower panel); compare lanes 4 and 6). Thus, the increase in DAF-16 DNA binding activity shown reflects an increase in its specific DNA binding activity indicating that LY294002 can prevent negative regulation of DAF-16 DNA binding activity by a PI 3-kinase-mediated mechanism.

We also examined the effect of PI 3-kinase inhibition on regulation of DAF-16 AKT site mutants that do not bind 14-3-3 *in vivo*, DAF-16 2A and DAF-16 4A (Fig. 5C, upper panel). Both LY294002 and wortmannin increased the DNA binding activity of wild-type DAF-16 (Fig. 5C, upper panel, compare lane 4 to lanes 5 and 6). In exponentially growing cells mutants of DAF-16 impaired in 14-3-3 binding, DAF-16 2A, 3A, and 4A were confined strictly to the nucleus (Fig. 5C, lower panel, compare lanes 9 and 10, lanes 11 and 12, and lanes 13 and 14). Nevertheless, similar to DAF-16 WT (Fig. 5C, lanes 4 and 5), the DNA binding activity of DAF-16 2A and DAF-16 4A was enhanced by PI 3-kinase inhibition (Fig. 5C, upper panel, compare lanes 7 and 8 and lanes 9 and 10).

In the insulin-responsive HepG2 cell line, serum inhibits the effect of endogenous factors on IGF1P gene transcription by 90% (Fig. 5D, bar B) relative to the activity seen in serum-deprived cells (bar A). The PI 3-kinase inhibitor enhances IG-

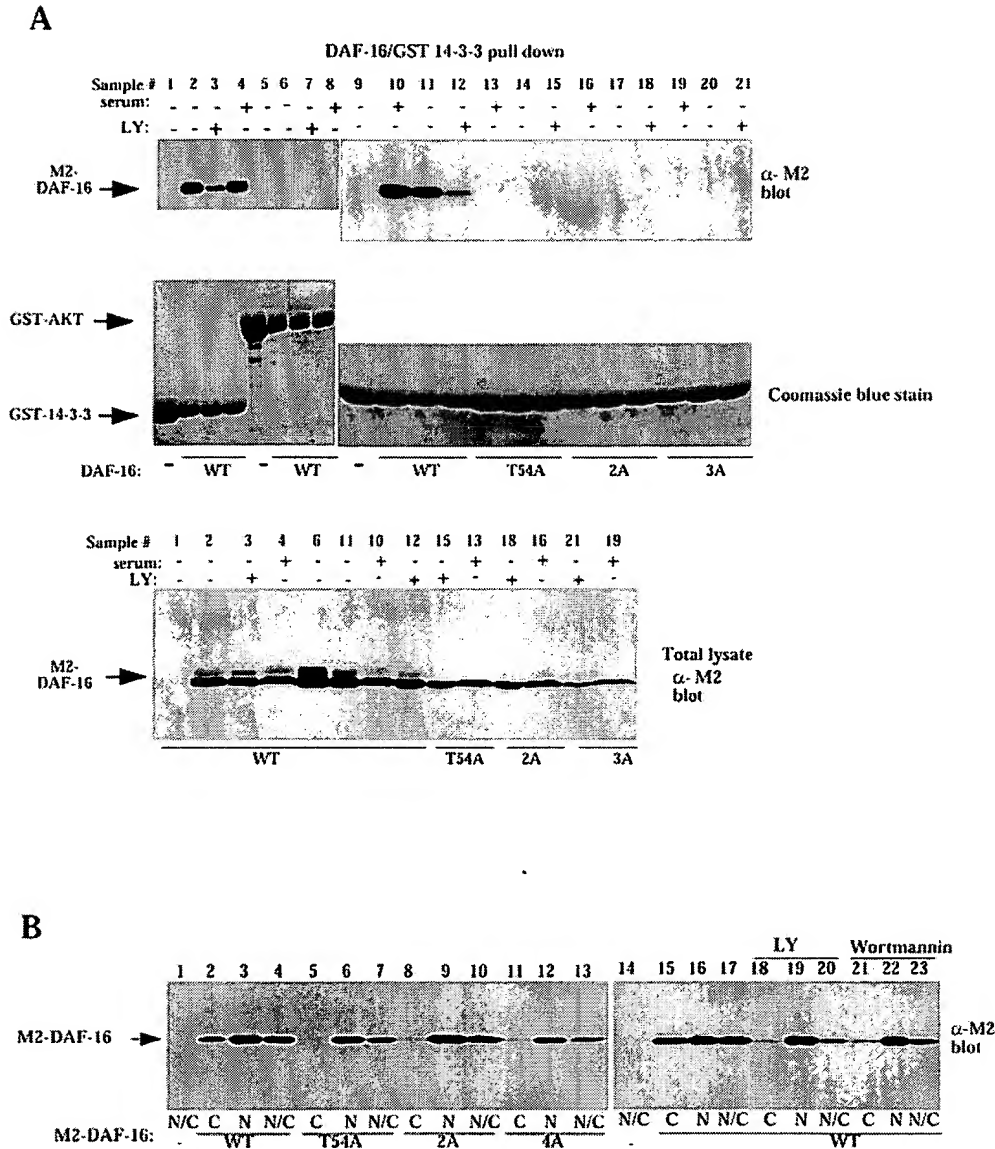


FIG. 4. Serum growth factors signaling to PI 3-kinase regulate DAF-16 nuclear/cytoplasmic distribution by regulating DAF-16/14-3-3 association. *A*, *in vivo* pull-down of Flag epitope-tagged DAF-16 with GST-tagged 14-3-3 or GST-AKT. Flag epitope-tagged DAF-16 (lanes 2–4, 6–8, and 10–12), DAF-16 mutants; T54A (lanes 13–15), 2A (lanes 16–18), 3A (lanes 19–21), or control vector (lanes 1, 5, and 9) were coexpressed in 293 cells with GST-14-3-3 (lanes 1–4 and 9–21) or GST-AKT (lanes 5–8). After transfection (24 h), cells were either grown in serum (lanes 4, 8, 10, 13, 16, and 19) or were serum-deprived in the presence of the PI 3-kinase inhibitor LY294002 (lanes 3, 7, 12, 15, 18, and 21) or vehicle (lanes 1, 2, 5, 6, 9, 11, 14, 17, and 20) for 24 h. Following affinity purification of GST fusions on GSH beads, associated DAF-16 was detected by anti-Flag immunoblot (using monoclonal antibody M2 (Sigma), top panel). The blots were Coomassie-stained for GST fusion recovery evaluation (middle panel). Representative samples of total lysates were analyzed for DAF-16 expression by anti-Flag immunoblot (bottom panel). *B*, subcellular localization of DAF-16 WT and AKT site mutant derivatives in HEK 293 cells. Flag-epitope-tagged DAF-16 (lanes 2–4 and 15–23), DAF-16 mutants T54A (lanes 5–7), 2A (lanes 8–10), 4A (lanes 11–13), or control vector (lane 1) were expressed in 293 cells. 24 h after transfection, cells were maintained in serum (lanes 1–17) or deprived of serum in the presence of PI 3-kinase inhibitors: LY294002 (10 μ M, lanes 18–20) or wortmannin (10 nM, lanes 21–23). Cells were harvested and fractionated into nuclear and cytoplasmic fractions using the NE-PER kit (Pierce). 30 μ g of nuclear (N, lanes 3, 6, 9, 12, 16, 19, and 22), 100 μ g of cytoplasmic (C, lanes 2, 5, 8, 11, 15, 18, and 21), and a combination of 15 μ g of nuclear and 50 μ g of cytoplasmic (N/C, lanes 1, 4, 7, 10, 13, 14, 17, 20, and 23) extracts were resolved on SDS-PAGE and assayed for the presence of DAF-16 by anti-Flag immunoblot.

FBP-1 gene transcription 2-fold above that seen in serum-starved cells (compare bars A and C). DAF-16 activates the IGF1R promoter (compare bar A to bar D) and serum inhibits the activity of exogenous DAF-16 by 50% (compare bars D and E), while LY294002 increases DAF-16 activity 2.5-fold over control levels (compare bars D and F).

The transcriptional activity of both wild type and mutant derivatives of DAF-16 was similarly regulated by PI 3-kinase inhibition in HepG2 cells (Fig. 5E). Whether wild-type or mutant DAF-16 derivatives are expressed in the pcDNA ex-

pression system (panel D) or as GAL4 fusion proteins compare (panel E), their activity is stimulated above basal in response to LY294002 (Fig. 5E, bars B, D, and F). However, when activity is assessed using the GAL4 DNA binding site to direct gene expression, LY294002 does not activate the GAL4-DAF-16 derivatives (Fig. 5F, bars B, D, and F). Thus, we conclude that the stimulatory effect of LY294002 is also mediated at the level of DNA binding *in vivo*.

The enhancing effect of LY294002 on GAL4-DAF-16 WT is greater than its enhancing effect on GAL4-DAF-16 3A and 4A

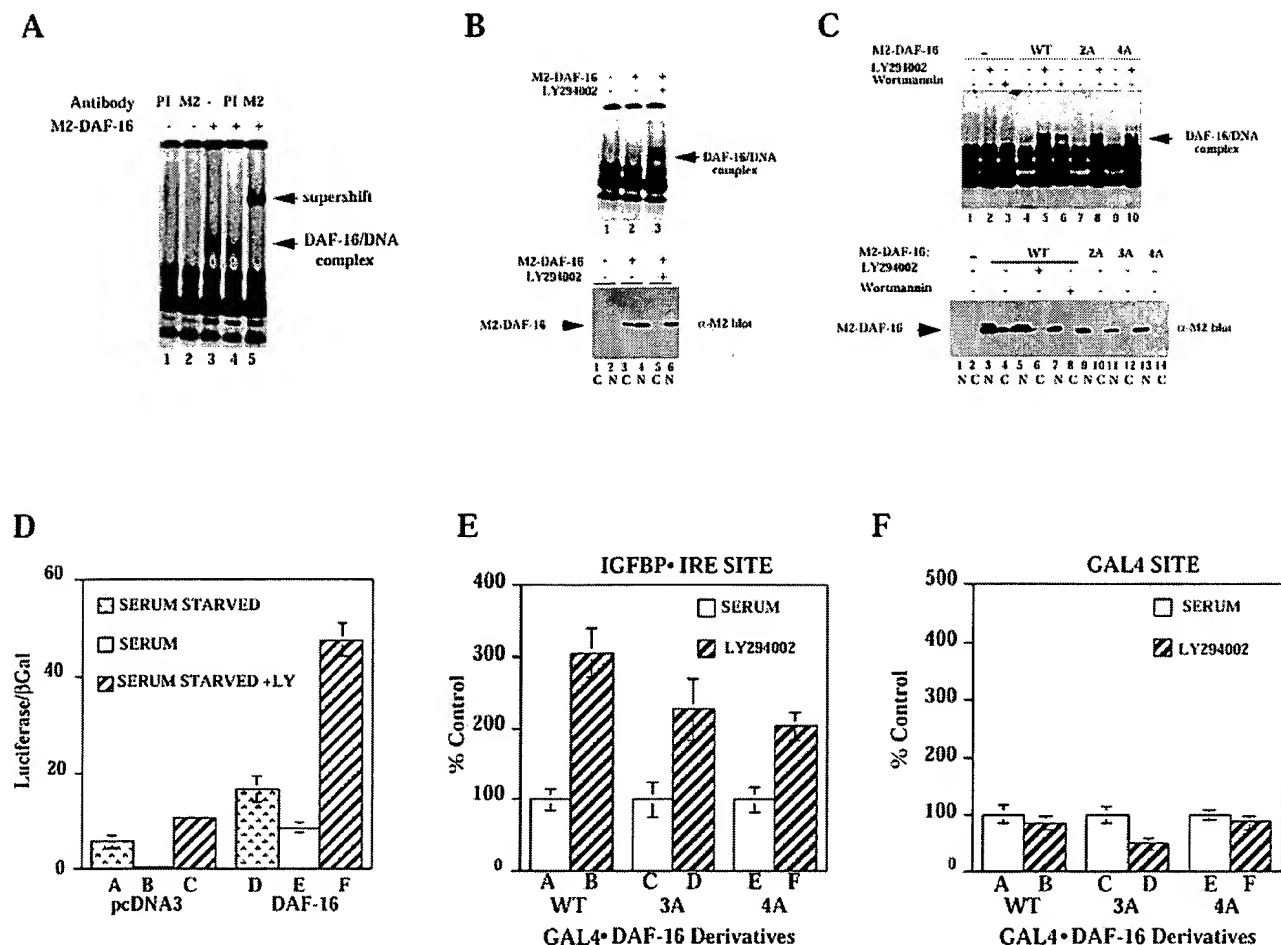


FIG. 5. PI 3-kinase inhibition enhances DAF-16 DNA binding and transcriptional activity via an AKT/14-3-3 site-independent pathway. *A*, identification of DAF-16 DNA binding activity in 293 cell nuclear extract. Nuclear extract was isolated from 293 cells expressing Flag epitope-tagged DAF-16 (M2-DAF-16) (lanes 3–5) or pcDNA alone (lanes 1 and 2) and assayed for binding to the 32 P-labeled IGF1R-IRE as in Fig. 2A. Preimmune serum (PI, lanes 1 and 4) or anti-Flag antibody (M2, lanes 2 and 5) was used to supershift DAF-16/DNA complexes. The location of the DAF-16/DNA complex and M2/DAF-16/DNA complex (supershift) is indicated. *B*, inhibition of endogenous PI 3-kinase activity enhances binding of DAF-16 to IRE DNA. *Upper panel*, nuclear extracts of 293 cells expressing Flag-epitope-tagged DAF-16 (M2-DAF-16) (lanes 2 and 3) or vehicle (lane 1) grown in serum (lanes 1 and 2) or serum-deprived in the presence of LY294002 (10 μ M, lane 3) were prepared as in Fig. 4B and assayed for binding to the IGF1R-IRE as described in Fig. 2A and “Experimental Procedures.” *Lower panel*, expression of DAF-16 in the nuclear (N) and cytoplasmic (C) fractions of the extracts shown was determined by anti-Flag immunoblotting. *C*, inhibition of endogenous PI 3-kinase with LY294002 enhances binding of DAF-16 AKT site mutants to IRE DNA. *Upper panel*, nuclear extract was isolated from 293 cells transfected with pcDNA alone (lanes 1–3), Flag-epitope-tagged DAF-16 (lanes 4–6), DAF-16 2A (lanes 7 and 8), or DAF-16 4A (lanes 9 and 10). Cells were grown in serum (lanes 1, 4, 7, and 9) or serum-deprived in the presence of LY294002 (10 μ M, lanes 2, 5, 8, and 10) or wortmannin (10 nM, lanes 3 and 6). Binding to IGF1R-IRE was assayed as in Fig. 2A. *Lower panel*, expression of DAF-16 in the nuclear (N) and cytoplasmic (C) fractions was determined by anti-Flag immunoblotting. *D*, serum growth factors regulate DAF-16 transcription activation. Insulin-responsive HepG2 hepatoma cells were cotransfected with a luciferase reporter gene under the control of the native IGF1R promoter (15 μ g) and pcDNA3-DAF-16 (2 μ g/ml) (bars D–F) or a control pcDNA3 vector (2 μ g/ml) (bars A–C) together with RSV- β -galactosidase to correct for transfection efficiency. 4 h after transfection, cells were changed to serum-containing media (bars B and E) or serum deprivation media (starved) (bars A, C, D, and F) in the absence (bars A and D) or presence (bars C and F) of LY294002 (10 μ M). Cells were harvested and assayed for luciferase (Promega kit) and β -galactosidase (Tropix kit) expression according to the manufacturers instructions. The mean ratios \pm S.E. of luciferase/ β -galactosidase triplicates are presented. *E*, inhibition of endogenous PI 3-kinase activity enhances transcription activity of DAF-16 WT and AKT site mutants DAF-16 3A and DAF-16 4A on the IGF1R-IRE. HepG2 cells were transiently cotransfected with an expression vector encoding the wild-type GAL4-DAF-16 (bars A and B), or mutant GAL4-DAF-16 derivatives 3A (bars C and D) or 4A (bars E and F) (2 μ g), the IGF1R-luciferase reporter gene (15 μ g), and the RSV- β galactosidase reporter gene (2 μ g). Control cells growing exponentially in serum were stimulated with vehicle (bars A, C, and E) or serum-starved cells were stimulated with LY294002 (bars B, D, and F). The effect of LY294002 is shown as the percentage of control value. *F*, inhibition of endogenous PI 3-kinase activity does not affect transcriptional activity of DAF-16 WT or mutants on the GAL4 site. HepG2 cells were transiently cotransfected with GAL4-DAF-16 derivatives (2 μ g/ml) and the GAL4-LUC (15 μ g) reporter gene. Control cells growing exponentially in serum (bars A, C, and E) were compared with serum-starved cells stimulated with LY294002 (bars B, D, and F). Luciferase activity was normalized for β -galactosidase gene expression and is presented as the percentage of the serum value for each plasmid.

on the IGF1R-IRE (Fig. 5E, compare bar B to bars D and F), which suggests that DAF-16 WT is subject to both 14-3-3-dependent and independent regulation by LY294002 *in vivo*. The ability of LY294002 to enhance the activity of DAF-16 AKT/14-3-3 site mutants that are confined strictly to the nucleus (Fig. 5C, lower panel, lanes 9–14, DAF-16 2A, 3A, and 4A) indicates that a PI 3-kinase-responsive, 14-3-3/AKT site-independent

mechanism can control DAF-16 DNA binding and transcription activity.

DISCUSSION

Our results reveal the existence of at least two mechanisms that cooperate to inhibit DAF-16 DNA binding in response to factors that activate PI 3-kinase-dependent signaling path-

TABLE I
Inhibition of DAF-16 DNA binding via 14-3-3-dependent (I) and -independent (II) pathways

Pathway I, 14-3-3 associates with AKT-phosphorylated DAF-16 WT *in vitro* and blocks its ability to bind to the IRE DNA. *In vivo* DAF-16 WT associates with 14-3-3 and is translocated from the nucleus to the cytoplasm. Insulin inhibits transcription activation of DAF-16 WT when activity is assessed on IRE DNA, but not GAL4 DNA pointing to the importance of DAF-16/IRE binding as a mode of regulation by insulin. Insulin does not regulate the activity of the AKT/14-3-3 site mutant DAF-16 4A. Pathway II, a 14-3-3-independent mode of DAF-16 regulation is manifested by DAF-16 4A, which lacks all four AKT sites, does not bind 14-3-3, is not exported from the nucleus but, like DAF-16 WT, is subject to DNA binding regulation by the PI3 kinase inhibitor LY294002. LY294002 enhances DNA binding and transcription activity of both DAF-16 WT and 4A and therefore mediates its effect at least in part via an AKT site/14-3-3-independent pathway. Again regulation by LY294002 of GAL4 DAF-16 WT and 4A on an IRE but not a GAL4 DNA site, indicates that this effect is mediated primarily at the level of DNA binding.

Pathway	DAF-16	Association <i>in vitro</i> with 14-3-3	Ability of 14-3-3 to inhibit DNA binding <i>in vitro</i>	Association <i>in vivo</i> with 14-3-3	Translocation	Insulin inhibition on IRE site	LY294002 activation on IRE site	Effect of insulin or LY294002 on GAL4 site
I	WT	+	+	+	+	+	+	-
II	4A	-	-	-	-	-	+	-

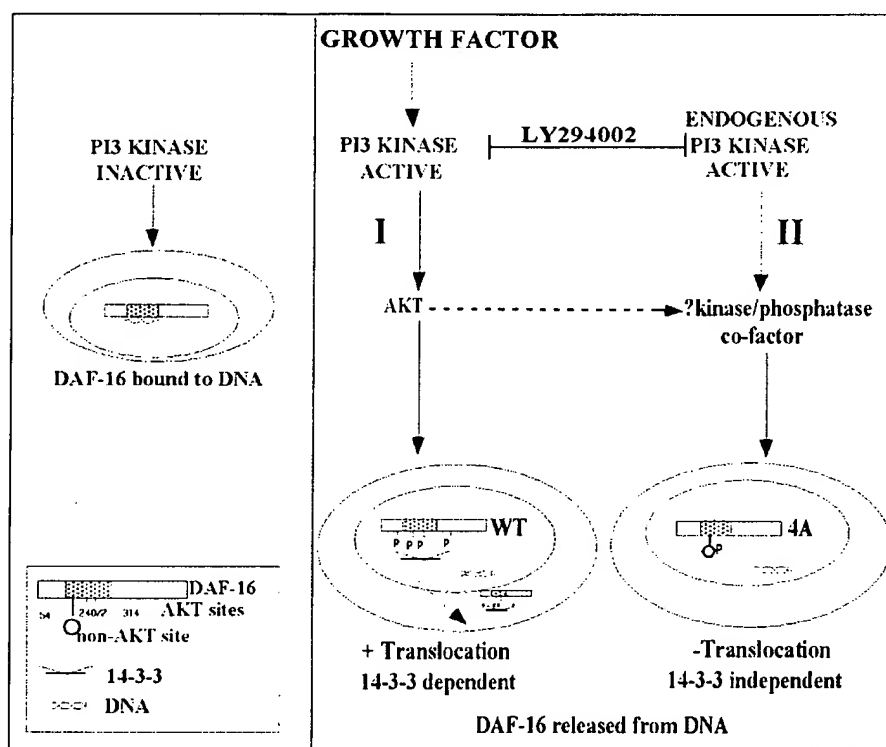


FIG. 6. Proposed model of DAF-16 regulation by growth factor signaling to PI 3-kinase. Under conditions in which PI 3-kinase is inactive, DAF-16 is found in the nucleus and is bound to DNA. Pathway I, following growth factor stimulation and activation of PI 3-kinase, AKT phosphorylates DAF-16 on Thr-54, Ser-240/242, and Ser-314, 14-3-3 binds the Thr-54 and Ser-314 sites and prevents the interaction of DAF-16 with DNA. DAF-16 is then translocated to the cytoplasm. Pathway II, endogenous PI 3-kinase signaling to DAF-16 WT and DAF-16 4A, which lacks AKT/14-3-3 binding sites, inhibits their ability to binding DNA. This effect occurs in the absence of 14-3-3 association or DAF-16 translocation. We propose that endogenous PI 3-kinase activates a kinase (or phosphatase) other than AKT that phosphorylates DAF-16 4A and inhibits DAF-16 4A DNA binding activity directly or by recruiting a cofactor that interacts with DAF-16 in a manner analogous to 14-3-3. Alternatively AKT or another kinase could phosphorylate the cofactor that interacts with DAF-16. Regulation of DAF-16 WT DNA binding *in vivo* may occur via a combination of pathways I and II.

ways. First, we show that in addition to its proposed role in promoting nuclear export/cytoplasmic retention of forkhead proteins, 14-3-3 can directly inhibit binding of AKT-phosphorylated DAF-16 to DNA (Table I and Fig. 6, pathway I). Second we describe a novel PI 3-kinase-dependent pathway that inhibits the DNA binding activity of DAF-16 4A, an AKT/14-3-3 site mutant that cannot bind 14-3-3 and is not subject to PI3-kinase-dependent nuclear export (Table I and Fig. 6, pathway II). The ability of endogenous PI 3-kinase signaling to prevent DAF-16 DNA binding independent of 14-3-3 may involve a phosphorylation-dependent interaction of DAF-16 with an interacting protein. This cofactor could have an analogous function to 14-3-3 and inhibit DAF-16 DNA binding activity in response to PI 3-kinase signaling. On the other hand, a cofactor that acts to stabilize DAF-16 DNA binding activity might dissociate from

DAF-16 in response to PI 3-kinase signaling. In a third scenario, a non-AKT kinase (or phosphatase) downstream of endogenous PI 3-kinase could directly phosphorylate DAF-16 or DAF-16 4A and inhibit their ability to bind DNA.

In HepG2 cells, we find that insulin inhibition of DAF-16 function occurs via an AKT/14-3-3 site-dependent pathway (Fig. 6, pathway I), consistent with the observed ability of dimeric 14-3-3 to bind AKT phosphorylated DAF-16. Our observation that insulin fails to inhibit the activity of GAL4-DAF16 bound to the GAL4 DNA site, as opposed to the IRE DNA site, implies that GAL4-DAF-16 is not subject to insulin-mediated inhibition of DNA binding or nuclear export when it is tethered to GAL4 DNA. Thus, we propose that, in HepG2 and 293 cells, growth factors that regulate PI 3-kinase activity may act primarily to inhibit DAF-16 DNA binding via an interaction

with 14-3-3 and that this step is permissive for nuclear export.

Our finding that insulin inhibition of DAF-16 is prevented by mutation of its AKT sites in HepG2 cells confirms that of Guo *et al.* (16), who reported similar results for FKHR. In Fig. 6 (pathway II), we propose a role for a kinase (or phosphatase) other than AKT in mediating the effect of PI 3-kinase signaling on DAF-16 DNA binding and function. Two observations suggest that the endogenous PI 3-kinase activity observed in serum-starved HepG2 and 293 cells may act via a distinct pathway from that which mediates the effect of insulin in HepG2 cells. First, whereas insulin signaling via PI 3-kinase inhibits DAF-16 function via its AKT sites in HepG2 cells (Fig. 3), the effect of LY294002 to inhibit endogenous PI 3-kinase activity and enhance DAF-16 DNA binding and transcription function is seen on both wild-type DAF-16 and DAF-16 4A (Fig. 5). Second, in our hands LY294002 stimulated wild-type and mutant DAF-16 4A activity over the control levels observed in serum-starved 293 and HepG2 cells (Fig. 5) rather than simply reversing the negative effect of serum or insulin (14, 16). Thus, we conclude that the endogenous PI 3-kinase activity expressed in serum-starved 293 and HepG2 cells signals to a kinase other than AKT. Alternatively, endogenous PI 3-kinase signaling to AKT could modify the phosphorylation of a cofactor that interacts with DAF-16/DAF-16 4A.

The observation that growth factor signaling activates distinct effectors downstream of PI 3-kinase to regulate the activity of DAF-16-like proteins is supported by three published reports. First, in the insulin-responsive H4 hepatoma cell line, insulin signaling via an AKT site-independent mechanism inhibits the transcription activity of GAL4-FKHR; this effect occurs whether activity is assessed using the GAL4 DNA binding site or the IGFBP-IRE site (35). This observation is consistent with a direct effect of insulin on FKHR transcription activity or localization and suggests that distinct insulin signaling pathways to DAF-16-like FKH proteins may be operative in specific cells. It is notable that the existence of insulin-regulated, AKT-independent mechanisms for DAF-16 regulation were proposed based on genetic data in *C. elegans* (3). Second, although the DAF-16 homolog FKHL1 can bind multimers of the PEPCK-IRE site and mediate the negative effect of insulin in H4IIE cells, mutation of the AKT sites in FKHL1 inhibits the effect of insulin by 50% (36). Furthermore, insulin activation of AKT does not appear to explain all the effects of insulin-stimulated PI 3-kinase activity on PEPCK gene transcription; negative regulation of this gene in H4 hepatoma cells requires downstream effectors of PI 3-kinase distinct from AKT, the atypical protein kinase C α and Rac (37). Third, although insulin and IGF-1 can stimulate AKT activity equivalently in wild-type and insulin receptor-deficient SV40-transformed hepatocytes, respectively, only insulin stimulates phosphorylation of FKHR at site Thr-24 in these cells (33); thus, only insulin, and not IGF-1, stimulates nuclear export of FKHR in these cells.

In HepG2 cells both insulin and LY294002 regulate IGFBP promoter activity in the absence of exogenously expressed DAF-16. This observation suggests that the pathways we describe for DAF-16 are also relevant for endogenously expressed mammalian homologues such as FKHR (16) in HepG2 cells. Although it is formally possible that LY294002 activation of endogenous FKHR could require new protein synthesis, we show in Fig. 5B that the effect of LY294002 to enhance DAF-16 DNA binding activity is not due to an increase in DAF-16 protein expression or nuclear content. Thus, LY294002 appears to have a direct effect on the specific DNA binding activity of DAF-16.

The proposed model of multistep regulation of DAF-16 at the level of DNA binding as well as regulation of subcellular localization by 14-3-3 underscores the complexity of the PI 3-kinase signaling pathways to forkhead proteins. Analogous results have been described for PHO4, where four distinct phosphorylation sites cooperate to regulate nuclear import, nuclear export, and transcription activation of the target gene for PHO5 (38). Understanding the complex regulation of DAF-16 and its mammalian homologues will provide valuable insights into the mechanism that underlie the diverse effects of insulin on the metabolism, growth, and survival of its target tissues.

Acknowledgments—We thank Joseph Avruch, Jack Rogers, and Phil Daniel for critical reading of the manuscript. We thank Simin Nui for construction of GAL4-DAF-16 plasmids.

REFERENCES

- Kimura, K. D., Tissenbaum, H. A., Liu, Y., and Ruvkun, G. (1997) *Science* **277**, 942–946
- Morris, J. Z., Tissenbaum, H. A., and Ruvkun, G. (1996) *Nature* **382**, 536–539
- Paradis, S., and Ruvkun, G. (1998) *Genes Dev.* **12**, 2488–2498
- Paradis, S., Ailion, M., Tokar, A., Thomas, J. H., and Ruvkun, G. (1999) *Genes Dev.* **13**, 1438–1452
- Ogg, S., and Ruvkun, G. (1998) *Mol. Cell* **2**, 887–893
- Lin, K., Dorman, J. B., Rodan, A., and Kenyon, C. (1997) *Science* **278**, 1319–1322
- Ogg, S., Paradis, S., Gottlieb, S., Patterson, G. I., Lee, L., Tissenbaum, H. A., and Ruvkun, G. (1997) *Nature* **389**, 994–999
- Gottlieb, S., and Ruvkun, G. (1994) *Genetics* **137**, 107–120
- Alessi, D. R., and Cohen, P. (1998) *Curr. Opin. Genet. Dev.* **8**, 55–62
- Cheatham, B., Vlahos, C., Cheatham, L., Wang, L., Blenis, J., and Khan, C. (1994) *Mol. Cell. Biol.* **14**, 4902–4911
- Avruch, J. (1998) *Mol. Cell. Biochem.* **183**, 31–48
- O'Brien, R. M., Nois, E. L., Suwanichkul, A., Yamasaki, T., Lucas, P. C., Wang, J., Powell, D. R., and Granner, D. K. (1995) *Mol. Cell. Biol.* **15**, 1747–1758
- Cichy, S. B., Uddin, S., Danilkovich, A., Guo, S., Klippel, A., and Unterman, T. G. (1998) *J. Biol. Chem.* **273**, 6482–6487
- Brunet, A., Bonni, A., Zigmond, M., Lin, M., Juo, P., Hu, L., Anderson, M., Arden, K., Blenis, J., and Greenberg, M. (1999) *Cell* **96**, 857–868
- Kops, G., de Ruiter, N., De Vries-Smits, A., Powell, D., Bos, J., and Burgering, B. (1999) *Nature* **398**, 630–634
- Guo, S., Rena, G., Cichy, S., He, X., Cohen, P., and Unterman, T. (1999) *J. Biol. Chem.* **274**, 17184–17192
- Tang, E., Nunez, G., Barr, F., and Guan, K.-L. (1999) *J. Biol. Chem.* **274**, 16741–16746
- Durham, S., Suwanichkul, A., Scheimann, A., Yee, D., Jackson, J., Barr, F., and Powell, D. (1999) *Endocrinology* **140**, 3140–3146
- Rena, G., Guo, S., Cichy, S., Unterman, T., and Cohen, P. (1999) *J. Biol. Chem.* **274**, 17179–17183
- Nakae, J., Park, B.-C., and Accili, D. (1999) *J. Biol. Chem.* **274**, 15982–15985
- Nasrin, N., Ogg, S., Cahill, C., W., B., Nui, S., Dore, J., Calvo, D., Shi, Y., Ruvkun, G., and Alexander-Bridges, M. C. (2000) *Proc. Natl. Acad. Sci. U. S. A.* **97**, 10412–10417
- Yaffe, M. B., Rittinger, K., Volinia, S., Caron, P. R., Aitken, A., Leffers, H., Smerdon, S. J., and Cantley, L. C. (1997) *Cell* **7**, 961–971
- Lopez-Girona, A., Furnari, B., Mondesert, O., and Russell, P. (1999) *Nature* **398**, 172–175
- Kumagai, A., and Dunphy, W. G. (1999) *Genes Dev.* **13**, 1067–1072
- Yang, J., Winkler, K., Yoshida, M., and Kornbluth, S. (1999) *EMBO J.* **18**, 2174–2183
- Tzivion, G., Luo, Z. J., and Avruch, J. (1998) *Nature* **394**, 88–92
- Luo, Z.-J., Zhang, X.-F., Rapp, U., and Avruch, J. (1995) *J. Biol. Chem.* **270**, 23681–23687
- Waterman, M., Stavridi, E., Waterman, J., and Halazonetis, T. (1998) *Nat. Genet.* **19**, 175–178
- Matta-Yelin, M., Aitken, A., and Ravid, S. (1997) *Mol. Biol. Cell* **8**, 1889–1899
- Datta, S. R., Dudek, H., Tao, X., Masters, S., Fu, H., Gotoh, Y., and Greenberg, M. E. (1997) *Cell* **91**, 231–241
- Zha, J., Harda, H., Yang, E., Jockel, J., and Korsmeyer, S. J. (1996) *Cell* **87**, 619–628
- Biggs, W. H., Meisenhelder, J., Hunter, T., Cavenee, W. K., and Arden, K. C. (1999) *Proc. Natl. Acad. Sci. U. S. A.* **96**, 7421–7426
- Nakae, J., Barr, V., and Accili, D. (2000) *EMBO J.* **19**, 989–996
- Takaishi, H., Konishi, H., Matsuzaki, H., Ono, Y., Shirai, Y., Saito, N., Kitamura, T., Ogawa, W., Kasuga, M., Kikkawa, U., and Nishizuka, Y. (1999) *Proc. Natl. Acad. Sci. U. S. A.* **96**, 11836–11841
- Tomizawa, M., Kumar, A., Perrot, V., Nakae, J., Accili, D., and Rechler, M. M. (2000) *J. Biol. Chem.* **275**, 7289–7295
- Hall, R. K., Yamasaki, T., Kucera, T., O'Brien, R. M., and Granner, D. K. (2000) *J. Biol. Chem.* **275**, 30169–30175
- Kotani, K., Ogawa, W., Matsumoto, M., Kitamura, T., Sakaue, H., Hino, Y., Miyake, K., Sano, W., Akimoto, K., and Kasuga, M. (1998) *Mol. Cell. Biol.* **18**, 6972–6982
- Komeili, A., and O'Shea, E. K. (1999) *Science* **284**, 977–980

Skeletal Muscle FOXO1 (FKHR) Transgenic Mice Have Less Skeletal Muscle Mass, Down-regulated Type I (Slow Twitch/Red Muscle) Fiber Genes, and Impaired Glycemic Control*[§]

Received for publication, January 21, 2004, and in revised form, July 9, 2004
Published, JBC Papers in Press, July 21, 2004, DOI 10.1074/jbc.M400674200

Yasutomi Kamei^{†§¶}, Shinji Miura[§], Miki Suzuki[§], Yuko Kai[§], Junko Mizukami^{||},
Tomoyasu Taniguchi^{||}, Keiji Mochida^{**}, Tomoko Hata^{‡‡}, Junichiro Matsuda^{‡‡},
Hiroyuki Aburatani^{§§}, Ichizo Nishino^{¶¶}, and Osamu Ezaki[§]

From the [†]PRESTO, Japan Science and Technology Agency, [§]Division of Clinical Nutrition, National Institute of Health and Nutrition, 1-23-1 Toyama, Shinjuku-ku, Tokyo 162-8636, ^{||}Lead Generation Research Laboratory, Tanabe Seiyaku Co., Ltd., 3-16-89 Kashima, Yodogawa-ku, Osaka 532-8505, ^{**}Bioresource Center, Institute of Physical and Chemical Research, 3-1-1 Koyadai, Tsukuba-shi, Ibaraki 305-0074, the ^{‡‡}Department of Veterinary Science, National Institute of Infectious Diseases, 1-23-1 Toyama, Shinjuku-ku, Tokyo 162-8640, ^{§§}Research Center for Advanced Science and Technology, University of Tokyo, 4-6-1 Komaba, Meguro-ku, Tokyo 153-8904, and the ^{¶¶}Department of Neuromuscular Research, National Institute of Neuroscience, National Center of Neurology and Psychiatry, 4-1-1 Ogawahigashi-cho, Kodaira, Tokyo 187-8502, Japan

FOXO1, a member of the FOXO forkhead type transcription factors, is markedly up-regulated in skeletal muscle in energy-deprived states such as fasting and severe diabetes, but its functions in skeletal muscle have remained poorly understood. In this study, we created transgenic mice specifically overexpressing FOXO1 in skeletal muscle. These mice weighed less than the wild-type control mice, had a reduced skeletal muscle mass, and the muscle was paler in color. Microarray analysis revealed that the expression of many genes related to the structural proteins of type I muscles (slow twitch, red muscle) was decreased. Histological analyses showed a marked decrease in size of both type I and type II fibers and a significant decrease in the number of type I fibers in the skeletal muscle of FOXO1 mice. Enhanced gene expression of a lysosomal proteinase, cathepsin L, which is known to be up-regulated during skeletal muscle atrophy, suggested increased protein degradation in the skeletal muscle of FOXO1 mice. Running wheel activity (spontaneous locomotive activity) was significantly reduced in FOXO1 mice compared with control mice. Moreover, the FOXO1 mice showed impaired glycemic control after oral glucose and intraperitoneal insulin administration. These results suggest that FOXO1 negatively regulates skeletal muscle mass and type I fiber gene expression and leads to impaired skeletal muscle function. Activation of FOXO1 may be involved in the pathogenesis of sarcopenia, the age-related decline in muscle mass in humans, which leads to obesity and diabetes.

Skeletal muscle is the largest organ in the human body, comprising about 40% of the body weight. The mass and composition of skeletal muscle are critical for its functions, such as exercise, energy expenditure, and glucose metabolism (1, 2). Elderly humans are known to undergo a progressive loss of muscle fibers associated with diabetes, obesity, and decreased physical activity (sarcopenia) (3). In human skeletal muscle, there are two major classifications of fiber type: type I (slow-twitch oxidative, so-called red muscle) and type II (fast-twitch glycolytic, so-called white muscle) fibers (2). Mass, fiber size, and fiber composition in adult skeletal muscle are regulated in response to changes in physical activity, environment, or pathological conditions. For example, space flight experiments using rats showed a reduction in total skeletal muscle mass of up to 37% as well as a significant loss of contractile proteins in type I but not type II fibers by 1–2 weeks of microgravity (4). Furthermore, the ratio of type I to type II fibers is associated with obesity and diabetes; the number of type I fibers is reduced in obese subjects and diabetic subjects compared with that in controls (5–7).

Skeletal muscle mass is positively regulated by hormones such as insulin-like growth factors (IGFs)¹ and growth hormone (8). Induction of hypertrophy in adult skeletal muscle by increased load is accompanied by the increased expression of IGF-1 (9). Systemic administration of IGF-1 results in increased skeletal muscle protein and reduced protein degradation (10). In addition, overexpression of IGF-1 blocks the age-related loss of skeletal muscle (11). Supplementation of IGF-1 to muscle cells *in vitro* promotes myotube hypertrophy, suggesting that hypertrophy can be mediated by autocrine- or paracrine-produced IGF-1 (12). Thus, delivery of the *IGF-1* gene specifically into skeletal muscle has been proposed as a genetic therapy for skeletal muscle disorders. A better understanding of the role of IGF-1 in skeletal muscle is therefore of great importance.

Specialized/differentiated myofiber phenotypes, including type I and type II fibers, are plastic and are physiologically

* This work was supported in part by research grants from the Japanese Ministry of Health, Labor, and Welfare (Tokyo) and by a grant from the Promotion of Fundamental Studies in Health Sciences of the Organization for Pharmaceutical Safety and Research. The costs of publication of this article were defrayed in part by the payment of page charges. This article must therefore be hereby marked "advertisement" in accordance with 18 U.S.C. Section 1734 solely to indicate this fact.

[§] The on-line version of this article (available at <http://www.jbc.org>) contains Information 1 and 2.

[¶] To whom correspondence should be addressed: Division of Clinical Nutrition, National Institute of Health and Nutrition, 1-23-1 Toyama, Shinjuku-ku, Tokyo 162-8636, Japan. Tel.: 81-3-3203-5725; Fax: 81-3-3207-3520; E-mail: ykamei@nih.go.jp.

¹ The abbreviations used are: IGF, insulin-like growth factor; CaMK, calmodulin-dependent kinase; PGC-1 α , peroxisome proliferator activated receptor- γ coactivator-1 α ; STZ, streptozotocin; MLC, myosin light chain; mtCK, mitochondrial creatine kinase; IGFBP, IGF-binding protein; COX, cytochrome c oxidase; DEXA, dual energy X-ray absorptiometry; EDL, extensor digitorum longus.

controlled by variations in motor neuron activity. The influence of motor neuron activity on different types of skeletal muscle fibers is considered to be transduced via calcium signaling and downstream molecules such as calcineurin and the calmodulin-dependent kinase (CaMK) pathway (13). Signals generated by calcium/calcineurin/CaMK augment the transactivating function of Mef2 and/or NFAT and enhance type I fiber-specific gene expression (13–18). More recently, it has been shown that a nuclear receptor cofactor (19, 20), peroxisome proliferator-activated receptor- γ coactivator-1 α (PGC-1 α) (21), drives the formation of type I fibers. Specifically, in transgenic mice expressing PGC-1 α , type II fibers are red in color, and PGC-1 α activates expression of type I fiber-specific genes (22). We also reproduced the PGC-1 α -induced red appearance of skeletal muscle; both type I and type II fibers appear redder in transgenic mice overexpressing PGC-1 α in skeletal muscle (23).

FOXO1 (FKHR), FOXO4 (AFX), and FOXO3a (FKHRL1) are a subfamily of the forkhead type transcription factors (24, 25). FOXO1 was originally cloned from a rhabdomyosarcoma because of its aberrant fusion with another transcription factor, PAX3, resulting from a chromosomal translocation (26). Recent studies have shown that the FOXO protein can also act as a cofactor of nuclear receptor activity (27–30). FOXO family members have been shown to regulate various cellular functions. FOXOs influence the transcription of genes involved in metabolism (31–34), the cell cycle (35, 36), and apoptosis (37, 38). In addition, FOXO1 can modulate cell differentiation; the constitutive active form of FOXO1 prevents the differentiation of preadipocytes (39) and stimulates myotube fusion of primary mouse myoblasts (40). Moreover, a FOXO1 knockout mouse has been reported; *Foxo1* haploinsufficiency restores insulin sensitivity and rescues the diabetic phenotype in insulin-resistant mice by reducing the hepatic expression of glucogenetic genes and by increasing the adipocytic expression of insulin-sensitizing genes (41). We have shown that FOXO1 expression is increased in skeletal muscle in energy-deprived states, such as in fasting mice, in mice with streptozotocin (STZ)-induced diabetes, and in mice after treadmill running (42). However, the physiological role of FOXO1 in skeletal muscle is still unclear. Although many studies have been performed using cultured cells, studies using animals with genetic modifications focused to the skeletal muscle remain to be conducted in order to understand the function of the FOXO family proteins *in vivo*. Meanwhile, it has been reported that FOXO1 and PGC-1 α can physically interact and regulate gene expression in the liver (43). Given that PGC-1 α is important for the differentiation of type I fibers, FOXO1 might be involved in this process. (Hereafter, we use “differentiation of muscle fiber” to mean “a switch from one fiber type to another fiber type.”) On the other hand, a genetic study of *Caenorhabditis elegans* showed that DAF16, the worm counterpart of FOXO, functions as a suppressor of insulin receptor-like signaling (44). Thus, the FOXO family may act negatively in mammals as a downstream player in insulin or IGF signaling. As IGF-1 plays an important role in controlling skeletal muscle mass, FOXO1 might also be involved in this process.

To gain insight into the potential role of FOXO1 in skeletal muscle, including the control of skeletal muscle mass and the control of differentiation of muscle fiber type, we established transgenic mice specifically overexpressing FOXO1 in their skeletal muscle. Most interestingly, these mice showed reduced skeletal muscle mass, and the muscle was paler in color. Histochemical, physiological, and microarray analyses of these FOXO1 transgenic mice showed that FOXO1 is involved in the regulation of skeletal muscle mass and type I fiber gene expression. In addition, our results suggest that FOXO1 activa-

tion may play a role in the impairment of skeletal muscle function including glycemic control.

EXPERIMENTAL PROCEDURES

RNA Analysis—Northern blot analyses were performed as described previously (42). The cDNA probes for Gadd45 α (GenBank™ accession number, U00937), troponin C (slow) (M29793), troponin T (slow) (AV213431), myosin light chain (MLC) (slow) (M91602), myoglobin (X04405), mitochondrial creatine kinase (mtCK, AV250974), F₀F₁-ATPase (AF030559), MLC (fast) (U77943), troponin I (fast) (J04992), troponin T (fast) (L48989), cathepsin L (X06086), IGF-binding protein 5 (IGFBP5) (L12447), MuRF1 (AF294790), and atrogen 1 (AF441120) were obtained by reverse transcription-PCR. The PCR primers used are as follows: Gadd45 α , forward, 5'-TCGCACCTTGCAATATGACTT-3', and reverse, 5'-CGGATGCCATCACCGTTCCG-3'; troponin C (slow), forward, 5'-AGCTGCGGTAGAACAGTTGA-3', and reverse, 5'-TCACCTGTGGCC-TGCAGCAT-3'; troponin T (slow), forward, 5'-TTCTGTCCACATGGG-AGCT-3', and reverse, 5'-TCGGAATTTCTGGCGTGGC-3'; MLC (slow), forward, 5'-GAGTTCGAAGGAAGCCTTCAC-3', and reverse, 5'-CTGCGA-ACATCTGGTTCGATC-3'; myoglobin, forward, 5'-CACCATGGGCTCA-TGTATG-3', and reverse, 5'-CTCAGCCCTGGAAGCCTAGC-3'; mtCK, forward, 5'-AAAGGAAGTGAACGATTAA-3', and reverse, 5'-TTGATG-TCTTGGCCTCTCTC-3'; F₀F₁-ATPase, forward, 5'-ACTGACCTGCCCTGCAAC-3', and reverse, 5'-CAAGGCTCTGTGTGGCCTG-3'; MLC (fast), forward, 5'-AGGGATGGCATTATCGACAA-3', and reverse, 5'-CATGTTCTTGTAGTCCAC-3'; troponin I, (fast), forward, 5'-AGGAAAG-CCGCCGAGAATCT-3', and reverse, 5'-TACTGGGAAGTGGGCAGTT-3'; troponin T (fast), forward, 5'-CAGCAAAGAATTCGGCTGA-3', and reverse, 5'-GGCCTTCTGTGCTGTGCTTCT-3'; cathepsin L, forward, 5'-CGAGGAGTCTTACCCTAT-3', and reverse, 5'-CTACCCTCAATTCA-CGACA-3'; IGFBP5, forward, 5'-GCTATGCCGTACCGGTCA-3', and reverse, 5'-CTTCACAGCCTCAGCCTTCA-3'; MuRF1, forward, 5'-ATG-AACTTCAACGGTGGGTTT-3', and reverse, 5'-TCAGTGCAGGCTGAG-CCTT-3'; and atrogen 1, forward, 5'-ATGCCGTTCCCTTGGGCAGGA-3', and reverse, 5'-TCAGAAGTTGAACAAATTGA-3'. FOXO1, FOXO3a, and FOXO4 cDNA probes were prepared as reported previously (42). COXII, COXIV, Mef2c, PGC-1 α , and glucose transporter 4 cDNA probes were prepared as described previously (23). NFAT (IMAGE clone 4109469) and CaMK II β (IMAGE clone 5014712) cDNA probes were purchased from Invitrogen.

Generating Transgenic Mice—The human skeletal muscle α -actin promoter (45) was provided by Drs. E. D. Hardeman and K. Guven (Children's Medical Research Institute, Australia). The human FOXO1 cDNA was as described previously (42). The transgene (Fig. 1A) was excised from agarose gel and purified for injection (2 ng μ l⁻¹). Fertilized eggs were recovered from C57BL/6 females crossed with C57BL/6 males and microinjected at Japan SLC Inc. (Hamamatsu, Japan). The mice were maintained at a constant temperature of 22 °C with fixed artificial light (12-h light and 12-h dark cycle). Care of the mice was conducted in accordance with the institutional guidelines.

Body Composition Analysis—Mice were anesthetized with pentobarbital sodium, Nembutal (0.08 mg/g body weight, Abbott), and scanned with a Lunar PIXi mus2 densitometer (Lunar Corp., Madison, WI), equipped for dual energy x-ray absorptiometry (DEXA) (46).

Immunoblotting—Protein extracts from skeletal muscles were prepared by centrifugation of the tissue homogenates as described previously (47). Protein extracts (30 μ g) separated by SDS-PAGE were electrophoretically transferred to Immobilon P membranes (Millipore, Bedford, MA). Immunoblotting was performed by using goat anti-FOXO1 IgG (N-18, Santa Cruz Biotechnology, Inc. Santa Cruz, CA), goat anti-troponin I (slow) (C-19, Santa Cruz Biotechnology), goat anti-troponin I (fast) (C-19, Santa Cruz Biotechnology), goat anti-myoglobin (M-109, Santa Cruz Biotechnology), or rabbit anti-PGC-1 α (C terminus, Calbiochem) as primary antibodies (1:1000) and anti-goat IgG or anti-rabbit IgG conjugated with horseradish peroxidase as secondary antibodies (1:1000). Bands were visualized with the enhanced chemiluminescence system (Amersham Biosciences).

Histological Analyses—Skeletal muscle (soleus) samples were frozen in liquid nitrogen-cooled isopentane, and transverse serial sections were stained with ATPase at pH 4.3 to detect type I fibers and at pH 10.5 to detect type II fibers (48). The ratio of type I fibers to type II fibers and the size (area) of skeletal muscle cells were determined by counting cell numbers in six randomly selected cross-section areas (each 900 μ m²) stained with ATPase at pH 4.3.

Blood Analysis—Blood samples were obtained from mice tail tips for hormone and metabolite determination under feeding conditions. Immunoreactive insulin was measured by an insulin assay kit (Morinaga,

Kanagawa, Japan), free fatty acid by NEFA C-test Wako (Wako Biochemicals, Osaka, Japan), lactate by the lactate reagent (Sigma), and glucose by the TIDEX glucose analyzer (Sankyo, Tokyo, Japan).

Running Wheel Activity—Mice were housed individually in cages (9 × 22 × 9 cm) equipped with a running wheel (20-cm in diameter, Shinano Co., Tokyo, Japan). Each wheel revolution was registered by a magnetic switch, which was connected to a counter. The number of revolutions was recorded daily for 6 days.

Oral Glucose and Insulin Tolerance Test—For the oral glucose tolerance test, D-glucose (1 mg/g of body weight, 10% (w/v) glucose solution) was administered with a stomach tube after an overnight fast. Blood samples were obtained by cutting the tail tip before and 30, 60, and 120 min after glucose administration. For the insulin tolerance test, human insulin (Humulin R; Lilly) was injected intraperitoneally (0.75 milliunits/g of body weight) into fed animals. Blood glucose concentrations were measured using a TIDEX glucose analyzer (Sankyo, Tokyo, Japan).

Microarray Analyses—RNA was isolated from skeletal muscle (quadriceps) of sex- and age-matched FOXO1 mice (A1 and A2 lines) and control mice (males at 4 months of age, RNA from three mice of each group were combined). Each of the combined samples was hybridized to the Affymetrix MGU74A microarray, which contains 12,489 genes including ESTs, and analyzed with the Affymetrix Gene Chip 3.1 software as described previously (49). Of the 12,489 genes including ESTs analyzed, 2500 (nontransgenic control mice), 2490 (line A1, transgenic), and 2510 (line A2, transgenic) genes were expressed at a substantial level (absolute call is present and average difference is above 150). Genes were classified on the basis of the biological function of the encoded protein, using a previously established classification scheme (50). The classification scheme was composed of seven major functional categories and several minor functional categories within the major categories.

Statistical Analyses—Statistical comparisons of data from the experimental groups were performed by the one-way analysis of variance, and groups were compared using the Fisher's protected least significant difference test (Statview 5.0, Abacus Concepts, Inc., Berkeley, CA). The glucose and insulin tolerance curves were compared by repeated measure analysis (Statview 5.0, Abacus Concepts). When significant, groups were compared by the Fisher's protected least significant difference test. Statistical significance was defined as $p < 0.05$.

RESULTS

Creation of FOXO1 Mice—The human skeletal muscle α -actin promoter (45) was used to drive the expression of the human FOXO1 transgene in mice (Fig. 1A). During development, cardiac muscle α -actin is the predominant isoform of sarcomeric α -actin in mice, and the switch to skeletal muscle α -actin occurs postpartum (45). Thus, by using the skeletal muscle α -actin promoter, the possibility that embryonic expression of FOXO1 might interfere with development was minimized. We obtained two independent lines of transgenic mice (lines A1 and A2). Southern blot analysis of DNA obtained from mouse tails was performed as shown in Fig. 1B. The transgene copy number of each animal was estimated by densitometric scanning of the autoradiographs from the Southern blots.

Expression of the FOXO1 transgene was evaluated by Northern blot analysis with RNA isolated from the tissues of FOXO1 mice and age-matched control mice at 8 weeks of age (Fig. 1C). The use of this promoter resulted in predominantly high expression levels of the FOXO1 transgene in skeletal muscle (about 3.5 kb). The A2 line showed expression levels of the FOXO1 transgene in skeletal muscle that were similar to or slightly higher than that in the A1 line. Transgene expression was observed not only in the gastrocnemius and quadriceps but also in other areas of skeletal muscle including the tibialis anterior, extensor digitorum longus (EDL), and soleus (not shown). The blot was then re-hybridized with a cDNA probe of Gadd45 α , an authentic target gene of FOXO1 (51, 52). As expected, induction of the expression of Gadd45 α was observed in skeletal muscle but not in other tissues in both FOXO1 transgenic mouse lines (Fig. 1C), indicating that the transgene expressed a functional FOXO1 protein. By using an antibody that recognizes both human and mouse FOXO1, we confirmed

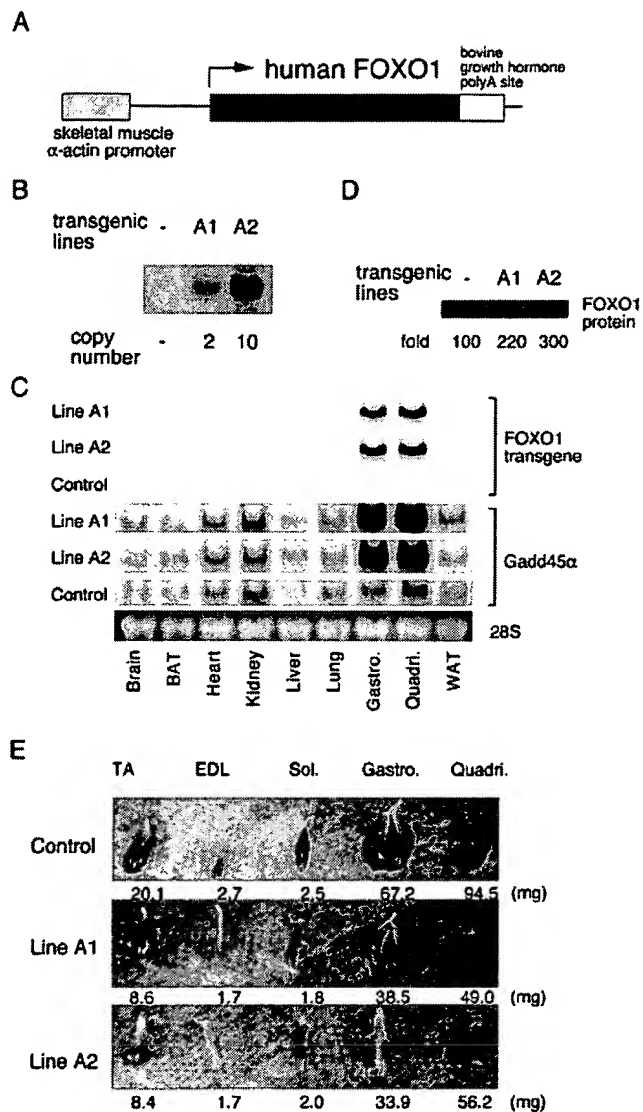


FIG. 1. Creation of FOXO1 transgenic mice. A, map of the 5-kb construct used for transgenic microinjection. The transgene was under the control of the human skeletal muscle α -actin promoter and included exon 1 and the intron of the human skeletal muscle α -actin gene as well as the bovine growth hormone polyadenylation site (45). B, characterization of FOXO1 mice. Two transgenic lines, A1 and A2, were identified by Southern blot analyses of DNA obtained from the tail of each mouse. The copy number was 2 for A1 and 10 for A2, as estimated by densitometric scanning of the autoradiographs of the Southern blot. C, expression of the FOXO1 transgene in mice. Northern blot analysis of human FOXO1 mRNA expression in tissues from FOXO1 mice (line A1 and A2) and nontransgenic control mice. RNAs from brain, brown adipose tissue (BAT), heart, kidney, liver, lung, skeletal muscle (gastrocnemius (Gastro.) and quadriceps (Quadri.)), and white adipose tissue (WAT) were analyzed. The blots were re-hybridized with the Gadd45 α probe. Each lane contained 20 μ g of total RNA. 28 S ribosomal RNA staining of a sample from control mice is shown. Similar staining was observed in samples from transgenic mice (not shown). D, expression of the FOXO1 protein in the skeletal muscle of FOXO1 mice. Protein extracts (30 μ g per lane) were subjected to SDS-PAGE. The FOXO1 protein was detected by immunoblotting. The densitometric ratio is shown below the autoradiogram (the control was set as 100). E, comparison of representative samples of dissected skeletal muscle (TA, tibialis anterior; Sol., soleus; Gastro, gastrocnemius; Quadri, quadriceps) between FOXO1 mice and littermate control mice. Legs were removed from 4-month-old (lines A1 and A2) transgenic mice and age-matched control mice. Tibialis anterior, gastrocnemius, and quadriceps contain a mixture of type I and II fibers; EDL is enriched in type II fibers, and soleus is enriched in type I fibers (control). Average dry mass ($n = 3$ in each group) is shown below the panel. Muscles were smaller in size and paler in color in FOXO1 mice than in control mice.

TABLE I
FOXO1 mice are smaller in body weight and lean body mass

FOXO1 mice weighed less (body weight and lean body mass) than nontransgenic, age- and sex-matched controls, when measured at 5 months of age (line A1) and at 4 months of age (line A2). Fat content per body weight of control and FOXO1 mice did not differ significantly. Data on both male and female mice are shown. Food intake and blood analyses of these mice are also shown. Values represent means \pm S.E.

Mice	Numbers	Sex	Age	Body weight	Lean body mass	Fat content	Food intake	Free fatty acid	Lactate	Glucose	Insulin
				g	g	%	g/g/day	mEq/liter	mg/ml	mg/dl	pg/ml
Control	4	Male	5 months	29.0 \pm 1.0	24.1 \pm 0.3	20.8 \pm 1.6	0.18 \pm 0.005	0.30 \pm 0.025	53.0 \pm 4.3	163 \pm 2.9	1775 \pm 700
A1	4	Male		24.5 \pm 0.4 ^a	20.3 \pm 0.4 ^b	20.8 \pm 0.5	0.17 \pm 0.004	0.34 \pm 0.098	56.3 \pm 8.3	173 \pm 14	739 \pm 139
Control	4	Female		21.6 \pm 0.9	19.3 \pm 0.9	12.9 \pm 1.0	0.25 \pm 0.017	0.39 \pm 0.060	32.7 \pm 3.1	158 \pm 8.0	289 \pm 14
A1	6	Female		18.4 \pm 0.4 ^a	16.4 \pm 0.2 ^a	15.8 \pm 1.2	0.24 \pm 0.017	0.38 \pm 0.049	38.9 \pm 2.5	163 \pm 5.3	302 \pm 5
Control	4	Male	4 months	24.3 \pm 0.4	21.0 \pm 0.4	15.2 \pm 1.2	0.21 \pm 0.011	0.40 \pm 0.045	37.3 \pm 3.7	160 \pm 10	373 \pm 19
A2	4	Male		19.4 \pm 0.1 ^b	17.4 \pm 0.2 ^b	15.0 \pm 1.9	0.18 \pm 0.017	0.33 \pm 0.077	46.4 \pm 6.6	184 \pm 14	573 \pm 109
Control	4	Female		19.9 \pm 0.6	17.6 \pm 0.7	12.8 \pm 0.2	0.25 \pm 0.027	0.45 \pm 0.055	34.5 \pm 1.9	144 \pm 10	283 \pm 10
A2	4	Female		17.3 \pm 0.3 ^a	15.1 \pm 0.4 ^c	13.3 \pm 0.9	0.23 \pm 0.041	0.58 \pm 0.096	35.7 \pm 5.9	143 \pm 6.5	316 \pm 10

^a $p < 0.01$.

^b $p < 0.001$.

^c $p < 0.05$.

the presence of the FOXO1 protein in the skeletal muscle of FOXO1 mice (Fig. 1D). An \sim 2.2-fold (line A1) and 3-fold (line A2) increase in FOXO1 protein levels was observed. These increases were at the physiological level, since 24-h fasting has been shown to increase FOXO1 protein content by 2.5–3-fold (Ref. 53 and data not shown).

FOXO1 Mice Are Small—The apparent phenotype observed in FOXO1 mice was small stature and thinner legs than the control mice. Both male and female transgenic mice weighed about 10% less than the control mice at 5 weeks of age (not shown). We used DEXA to measure the lean body mass (body weight excluding fat weight) and the content of fat in the whole body of the A1 line (at 5 months of age) and the A2 line (at 4 months of age) in age- and sex-matched control mice (Table I). Both body weight and lean body mass were significantly lower in both male and female FOXO1 mice (both lines) than in control mice. However, the fat content per total body weight of both FOXO1 mouse lines was comparable with that of nontransgenic mice (Table I). Thus, the decrease in body weight of the FOXO1 mice is not caused by a decrease in body fat but by a decrease in lean body mass. Consistent with the data on decreased lean body mass, the skeletal muscles in FOXO1 mice were smaller in size and dry mass, as well as paler in color than those of control mice (Fig. 1E). Consumption of food per body weight was not significantly different between FOXO1 mice and control mice (Table I). Blood metabolite (free fatty acid, lactate, and glucose) and insulin levels did not differ significantly between FOXO1 mice and the controls (Table I).

Microarray Analysis—To obtain information on changes in gene expression in FOXO1 mice, we performed microarray analysis using RNA samples from skeletal muscle (quadriceps) of transgenic and control mice. Most interestingly, the largest category of genes with suppressed expression in the transgenic mice was those involved in cell structure. Namely, about half of the down-regulated genes were classified as cytoskeletal proteins (Table II). The FOXO1-induced genes were distributed throughout various categories (not shown, see Supplemental Material 1).

In the skeletal muscle of FOXO1 mice, there was a decrease in the expression levels of genes related to structural proteins of the type I fiber (slow twitch oxidative, red muscle), such as slow muscle isoforms of myosins (Table II, line numbers 1, 4, and 6), slow isoforms of troponins (Table II, line numbers 2, 5, and 7), α -tropomyosin slow type (Table II, line number 13), myoglobin (Table II, line number 12), and mtCK (Table II, line number 15), which are abundant in type I fibers (54). This is consistent with the observation that the skeletal muscles of FOXO1 mice are pale (Fig. 1E). In the microarray, the expression of mitochondrial oxidative metabolism genes, such as the

electron transport system, did not differ between FOXO1 mice and controls (not shown). In large mammals such as humans, type I fibers are higher in mitochondrial content and more dependent on oxidative metabolism than type II fibers. In small mammals (e.g. mouse and rat), a large amount of mitochondria is seen in type II fibers as well as type I fibers (2). The large amount of mitochondria in both type I and type II fibers in mice would explain the unchanged gene expression of the mitochondrial electron transport system, although expression of type I fiber genes was markedly suppressed. In addition, the gene expression of type II fiber isoforms did not differ (not shown). Namely, expression of genes preferentially abundant in type I fibers appears to be suppressed in the skeletal muscle of FOXO1 mice.

Northern Blot Analysis of Representative Genes—We recognize the limitation of single microarray assays, as they can contain certain noise in the data. Thus, to verify the changes of gene expression found in the microarray analysis, we performed Northern blot analysis by using probes for several genes. In addition to representative genes in the list (Table II), we also analyzed several additionally selected genes of type I fiber or type II fiber markers or genes that may be involved in fiber differentiation. FOXO1 overexpression did not significantly affect mRNA levels of the other FOXO members, FOXO4 and FOXO3a (Fig. 2A). Consistent with the microarray data, a reduction in gene expression was confirmed for type I fiber proteins, such as troponin C (slow) (Table II, line number 2), MLC (slow) (Table II, line number 6), troponin T (slow) (Table II, line number 7), myoglobin (Table II, line number 12), and mtCK (Table II, line number 15) (Fig. 2A). On the other hand, expression levels of genes for components of the mitochondrial electron transport system, such as cytochrome c oxidase II and IV (COX II and IV), and the F_0F_1 -ATPase, were not markedly changed in the skeletal muscle of FOXO1 mice. Next, we examined type II fiber genes. The expression of genes for troponin I (fast), troponin T (fast), and MLC (fast) did not differ between FOXO1 mice and control mice. Thus, the results of the microarray analysis were confirmed by Northern blot analysis. In addition, given that Mef2, NFAT, CaMK, and PGC-1 α have been implicated recently in regulating gene expression in type I fibers (14–18, 22), we also examined the level of their expression in skeletal muscle of control and FOXO1 mice. PGC-1 α mRNA levels were slightly increased in the skeletal muscle of FOXO1 mice (line A2). Most interestingly, expression levels of Mef2c and CaMK were reduced in FOXO1 mice. FOXO1-mediated down-regulation of type I fiber genes may, in part, be regulated by Mef2c and CaMK.

Moreover, we examined the expression levels of genes whose expression levels are known to be changed during skeletal

TABLE II
Gene with decreased expression in the skeletal muscle of FOXO1 mice

The expression levels of 22 genes were significantly decreased in both the A1 and A2 lines of FOXO1 mice. The genes are listed in the order of greatest fold change in expression in skeletal muscle from line A1 mice relative to control mice. Fold change calculations were carried out as an indication of the relative change of each transcript represented on the probe array. The average difference value is a marker of abundance of each gene. Categories and subcategories are based on a previously established classification scheme (50) and literature review. Change (↓) indicates that expression is significantly decreased compared with control mice.

	GenBank™ accession no.	Gene description	Categories	Subcategories	Fold change (line A1)	Fold change (line A2)	Average difference (control)	Average difference (line A1)	Average difference (line A2)
1	AJ223362	Myosin, heavy polypeptide 7, cardiac muscle, β	Cell structure	Cytoskeletal	-57.6 ↓	-41.8 ↓	418	-97	10
2	M29793	Troponin C (cardiac/slow skeletal isoform)	Cell structure	Cytoskeletal	-30.4 ↓	-9.7 ↓	260	2	39
3	U88623	Aquaporin 4	Metabolism	Transport	-21 ↓	-10.2 ↓	259	10	21
4	X12972	Myosin alkali light chain (ventricular/slow muscle isoform)	Cell structure	Cytoskeletal	-6.8 ↓	-2.1 ↓	937	129	450
5	AJ242874	Troponin I, skeletal, slow 1	Cell structure	Cytoskeletal	-6.7 ↓	-3.2 ↓	313	48	109
6	M91602	Myosin light chain 2 (cardiac ventricle isoform)	Cell structure	Cytoskeletal	-5.8 ↓	-3 ↓	1038	165	316
7	AV213431	Troponin T1 (slow twitch isoform)	Cell structure	Cytoskeletal	-4.4 ↓	-3.1 ↓	772	174	246
8	M74570	Aldehyde dehydrogenase II	Metabolism	Sugar/glycolysis	-4 ↓	-2.8 ↓	567	140	209
9	U34277	Platelet-activating factor acetylhydrolase	Cell defense	Homeostasis	-3.1 ↓	-2 ↓	238	77	120
10	AI646638	Clone MGC:37615 IMAGE:4989784, mRNA,	Not found in the list		-2.9 ↓	-2.2 ↓	150	51	68
11	D45203	Pentylentetrazole-related mRNA PTZ-17	Not found in the list		-2.8 ↓	-3 ↓	1232	434	411
12	X04405	Myoglobin	Cell defense	Homeostasis	-2.8 ↓	-1.8 ↓	2484	812	1410
13	U04541	Tropomyosin 3 (slow twitch isoform)	Cell structure	Cytoskeletal	-2.7 ↓	-2.4 ↓	662	243	273
14	X92665	Ubiquitin-conjugating enzyme E2E1	Protein expression	Post-translational modification	-2.1 ↓	-1.7 ↓	298	187	175
15	AV250974	Creatine kinase, mitochondrial 2	Metabolism	Sugar/glycolysis	-2 ↓	-1.8 ↓	671	300	339
16	X57349	Transferrin receptor	Cell defense	Homeostasis	-1.9 ↓	-2.8 ↓	276	121	82
17	L12447	Insulin-like growth factor-binding protein 5	Unclassified		-1.9 ↓	-1.9 ↓	2080	1111	1095
18	Z38015	Myotonic protein kinase	Cell signaling	Protein modification	-1.9 ↓	-1.8 ↓	684	361	374
19	AB010144	Mitsugumin29, a synaptophysin family	Cell structure	General	-1.8 ↓	-2.4 ↓	742	414	312
20	X63615	Calcium/calmodulin-dependent protein kinase II, β	Cell signaling	Protein modification	-1.8 ↓	-2.1 ↓	295	160	146
21	U00677	Syntrophin, acidic 1	Cell structure	Cytoskeletal	-1.7 ↓	-1.7 ↓	857	504	491
22	AF032099	Potassium voltage-gated channel	Cell signaling	Channel/transport	-1.5 ↓	-1.6 ↓	320	209	195

muscle atrophy such as caused by fasting, cachexia, and STZ-induced diabetes (55). Specifically, gene expression of atrogin 1/MuRF1, MuRF1 (both are ubiquitin ligases), and cathepsin L (a lysosomal protease) is up-regulated and IGFBP5 is down-regulated during skeletal muscle atrophy (55). In our Northern blot analysis, the level of atrogin 1 expression was increased in the A2 line of FOXO1 mice, which has less skeletal muscle, but not in the A1 line, which also has less skeletal muscle mass than nontransgenic controls. In both the A1 and A2 lines of FOXO1 mice, the expression of cathepsin L and IGFBP5 was increased and decreased, respectively. The MuRF1 mRNA level was not changed. Thus, atrophy-related gene expression changes including that of protein degradation likely occurred in the skeletal muscle of FOXO1 mice.

Western Blot Analysis of the Skeletal Muscle of FOXO1 Mice and PGC-1 α Mice—We examined the expression of various gene products of FOXO1 mice at the protein level by Western blot analysis (Fig. 2B). Protein extracts from the skeletal muscle of FOXO1 mice (A1 and A2 lines) and wild-type control mice were used. For comparison, we analyzed protein extracts from the skeletal muscle of PGC-1 α transgenic mice, which we previously analyzed (23). Protein levels of troponin I (slow) and myoglobin, which are rich in type I fibers, were increased in

PGC-1 α mice but decreased in FOXO1 mice (Fig. 2B). On the other hand, the protein level of troponin I (fast), which is rich in type II fibers, was decreased in PGC-1 α mice but not in FOXO1 mice (Fig. 2B). Thus, Western blot analysis of the protein expression of genes for type I and type II fibers was consistent with the results of mRNA expression analysis.

Histological Analysis of Skeletal Muscle of FOXO1 Mice—We examined the relationship between the change in type I fiber gene expression and actual muscle fiber morphology in the skeletal muscle (soleus) of transgenic mice using light microscopy and histochemical procedures (A1 line, 4 months after birth; A2 line, 3 months after birth). Distinction between type I and type II fibers can be made by myosin ATPase staining at different pH values. Specifically, at pH 10.5, type II fibers are well stained but not type I fibers, and at pH 4.3, type I fibers are well stained but not type II fibers (2). ATPase staining revealed that skeletal muscle cells (both type I and type II fibers) in the FOXO1 mice are smaller than those of the control mice (average cross-sectional area of muscle fibers; A1 line, $11.5 \pm 0.8 \mu\text{m}^2$ in FOXO1 mice and $20.0 \pm 2.7 \mu\text{m}^2$ in control mice; A2 line, $9.8 \pm 0.5 \mu\text{m}^2$ in FOXO1 mice and $14.1 \pm 1.9 \mu\text{m}^2$ in control mice) and had fewer type I fibers than those in the control mice (average; A1 line, $28.6 \pm 1.3\%$ in FOXO1 mice and

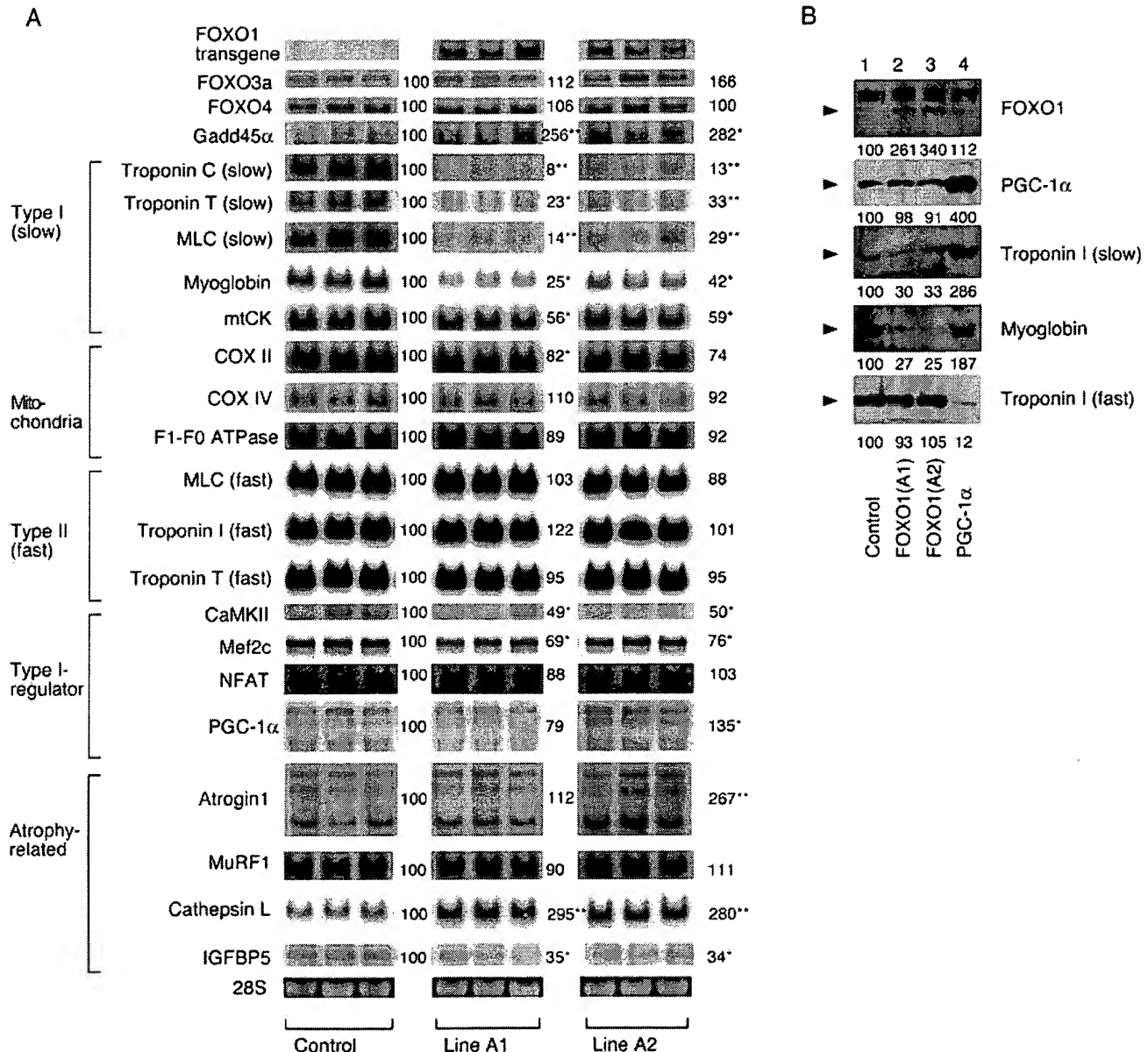


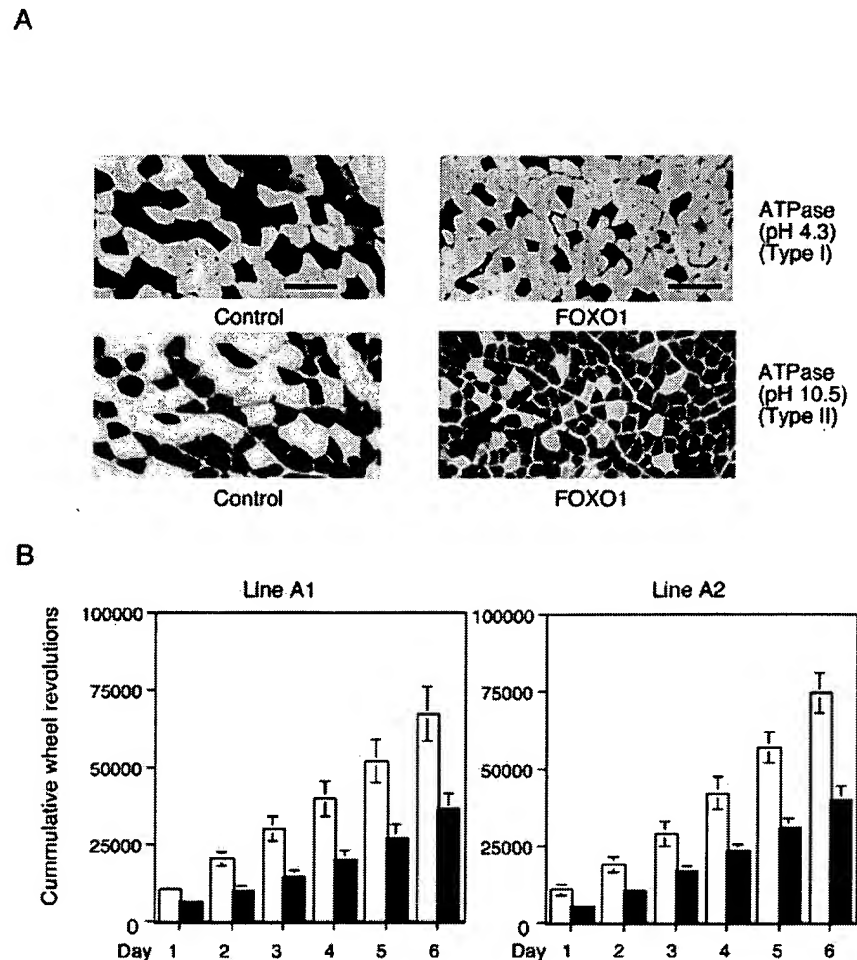
FIG. 2. Gene product levels in the skeletal muscle of FOXO1 mice. **A**, Northern blot analysis was performed on total RNA (20 μ g per lane) isolated from skeletal muscle (quadriceps) of FOXO1 mice (line A1 and line A2) and nontransgenic control mice. The same RNA sample sets were blotted onto multiple membranes and hybridized with the indicated probes. The names of genes examined are on the left of the autoradiograms, and average densitometric ratios (the control was set as 100) are on the right (*, $p < 0.05$; **, $p < 0.01$). Equal sample loading was confirmed by ethidium bromide staining of 28 S ribosomal RNA. Each lane represents a sample from an individual mouse. **B**, Western blot analysis was performed on protein extracts from the skeletal muscle of FOXO1 mice (A1 and A2 lines), PGC-1 α mice, and control mice. Antibodies against FOXO1, PGC-1 α , troponin I (slow), myoglobin, and troponin I (fast) were used. A typical autoradiogram, representative of three independent experiments with similar results, is shown. Numbers below the panels are values of the densitometric ratios (the signal of the control for each sample was set as 100). Corresponding bands are indicated by arrowheads. The approximate estimated molecular sizes are as follows: FOXO1, 70 kDa; PGC-1 α , 90 kDa; troponin I (slow), 30 kDa; myoglobin, 30 kDa; and troponin (fast), 40 kDa.

37.8 \pm 2.2% in control; A2 line, 20.2 \pm 2.3% in FOXO1 mice and 40.4 \pm 2.0% in control) (Fig. 3A). Immunohistochemistry with antibodies to myoglobin (present at high concentrations in type I fibers) confirmed the reduction in the number of type I fibers in the skeletal muscle of FOXO1 mice (not shown). Skeletal muscle samples from FOXO1 mice had no structural abnormalities such as mitochondrial abnormalities, glycogen accumulation, vacuolar formation, and muscle fiber degeneration (not shown).

Running Wheel Activity of FOXO1 Mice—The mass and fiber composition of skeletal muscle are important for physical ex-

ercise. Type I fibers are more resistant to fatigue than type II fibers (2). As the FOXO1 mice had decreased total skeletal muscle mass and fewer type I fibers, they may have a low capacity for endurance, such as that needed in a marathon. We then compared the running wheel activity (spontaneous locomotive activity) in FOXO1 mice and control mice. Mice were transferred to cages with a running wheel and monitored daily for the number of wheel revolutions made for 6 days. Both lines of FOXO1 mice showed significantly fewer wheel revolutions (Fig. 3B). The decrease in running wheel activity suggested that FOXO1 mice were less able to sustain continuous muscle

FIG. 3. A, histological analysis of skeletal muscle. Light microscopy of ATPase (pH 4.3 for type I fibers and pH 10.5 for type II fibers)-stained transverse sections of skeletal muscle (soleus) specimens from FOXO1 mice (line A2) and control littermates at 3 months of age. Bars, 50 μ m. Skeletal muscle fibers of FOXO1 mice were thinner and contained fewer type I fibers than that of control mice. B, running wheel activity of FOXO1 mice. Mice were housed individually in cages equipped with a running wheel (20 cm in diameter). The number of revolutions made was recorded daily for 6 days, and the cumulative values are shown. Open column, control; closed column, FOXO1 mice. Running wheel activity was significantly ($p < 0.05$) reduced in FOXO1 mice (line A1, left; line A2, right) compared with control mice. Mice used were females at 10 weeks (line A1) and 9 weeks (line A2) of age. Numbers of animals used are as follows: line A1, control, $n = 6$; FOXO1 mice, $n = 5$; line A2, control, $n = 4$; FOXO1 mice, $n = 3$. Because male mice responded similarly, only the data from female mice are shown. C and D, oral glucose tolerance tests (C) and insulin tolerance tests (D) on FOXO1 mice. For the oral glucose tolerance test, mice were fasted overnight and given D-glucose (1 mg/g body weight) orally by a stomach tube. Blood glucose levels were determined at the times indicated. For the insulin tolerance test, mice were allowed free access to food and then given 0.75 milliunits of human insulin/g of body weight. Blood glucose levels were measured at the indicated time points. Mice used were males at 10 weeks (line A1) and 9 weeks (line A2) of age. The numbers of animals used were: line A1, control, $n = 6$; FOXO1 mice, $n = 5$; line A2, control, $n = 5$; FOXO1 mice, $n = 4$.



contractions than control mice, which is consistent with the reduction in the mass of skeletal muscle and the number of type I fibers.

Oral Glucose Tolerance Test and Insulin Tolerance Test on FOXO1 Mice—Skeletal muscle is important for glucose metabolism. To examine whether the decreased skeletal muscle mass of FOXO1 mice is affecting their systemic glucose homeostasis, we examined oral glucose tolerance and insulin tolerance in FOXO1 mice. Glucose tolerance was impaired in both lines of FOXO1 mice, namely peak blood glucose values in FOXO1 mice were elevated significantly above those of the control mice (Fig. 3C). The insulin tolerance test clearly demonstrated that the glucose-lowering effects of insulin were impaired in both the A1 and A2 lines of FOXO1 mice, compared with those in age- and sex-matched control mice (Fig. 3D). FOXO1 mice showed a low capacity for glucose metabolism and decreased insulin sensitivity. Adipose tissue, another organ playing a role in glucose metabolism, appears not to be involved in this impaired glycemic control because 1) body fat did not differ between FOXO1 mice and control mice (Table I), and 2) gene expression of glucose transporter 4, which is a rate-limiting molecule of insulin-dependent glucose intake (56), was not decreased in adipose tissue of FOXO1 mice (see Supplemental Material 2). FOXO1 mice may therefore represent a certain type of diabetic state in humans.

Change in Endogenous FOXO1 Expression by Physical Inactivity—We performed Northern blot analysis with RNA from the skeletal muscle of mice maintained under a long period of physical inactivity. The right hindlimbs of wild-type mice were

immobilized in plaster casts, and the left hindlimbs were left freely moving for the control sample. After 3 weeks in the plaster casts, skeletal muscle (gastrocnemius) weight of the right hindlimbs was significantly decreased compared with that in the controls (average, 88 ± 12 mg for immobilized and 149 ± 6 mg for freely moving controls, $n = 3$, $p < 0.05$). As shown in Fig. 4, the gene expression of troponin C (slow), myoglobin, and mtCK but not MLC (fast) and troponin T (fast) was markedly decreased in the plaster-casted muscle. At the same time, endogenous FOXO1 mRNA was increased in the immobilized muscle (Fig. 4). Furthermore, Gadd45 α was increased in the same sample. In addition, cathepsin L, but not atrogin 1 and MuRF1, were increased (Fig. 4). Thus, mRNAs of endogenous FOXO1, Gadd45 α , and cathepsin L were increased; skeletal muscle mass was decreased, and the expression of type I fiber genes but not type II fiber genes were decreased. The gene expression changes observed in the plaster-casted skeletal muscle were similar to the changes observed in the FOXO1 mice (Fig. 2A). These results further support the involvement of FOXO1 in the negative regulation of skeletal muscle mass and the expression of type I fiber genes.

DISCUSSION

To gain insight into the role of FOXO1 in skeletal muscle *in vivo*, we established transgenic mice overexpressing human FOXO1. The FOXO1 transgene was predominantly expressed in the skeletal muscle, and the increase in FOXO1 protein expression was within physiological levels. Most interestingly, the skeletal muscle of FOXO1 mice weighed less and was paler

C

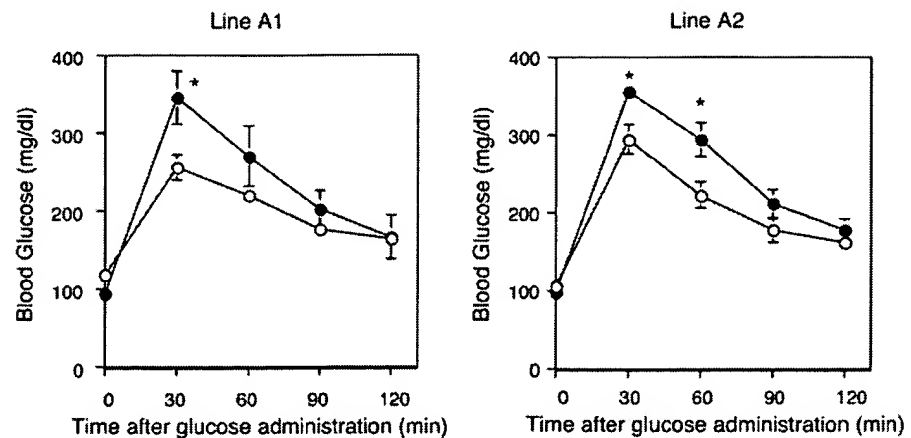
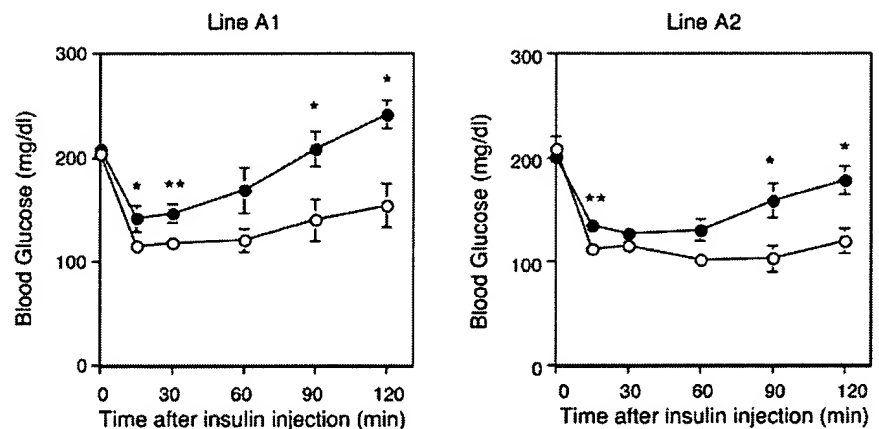


FIG. 3—continued

D



in color. The results of gene expression analyses showed that type I (red muscle) fiber-related gene expression was decreased in the skeletal muscle of FOXO1 mice. In addition, histological examinations showed that the skeletal muscle of FOXO1 mice had fewer type I fibers and smaller type I and type II fibers. Consistently, under long time physical inactivity by immobilizing skeletal muscle in plaster casts, an increased expression of endogenous FOXO1 mRNA and a markedly decreased expression of genes related to type I fibers were observed. These results suggest that FOXO1 is a negative regulator of skeletal muscle mass and expression of type I fiber-related genes. Moreover, FOXO1 mice showed poor glycemic control and low capacity for physical exercise, which involves the skeletal muscles, especially type I fibers. These phenotypes are consistent with the decreased mass of skeletal muscle including type I fibers in FOXO1 mice.

How does FOXO1 affect the skeletal muscle, including the reduction of mass of both type I and type II fibers and the suppressed expression of type I fiber genes? In the following, we discuss the possibility of involvement of FOXO1 in 1) growth, 2) protein degradation, and 3) differentiation of skeletal muscle.

1) FOXO1 may suppress increase of skeletal muscle mass. A genetic study of *C. elegans* showed that DAF16, the worm counterpart of FOXO, functions as a suppressor of insulin receptor-like signaling (44). Thus, the FOXO family might act negatively in mammals as a downstream player in insulin or IGF signaling. IGF-1 stimulates the proliferation of skeletal

muscle satellite cells (57). Mature skeletal muscle fibers are not able to proliferate. Skeletal muscle satellite cells, mononuclear cells located between the basement membrane and the plasma membrane of myofibers in mature cells, are important in post-natal skeletal muscle hypertrophy because of their ability to add new myonuclei into growing myofibers. Machida *et al.* (58) showed that FOXO1 inhibited IGF-1-mediated skeletal muscle cell proliferation. In primary skeletal muscle satellite cells, FOXO1 activates the promoter of p27 Kip1, an inhibitor of the cell cycle at the G₁ stage, which leads to inhibition of cell proliferation, and addition of IGF-1 reverses the FOXO1-mediated activation of the p27 Kip1 promoter (58). Unexpectedly, p27 Kip1 mRNA expression was unchanged in the skeletal muscle of FOXO1 mice compared with that of controls (not shown). As the ratio of satellite cells is very small in total skeletal muscle, the increased expression of p27 Kip1 in satellite cells may not have been detected in our assay. On the other hand, we showed enhanced expression of Gadd45 α , an inhibitor of the cell cycle at the G₂ stage (51, 52), in the skeletal muscle of FOXO1 mice (Figs. 1 and 2A). As a 0.7-kb stretch of the rat skeletal muscle α -actin promoter is active in skeletal muscle satellite cells (59), the FOXO1 transgene, driven by a 2-kb stretch of the human skeletal muscle α -actin promoter (45), is likely to be expressed in the skeletal muscle satellite cells of the FOXO1 mice. Thus, the increased amount of Gadd45 α and possibly p27 Kip1 in the skeletal muscle satellite cells of FOXO1 mice may have suppressed the proliferation of satellite cells and caused a decrease in skeletal muscle mass (size).

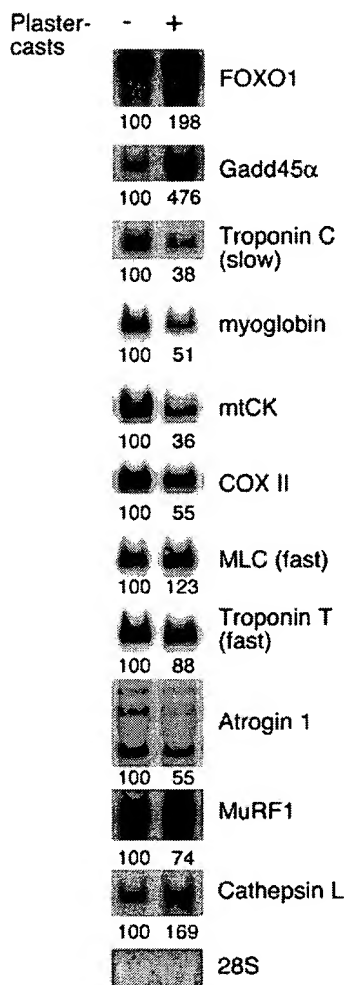


FIG. 4. Gene expression in skeletal muscle immobilized in plaster casts. The right hindlimbs of mice at 9 weeks of age were immobilized in plaster casts, and left hindlimbs of the mice were kept free for the control sample. After 3 weeks of immobilization in plaster casts, Northern analysis was performed on total RNA (20 μ g per lane) isolated from the skeletal muscle (gastrocnemius) of right hindlimbs and left hindlimbs. Plus and minus denote with or without immobilization, respectively. The names of the genes examined are on the right of the autoradiograms. A typical autoradiogram, representative of three independent mice with similar results, is shown. The densitometric ratio is shown below the autoradiograms (the control was set as 100).

2) FOXO1 may increase the degradation rate of skeletal muscle proteins. Gene expression of atrogin 1, MuRF1 (both are ubiquitin ligases), and cathepsin L (a lysosomal protease) is up-regulated and IGFBP5 is down-regulated during skeletal muscle atrophy caused by fasting, cachexia, STZ-induced diabetes, and other diseases (55). After we submitted our manuscript, a member of the FOXO family, FOXO3a, was reported to activate the gene expression of atrogin 1, and addition of IGF-1 was found to reverse the FOXO3a-mediated activation of the atrogin 1 promoter (60). Overexpression of an active form of FOXO3a reduces the size of skeletal muscle fibers, both *in vivo* and *in vitro* (60). In addition, another group reported that overexpression of an active form of FOXO1 in C2C12 muscle cells did not change the base-line expression of atrogin 1 and MuRF1, but the active form of FOXO1 suppresses IGF-1-mediated repression of atrogin 1 and MuRF1 expression induced by glucocorticoids (61). This suggests that FOXO1 expression is not sufficient for inducing atrophy-related genes, but FOXO1 is negatively involved in IGF-1-mediated suppression of atrophy of skeletal muscle. In our Northern blot analysis, the level of

atrogin 1 was increased in the A2 line but not in the A1 line of FOXO1 mice, although both had less skeletal muscle mass than the nontransgenic controls. In both the A1 and A2 lines of FOXO1 mice, the expression of cathepsin L and IGFBP5 was increased and decreased, respectively. MuRF1 mRNA levels were not altered in both lines. Thus, atrophy-related protein degradation probably occurs in the skeletal muscle of FOXO1 mice and could explain, in part, the decrease in skeletal muscle mass of the FOXO1 mice. However, the increase in atrogin 1 is unlikely to be enough to cause the decrease in skeletal muscle mass of FOXO1 mice, because the expression level did not change in the A1 line of FOXO1 mice. This is consistent with the description by Sandri *et al.* (60) that overexpression of atrogin 1 alone does not cause myotube or muscle atrophy. On the other hand, IGFBP5 is reported to modulate the activity of IGF-1 (62), and hence decreased expression of IGFBP5 may contribute to the decrease in skeletal muscle mass by affecting IGF-1 action. FOXO1 transgene expression was observed in both type I fiber-rich soleus and type II fiber-rich EDL. Thus, changes in the expression of atrophy-related genes may be an alternative molecular explanation for the decreased skeletal muscle mass, including the size of both type I and type II fibers of FOXO1 mice.

3) Does FOXO1 inhibit the differentiation of type I fibers? The FOXO1 transgene is expressed in muscles rich in both type I and type II fibers. How does it cause the selective reduction of gene expression in type I fibers but not in type II fibers? It is possible that FOXO1 suppresses the function of a factor(s) that is preferentially expressed in type I fibers and therefore activates gene expression only in type I fibers. One candidate for such a factor is PGC-1 α , which is known to be preferentially expressed in type I fibers and enhances type I fiber gene expression (22). As the FOXO1 protein can interact with the PGC-1 α protein (43), FOXO1 may affect certain functions of PGC-1 α . FOXO1 may inhibit PGC-1 α function via its binding to PGC-1 α . FOXO1 itself is a transcription factor. In addition, several reports (27–30) have shown that FOXO1 acts as a corepressor of nuclear receptors, whereas PGC-1 α can activate many nuclear receptors (21, 63). Although to our knowledge nuclear receptors have not been shown to be involved in type I fiber-specific gene expression, a certain nuclear receptor(s) and transcription factor(s), which can interact with both FOXO1 and PGC-1 α , may be involved in a process positively and negatively regulated by PGC-1 α and FOXO1, respectively. Further studies are required to examine this possibility. Besides, although PGC-1 α stimulates the differentiation of type I fibers, in FOXO1 mice, gene expression was reduced in type I fibers but was not affected in type II fibers. Thus, fiber differentiation (switching) from type I to type II is not likely to occur in FOXO1 mice, and FOXO1 appears not to be involved in fiber differentiation.

Calcineurin (14, 17) and CaMK (15), downstream molecules of calcium signaling (13), the transcription factors Mef2c (14–16, 18) and NFAT (14, 15, 17), as well as the nuclear receptor coactivator PGC-1 α (22) are known to promote type I fiber differentiation and type I fiber gene expression. In skeletal muscle of FOXO1 mice, mRNA levels of Mef2c and CaMK are significantly decreased (Fig. 2A). FOXO1 may reduce gene expression in type I fiber by suppressing gene expression of Mef2c and CaMK.

FOXO1 mice showed a clear phenotype related to the function of skeletal muscle. Specifically, spontaneous locomotor activity was lower in FOXO1 mice than in control mice (Fig. 3B). In addition, FOXO1 mice had impaired oral glucose tolerance and impaired insulin-mediated glucose-lowering effects (Fig. 3, C and D). Elderly humans have been reported to show

a progressive loss of muscle fibers associated with diabetes, obesity, and decreased physical activity (sarcopenia). Overexpression of IGF-1 in skeletal muscle prevents the age-related decline in muscle mass (11, 57). As described above, the reduced skeletal muscle mass in FOXO1 mice may be caused by the suppression of IGF signaling during skeletal muscle formation, and FOXO1 may therefore be involved in age-related sarcopenia in humans. FOXO1 mice may be valuable as a model for human diseases related to loss of muscle fibers. Further analysis of the molecular mechanisms of FOXO1 action in skeletal muscle is important from a clinical as well as a sports science perspective.

Acknowledgments—We thank H. Meguro for technical assistance, Dr. S. Machida (University of Missouri, Columbia) for valuable comments, and Dr. H. A. Popiel for proofreading.

REFERENCES

- Zurlo, F., Larson, K., Bogardus, C., and Ravussin, E. (1990) *J. Clin. Invest.* **86**, 1423–1427
- Berchtold, M. W., Brinkmeier, H., and Muntener, M. (2000) *Physiol. Rev.* **80**, 1215–1265
- Proctor, D., Balagopal, P., and Nair, K. (1998) *J. Nutr.* **128**, S351–S355
- Fitts, R., Riley, D., and Widrick, J. (2001) *J. Exp. Biol.* **204**, 3201–3208
- Hickey, M. S., Carey, J. O., Azevedo, J. L., Houmard, J. A., Pories, W. J., Israel, R. G., and Dohm, G. L. (1995) *Am. J. Physiol.* **268**, E453–E457
- Gaster, M., Staehr, P., Beck-Nielsen, H., Schroder, H. D., and Handberg, A. (2001) *Diabetes* **50**, 1324–1329
- Tanner, C. J., Barakat, H. A., Dohm, G. L., Pories, W. J., MacDonald, K. G., Cunningham, P. R., Swanson, M. S., and Houmard, J. A. (2002) *Am. J. Physiol.* **282**, E1191–E1196
- Frost, R. A., and Lang, C. H. (2003) *Minerva Endocrinol.* **28**, 53–73
- DeVol, D., Rotwein, P., Sadow, J., Novakofski, J., and Bechtel, P. (1990) *Am. J. Physiol.* **259**, E89–E95
- Zdanowicz, M., Moysse, J., Wingertzahn, M., O'Connor, M., Teichberg, S., and Slonim, A. (1995) *Endocrinology* **136**, 4880–4886
- Barton-Davis, E. R., Shotorbani, D. I., Musaro, A., Rosenthal, N., and Sweeney, H. L. (1998) *Proc. Natl. Acad. Sci. U. S. A.* **95**, 15603–15607
- Florini, J., Ewton, D., and Coolican, S. (1996) *Endocr. Rev.* **17**, 481–517
- Stull, J. T. (2001) *J. Biol. Chem.* **276**, 2311–2312
- Chin, E. R., Olson, E. N., Richardson, J. A., Yang, Q., Humphries, C., Shelton, J. M., Wu, H., Zhu, W., Bassel-Duby, R., and Williams, R. S. (1998) *Genes Dev.* **12**, 2499–2509
- Wu, H., Naya, F. J., McKinsey, T. A., Mercer, B., Shelton, J. M., Chin, E. R., Simard, A. R., Michel, R. N., Bassel-Duby, R., Olson, E. N., and Williams, R. S. (2000) *EMBO J.* **19**, 1963–1973
- Yan, Z., Serrano, A. L., Schiaffino, S., Bassel-Duby, R., and Williams, R. S. (2001) *J. Biol. Chem.* **276**, 17361–17366
- Chakkalakal, J. V., Stocksley, M. A., Harrison, M. A., Angus, L. M., Deschenes-Furry, J., St-Pierre, S., Megoney, L. A., Chin, E. R., Michel, R. N., and Jasmin, B. J. (2003) *Proc. Natl. Acad. Sci. U. S. A.* **100**, 7791–7796
- Karasheva, N., Tsika, G., Ji, J., Zhang, A., Mao, X., and Tsika, R. (2003) *Mol. Cell. Biol.* **23**, 5143–5164
- Kamei, Y., Xu, L., Heinzel, T., Torchia, J., Kurokawa, R., Gloss, B., Lin, S. C., Heyman, R. A., Rose, D. W., Glass, C. K., and Rosenfeld, M. G. (1996) *Cell* **85**, 403–414
- Glass, C. K., Rose, D. W., and Rosenfeld, M. G. (1997) *Curr. Opin. Cell Biol.* **9**, 222–232
- Puigserver, P., Wu, Z., Park, C. W., Graves, R., Wright, M., and Spiegelman, B. M. (1998) *Cell* **92**, 829–839
- Lin, J., Wu, H., Tarr, P. T., Zhang, C. Y., Wu, Z., Boss, O., Michael, L. F., Puigserver, P., Isotani, E., Olson, E. N., et al. (2002) *Nature* **418**, 797–801
- Miura, S., Kai, Y., Ono, M., and Ezaki, O. (2003) *J. Biol. Chem.* **278**, 31385–31390
- Anderson, M. J., Viars, C. S., Czekay, S., Cavenee, W. K., and Arden, K. C. (1998) *Genomics* **47**, 187–199
- Kaestner, K. H., Knochel, W., and Martinez, D. E. (2000) *Genes Dev.* **14**, 142–146
- Galili, N., Davis, R. J., Fredericks, W. J., Mukhopadhyay, S., Rauscher, F. J., 3rd, Emanuel, B. S., Rovera, G., and Barr, F. G. (1993) *Nat. Genet.* **5**, 230–235
- Schuur, E. R., Loktev, A. V., Sharma, M., Sun, Z., Roth, R. A., and Weigel, R. J. (2001) *J. Biol. Chem.* **276**, 33554–33560
- Zhao, H. H., Herrera, R. E., Coronado-Heinsohn, E., Yang, M. C., Ludes-Meyers, J. H., Seybold-Tilson, K. J., Nawaz, Z., Yee, D., Barr, F. G., Diab, S. G., Brown, P. H., Fuqua, S. A. W., and Osborne, C. K. (2001) *J. Biol. Chem.* **276**, 27907–27912
- Dowell, P., Otto, T. C., Adi, S., and Lane, M. D. (2003) *J. Biol. Chem.* **278**, 45485–45491
- Hirota, K., Daitoku, H., Matsuzaki, H., Araya, N., Yamagata, K., Asada, S., Sugaya, T., and Fukamizu, A. (2003) *J. Biol. Chem.* **278**, 13056–13060
- Ayala, J. E., Streeper, R. S., Desrosellier, J. S., Durham, S. K., Suwanichkul, A., Svitek, C. A., Goldman, J. K., Barr, F. G., Powell, D. R., and O'Brien, R. M. (1999) *Diabetes* **48**, 1885–1889
- Barthel, A., Schmoll, D., Bahrenberg, G., Walther, R., Roth, R. A., and Joost, H. G. (2001) *Biochem. Biophys. Res. Commun.* **285**, 897–902
- Nakae, J., Kitamura, T., Silver, D. L., and Accili, D. (2001) *J. Clin. Invest.* **108**, 1359–1367
- Nadal, A., Marrero, P. F., and Haro, D. (2002) *Biochem. J.* **366**, 289–297
- Dijkers, P. F., Medema, R. H., Pals, C., Banerji, L., Thomas, N. S. B., Lam, E. W. F., Burgering, B. M. T., Raaijmakers, J. A. M., Lammers, J. W. J., Koenderman, L., and Coffey, P. J. (2000) *Mol. Cell. Biol.* **20**, 9138–9148
- Medema, R. H., Kops, G. J. P. L., Bos, J. L., and Burgering, B. M. T. (2000) *Nature* **404**, 782–787
- Brunet, A., Bonni, A., Zigmond, M. J., Lin, M. Z., Juo, P., Hu, L. S., Anderson, M. J., Arden, K. C., Blenis, J., and Greenberg, M. E. (1999) *Cell* **96**, 857–868
- Kops, G. J. P. L., Dansen, T. B., Polderman, P. E., Saarloos, I., Wirtz, K. W. A., Coffey, P. J., Huang, T. T., Bos, J. L., Medema, R. H., and Burgering, B. M. T. (2002) *Nature* **419**, 316–321
- Nakae, J., Kitamura, T., Kitamura, Y., Biggs, W. H., III, Arden, K. C., and Accili, D. (2003) *Dev. Cell* **4**, 119–129
- Bois, P. R. J., and Grosfeld, G. C. (2003) *EMBO J.* **22**, 1147–1157
- Nakae, J., Biggs, W. H., III, Kitamura, T., Cavenee, W. K., Wright, C. V., Arden, K. C., and Accili, D. (2002) *Nat. Genet.* **32**, 245–253
- Kamei, Y., Mizukami, J., Miura, S., Suzuki, M., Takahashi, N., Kawada, T., Taniguchi, T., and Ezaki, O. (2003) *FEBS Lett.* **536**, 232–236
- Puigserver, P., Rhee, J., Donovan, J., Walkey, C. J., Yoon, J. C., Oriente, F., Kitamura, Y., Altomonte, J., Dong, H., Accili, D., and Spiegelman, B. M. (2003) *Nature* **423**, 550–555
- Ogg, S., Paradis, S., Gottlieb, S., Patterson, G. I., Lee, L., Tissenbaum, H. A., and Ruvkun, G. (1997) *Nature* **389**, 994–999
- Brennan, K. J., and Hardeman, E. C. (1993) *J. Biol. Chem.* **268**, 719–725
- Nagy, T. R., and Clair, A. L. (2000) *Obes. Res.* **8**, 392–398
- Hahn, C. G., and Covault, J. (1990) *Anal. Biochem.* **190**, 193–197
- Ogilvie, R. W., and Feedback, D. L. (1990) *Stain Technol.* **65**, 231–241
- Takahashi, M., Tsuboyama-Kasaoka, N., Nakatani, T., Ishii, M., Tsutsumi, S., Aburatani, H., and Ezaki, O. (2002) *Am. J. Physiol.* **282**, G338–G348
- Adams, M. D., Kerlavage, A. R., Fleischmann, R. D., Feldner, R. A., Bult, C. J., Lee, N. H., Kirkness, E. F., Weinstock, K. G., Gocayne, J. D., White, O., et al. (1995) *Nature* **377**, 3–174
- Furukawa-Hibi, Y., Yoshida-Araki, K., Ohta, T., Ikeda, K., and Motoyama, N. (2002) *J. Biol. Chem.* **277**, 26729–26732
- Tran, H., Brunet, A., Grenier, J. M., Datta, S. R., Fornace, A. J., Jr., DiStefano, P. S., Chiang, L. W., and Greenberg, M. E. (2002) *Science* **296**, 530–534
- Furuyama, T., Kitayama, K., Yamashita, H., and Mori, N. (2003) *Biochem. J.* **375**, 365–371
- Garry, D. J., Ordway, G. A., Lorenz, J. N., Radford, N. B., Chin, E. R., Grange, R. W., Bassel-Duby, R., and Williams, R. S. (1998) *Nature* **395**, 905–908
- Lecker, S., Jagoe, R., Gilbert, A., Gomes, M., Baracos, V., Bailey, J., Price, S., Mitch, W., and Goldberg, A. (2004) *FASEB J.* **18**, 39–51
- Ezaki, O. (1997) *Biochem. Biophys. Res. Commun.* **241**, 1–6
- Chakravarthy, M., Davis, B., and Booth, F. (2000) *J. Appl. Physiol.* **89**, 1365–1379
- Machida, S., Spangenburg, E., and Booth, F. (2003) *J. Cell. Physiol.* **196**, 523–531
- Yamanouchi, K., Soeta, C., Suzuki, S., Hasegawa, T., Naito, K., and Tojo, H. (2000) *J. Vet. Med. Sci.* **62**, 1213–1216
- Sandri, M., Sandri, C., Gilbert, A., Skurk, C., Calabria, E., Picard, A., Walsh, K., Schiaffino, S., Lecker, S., and Goldberg, A. (2004) *Cell* **117**, 399–412
- Stitt, T., Drujan, D., Clarke, B., Panaro, F., Timofeyeva, Y., Kline, W., Gonzalez, M., Yancopoulos, G., and Glass, D. (2004) *Mol. Cell* **14**, 395–403
- Schneider, M., Wolf, E., Hoeflich, A., and Lahm, H. (2002) *J. Endocrinol.* **172**, 423–440
- Kamei, Y., Ohizumi, H., Fujitani, Y., Nemoto, T., Tanaka, T., Takahashi, N., Kawada, T., Miyoshi, M., Ezaki, O., and Kakizuka, A. (2003) *Proc. Natl. Acad. Sci. U. S. A.* **100**, 12378–12383

Review

Obesity, Glucose Intolerance and Diabetes and Their Links to Cardiovascular Disease. Implications for Laboratory Medicine

Marek H. Dominiczak*

Department of Biochemistry, Gartnavel General Hospital, and the Medical Humanities Unit, North Glasgow University Hospitals NHS Trust, Glasgow, UK

This article provides an overview of the role of metabolite toxicity, low-grade inflammation and disturbed cellular signaling in obesity, glucose intolerance and diabetes. It also highlights links between this continuum of deteriorating glucose tolerance and atherosclerosis.

Obesity, diabetes mellitus, and cardiovascular disease are all related to diet and to the level of physical activity. They have reached epidemic proportions worldwide. Glucose intolerance and diabetes increase the risk of atherosclerotic events. Moreover, obesity, and glucose intolerance or diabetes, are components of the metabolic syndrome, which also imparts an increased cardiovascular risk. There is increasing recognition that common mechanisms contribute to diabetes and cardiovascular disease. Following increased calorie intake and/or decreased physical activity, fuel metabolism generates excess of 'toxic' metabolites, particularly glucose and fatty acids. Homeostasis is affected by the endocrine output from the adipose tissue. Reactive oxygen species are generated, creating oxidative stress, which exerts major effects on signaling pathways, further affecting cellular metabolism and triggering low-grade inflammatory reaction.

This perspective on the diabetic syndrome has been reflected in the approach to its treatment, which integrates maintenance of glycemic control with primary and secondary cardiovascular prevention. Laboratory medicine should support diabetes care with an integrated package of tests which, in addition to glycemic control, enable assessment and monitoring of the risk of microvascular complications as well as cardiovascular disease. Clin Chem Lab Med 2003; 41(9):1266–1278

Key words: Type 2 diabetes mellitus; Obesity; Cardiovascular disease; Metabolic syndrome.

Abbreviations: AGE, advanced glycosylation endproducts; apoE, apolipoprotein E; ARIC, Atherosclerosis in Communities Study; ATPIII, National Cholesterol Education Program: Adult Treatment Panel III; CHD, coronary heart disease; CPT-1, carnitine palmitoyl transferase-1; CRP, C-reactive protein; DCCT, Diabetes

Control and Complications Trial; FFA, free fatty acids; GLUT, glucose transporter; HDL, high-density lipoprotein; HNF, hepatocyte nuclear factor; IFG, impaired fasting glucose; IGT, impaired glucose tolerance; IL-6, interleukin-6; IRS, insulin receptor substrate; LDL, low-density lipoprotein; LPL, lipoprotein lipase; MAPK, mitogen-activated protein kinase; MI, myocardial infarction; MODY, maturity onset diabetes of the young; NFκB, nuclear factor-κB; OGTT, oral glucose tolerance test; OR, odds ratio; PAI-1, plasminogen activator inhibitor-1; PI3-kinase, phosphoinositide 3-kinase; PKC, protein kinase C; POCT, point-of-care testing; PPAR-γ, peroxisome proliferator-activated receptor-γ; RAGE, receptor for advanced glycosylation endproducts; ROS, reactive oxygen species; T1D, type 1 diabetes; T2D, type 2 diabetes; TNF-α, tumor necrosis factor-α; tPA, tissue-type plasminogen activator antigen; UKPDS, UK Prospective Diabetes Study; VLDL, very-low-density lipoprotein; VWF, von Willebrand factor.

Introduction

Diabetes mellitus is a heterogeneous disorder of fuel metabolism, which in the short-term may lead to dramatic metabolic and clinical decompensation, and in the long-term results in vascular complications. Diabetes has been defined as 'a lifestyle disorder with the highest prevalence seen in populations that have a heightened genetic susceptibility (where) environmental factors associated with lifestyle unmask the disease' (1).

The two main forms of diabetes are type 1 diabetes (T1D) and type 2 diabetes (T2D), with approximately 10 times more patients with T2D compared to T1D. T1D is caused by the autoimmune destruction of insulin secreting β-cells of the pancreatic islets (2), and T2D develops as a result of a combination of insulin resistance and deteriorating β-cell function. Cardiovascular disease is the most prevalent complication of diabetes and is the main cause of death among people with diabetes (3, 4).

Prevalence of diabetes is increasing worldwide, although the rates of increase differ very much between populations (1). T2D affects approximately 8% of the population of the USA (5), and in 1995 its worldwide prevalence was approximately 4% (6). Worryingly, it recently became to appear with greater frequency in adolescents (7, 8). Presently about 150 million people worldwide have diabetes, and this is likely to increase to 200 million by the year 2010 (9). The size of the problem and its relation to nutrition and lifestyle take the is-

*E-mail of the corresponding author:
m.h.dominiczak@clinmed.gla.ac.uk or
mhd1b@clinmed.gla.ac.uk

sue outside the realm of health care alone; its societal implications need to be seen together with development of new therapies (2, 8, 10). This article will focus on type 2 diabetes and, in particular, on its links with obesity as its antecedent, and cardiovascular disease as its major complication.

The Genetics of Type 2 Diabetes

There is a significant genetic component to T2D. First degree relatives of individuals with T2D have nearly threefold increased lifetime risk of developing the disease. Although the concordance rate is high in T2D, there is no consistent inheritance pattern (2, 11, 12). There is a genetic form of T2D, the maturity onset diabetes of the young (MODY) but it affects only a small minority of patients with T2D. MODY results from mutation of at least six different genes: glucokinase (*MODY2*), hepatocyte nuclear factor HNF-4 α (*MODY1*), HNF-1 α (*MODY3*), insulin promoter factor (*IPF-1*), HNF-1 α and β -cell transcription factor neuroD1 (also called *BETA2*) (10, 11). A mitochondrial DNA mutation leads to impaired oxidative phosphorylation and to 'mitochondrial diabetes' (2, 11). The influence of other genes can also alter metabolism: this includes genes encoding the insulin receptor, GLUT4 glucose transporter, hexokinase II enzyme, insulin (*INS*), sulfonylurea receptor-1 (*SUR-1* gene), insulin receptor substrate-1 (*IRS-1*), a membrane protein that inhibits the autophosphorylation of insulin receptor (*PC-1* gene), and finally the glycogen synthase (11). The NIDDM1 locus on chromosome 2 identified as a result of the genome-wide scan resulted in subsequent identification of the calpain-10 (calcium-activated neutral protease) diabetes susceptibility gene (13).

Genes associated with insulin resistance are the *LMNA* encoding for laminin type A and C and also mutations in the gene encoding the peroxisome proliferator-activated receptor- γ (*PPAR- γ*). An amino acid polymorphism (Pro12A1a) in *PPAR- γ* has also been associated, albeit inconsistently, with T2D (11). Candidate genes potentially likely to elucidate links between diabetes and cardiovascular disease (14) are those coding for, among others, lipoprotein lipase (LPL), apolipoprotein E (apoE), apoCIII, cholesteryl ester transfer protein, fatty acid synthase and carnitine palmitoyl transferase-1 (CPT-1). However, in the vast majority of T2D cases the genetic basis is not identifiable. The thrifty gene hypothesis was invoked to explain the differing incidence rates of T2D in various populations (1).

The Prediabetic Continuum: Obesity, Glucose Intolerance and the Metabolic Syndrome

Similarly to diabetes, the incidence of obesity has been increasing. An alarm has been raised concerning this yet another epidemic, with a particular concern about obesity in teenagers (10). The significance of obesity is that it is associated with an increased risk of a range of

chronic disorders: most importantly it is a major antecedent of diabetes mellitus, and it is associated with cardiovascular disease. It is also more frequent in dyslipidemia and hypertension. It leads to insulin resistance with an increased plasma insulin concentration (15, 16). It is strongly associated with prediabetic state, defined as either impaired fasting glucose (IFG) or impaired glucose tolerance (IGT). These in turn may transition to diabetes (17). With regard to cardiovascular disease, the Framingham Study showed that the incidence of cardiovascular disorders increases with increasing weight (18). The disease burden associated with obesity extends to disorders such as gallstones and osteoarthritis (19).

Obesity and prediabetic state (or diabetes) may present as a component of a heterogeneous entity defined as the metabolic syndrome (17, 20–23) where they combine with dyslipidemia and increased arterial blood pressure (24, 25). Contribution of each of these components to the metabolic syndrome differs in individual cases, and this heterogeneity had been emphasized in both its WHO (20) and Adult Treatment Panel III (ATP III) (21) definitions (Figure 1). The key question is whether the syndrome is a separate clinical entity or simply a cluster of independent processes. Recent factor analysis in persons with metabolic syndrome who developed diabetes, suggests that the syndrome is an independent cluster (26). Whatever the case, the metabolic syndrome is a stage where several risk factors for vascular damage operate at a high level of intensity. It signifies to the clinician that the combination of potentially harmful metabolic factors reached critical level beyond which the damage to the large arteries accelerates.

In diabetes the risk of coronary events increases twofold in men and fourfold in women, compared to non-diabetic individuals (27). In fact, the risk of a cardiovascular event in a person with diabetes seems to be similar to the risk of recurrence of an event in a patient with already present coronary disease (which is considerably higher than the risk of a first event) (28), although not all data confirm this (29). Associations between diabetes and cardiovascular disease had been long known, and they led to the development of the 'common soil' hypothesis (30). The idea of common mechanisms has also been the basis for the development of the concept of diabetes (obesity-associated diabetes); this concept posits inflammation as the major common denominator between the two conditions, with the dominant role played by the innate immune system (31, 32). Another fundamentally important fact is that the entire sequence obesity-metabolic-syndrome-T2D, and to an extent cardiovascular disease, may be prevented, or their progress delayed, by similar lifestyle interventions: weight reduction, diet and increased physical activity (33).

Indeed, in middle-aged persons with glucose intolerance, intervention based on weight reduction, reduction of fat intake, increase in fiber intake and increase in physical activity, resulted over 9.2 years in 58% reduction of the risk of developing diabetes (34). In another

Metabolic syndrome: the WHO definition

Impaired glucose tolerance or diabetes and/or insulin resistance

plus two of the following:

Blood pressure $> 160/90$ mm Hg;

Plasma triglycerides above 1.7 mmol/l (> 149 mg/dl) and/or HDL-cholesterol below 0.9 mmol/l (< 35 mg/dl) in men or below 1 mmol/l (< 39 mg/dl) in women;

Central obesity: In men waist-to-hip ratio greater than 0.90 , and in women greater than 0.85 , and/or BMI greater than 20 kg/m²;

Microalbuminuria: Urinary albumin excretion rate equal to, or above, 20 μ g/min or albumin/creatinine ratio equal to, or above, 20 mg/g.

Metabolic syndrome: the ATP III definition

Any three of the following:

Fasting glucose equal to or greater than 6.1 mmol/l (≥ 110 mg/dl);

Blood pressure equal to, or higher than, $130/85$ mm Hg;

Plasma triglycerides above 1.71 mmol/l (> 150 mg/dl);

HDL-cholesterol below 1.0 mmol/l (< 40 mg/dl) in men, or below 1.3 mmol/l (< 50 mg/dl) in women;

Central obesity: In men waist circumference greater than 102 cm (> 40 in), in women greater than 88 cm (> 35 in).

Figure 1 Definition of the metabolic syndrome according to the WHO (20) and the National Cholesterol Program Expert Panel on Detection, Evaluation and Treatment of High Blood Cholesterol in Adults (Adult Treatment Panel III; ATP III) (21).

Note that both definitions emphasize heterogeneity of the syndrome and its many possible permutations. ATP III guidelines set the cut-off level of HDL-cholesterol higher than WHO ones. The cut-off point for blood pressure values is set lower.

study involving persons at high risk of developing diabetes, an intervention lasting 2.8 years based on lifestyle changes (weight reduction and increase in the physical activity), or treatment with metformin, reduced the incidence of diabetes by 58% in the lifestyle group, and by 31% in the metformin group, compared with placebo (5).

Vascular Complications of Diabetes

Diabetes as a clinical entity is defined by the risk, or the presence, of microvascular complications. Diabetic microangiopathy is specific to the disease and leads to kidney failure and blindness, and also contributes to neuropathy and foot ulceration. In contrast to this, atherosclerosis is not specific to diabetes. Further, while microangiopathy is the consequence (and indeed a part) of existing diabetes, clinical manifestations of macrovascular disease might either precede, follow or occur in parallel with any degree of glucose intolerance.

The current view of the microvascular complications of diabetes emphasizes the toxicity of glucose (glucotoxicity) and of lipid-related substrates (lipotoxicity), in particular the derivatives long-chain acyl-CoA (35–39). Presently considered mechanisms of microvascular complications include glycoxidation and the formation of the advanced glycosylation endproducts (AGE) (40–42), associated with carbonyl (42, 43) and oxidative stress (40–46). Other proposed mechanisms are the increased flux through polyol and hexosamine pathways, and activation of protein kinase C (PKC) isoforms,

which affects cellular signaling systems and, through this, synthesis of growth factors and operation of ion channels (for review see ref. 44). Atherosclerosis is to a large extent driven by the cytokine/growth factor cross-talk between endothelial cells, macrophages and vascular smooth muscle cells (47–49). It is initiated by endothelial dysfunction in which a particularly important role is played by the nitric oxide (50) (the bioavailability of NO is impaired by the superoxide radical). Formation of atherosclerotic plaque is associated with lipid deposition in the vascular wall, and atherosclerosis progresses on the background of oxidative processes, low-grade inflammation and remodelling of the structure of the vascular wall. Inflammatory reaction in the atherosclerotic plaque is also a major determinant of plaque rupture, which is the direct cause of cardiac catastrophes.

Signaling Pathways in Diabetes

Progress in research into insulin signalling not only provided insight into insulin action, glucose transport and insulin secretion, but also revealed the existence of multifunctional signalling pathways which operate in diabetes and cardiovascular disease.

The first event in the insulin action is its binding to the α -subunit of the membrane receptor (51). This activates the β -subunit tyrosine kinase and leads to tyrosine autophosphorylation. The receptor also phosphorylates a range of other substrates such as four proteins belonging to the IRS family, and proteins des-

ignated Shc, Gab-1 p60^{src} Cbl and APS (51). Subsequently, other adaptor molecules dock on these and in turn activate G-proteins. Tyrosine phosphorylation of IRS proteins and/or Shc-interaction with adapter molecules lead to the activation of Ras-(mitogen-activated protein kinase) MAPK pathway. The IRS proteins interact with phosphoinositol signaling cascades, which involve phosphoinositol-3-(PI3)-kinase and generate phosphoinositol phosphates. PI3-phosphates regulate further signaling molecules: serine/threonine protein kinases (such as Akt), tyrosine kinases and the guanine nucleotide-exchange proteins (39, 51, 52). Insulin-dependent glucose entry into cells is mediated by glucose transporters, in particular GLUT4 which controls glucose uptake in the skeletal muscle and adipocytes. Insulin stimulates exocytosis of GLUT4 molecules to the surface of the cell membrane (53, 54). Recruitment of the transporter to the plasma membrane requires insulin binding to its receptor; tyrosine phosphorylation of IRS-1, phosphoinositol signaling and PI3-kinase activation. A simplified scheme of the insulin signaling systems is shown in Figure 2.

Insulin secretion is initiated by a sequence of events where glucose metabolism in the β -cells produces ATP, and the increased ATP/ADP ratio closes the ATP-sensitive K⁺ channel (K_{ATP}). This depolarizes the cell and

opens the voltage-dependent L-type calcium channel. The entry of calcium ions stimulates the first phase of insulin secretion. The second, more prolonged phase probably requires an increase in the concentration of the cytosolic long-chain acetyl-CoA molecules, ATP or GTP, and also the involvement of diacylglycerol and PKC (55).

Metabolites, cytokines and growth factors exert many of their effects by influencing signaling cascades. Proteins participating in the signaling cascades are often able to transduce multiple signals: for instance, the activation of Akt kinase by insulin prevents endothelial cell apoptosis induced by tumor necrosis factor- α (TNF- α) (56). In particular, the interference of the reactive oxygen species (ROS) and inflammatory mediators in the operation of signaling cascades is important in the development of microvascular complications of diabetes and cardiovascular disease.

Adipose Tissue and Lipid Transport in Diabetes

Adipose tissue is an active endocrine organ. Hormone-like substances – adipokines – leptin, adiponectin and resistin, and growth factors such as vascular endothelial growth factor (VEGF), as well as pro-inflammatory cytokines (TNF- α and Interleukin-6 (IL-6)) are all gener-

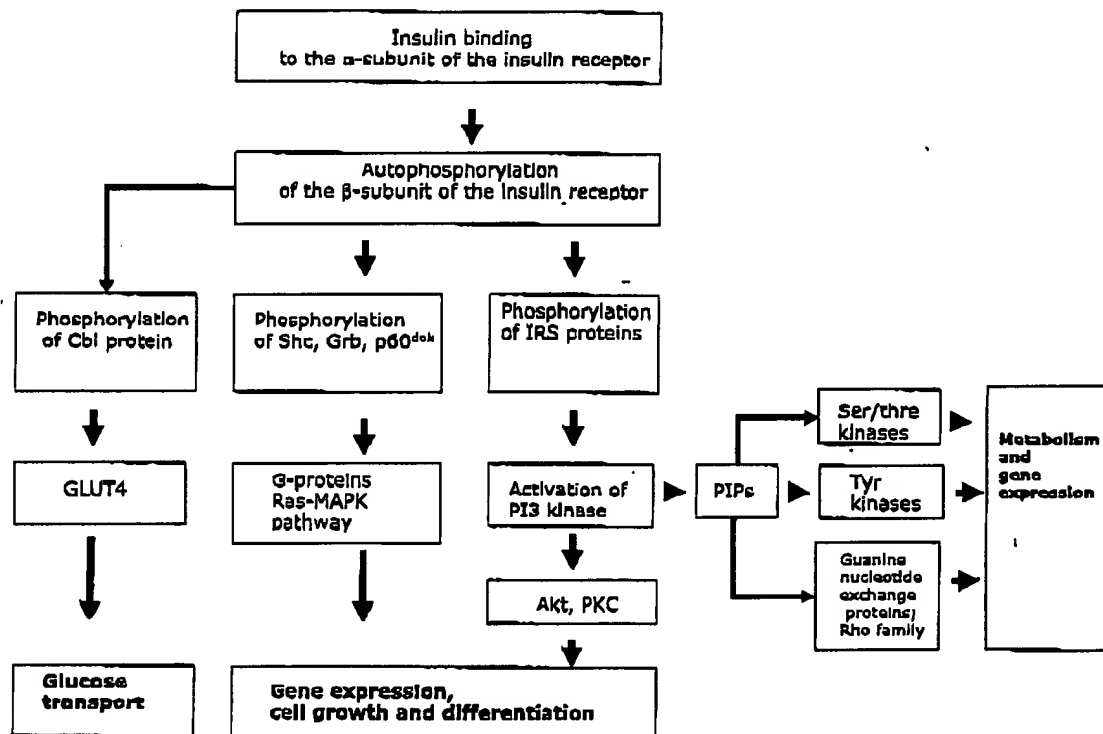


Figure 2 A simplified scheme of insulin signaling pathways. Insulin binds to the α -subunit of its membrane receptor and the binding stimulates the autophosphorylation of the β -subunit, and subsequently a range of substrates including the insulin receptor substrate (IRS) family and also Cbl, Gab-1 and Shc proteins. Then the adaptor molecules such as Grb2 dock on these and activate G-proteins. These events in turn lead to the activation of the mitogen-activated kinase pathway

(MAPK). Phosphorylated IRS-1 activates the phosphoinositide-3 (PI-3) kinase which generates phosphoinositide phosphates. These interact with serine/threonine protein kinases (including Akt kinase), tyrosine kinases and guanine nucleotide exchange proteins. These signals eventually affect glucose transport (the GLUT4 transporter), gene expression and a broad spectrum of metabolic actions.

ated by the adipocytes (54). Leptin regulates food intake and energy expenditure, and also has neuroendocrine function (57). Inefficient leptin action leads to hyperphagia, decreased fat oxidation, increased tissue triglycerides and insulin resistance: this translates into obesity and T2D. On the other hand, leptin treatment of normal animals causes hypophagia, leads to increased fat oxidation, depletion of tissue triglycerides and to increased insulin sensitivity.

Another adipokine, adiponectin, is specific to the adipose tissue. In non-diabetic persons plasma adiponectin concentration correlates with insulin sensitivity, measured either by the euglycemic-hyperinsulinemic clamp or by the oral glucose tolerance test (OGTT) (58). Adiponectin concentrations correlated positively with high-density lipoprotein (HDL)-cholesterol and inversely with triglycerides and free fatty acids (FFA) concentration at 120-minute sampling time during OGTT (58). Adiponectin has an insulin-sensitizing effect: it decreased glucose and FFA levels without affecting insulin concentration (59–61). In Pima Indians, adiponectin increased insulin sensitivity and was associated with a decrease of the risk of T2D (62). Adiponectin concentration decreases in insulin resistance while TNF- α and resistin concentrations increase. An example of the interference of adipocyte-generated signals in insulin signaling cascades is, for instance, the fact that adipocyte expression of TNF- α leads to serine phos-

phorylation of IRS-1, which in turn causes reduced insulin receptor kinase activity (63).

Hormonal activity of adipocytes is also associated with the ectopic presence of fat in muscle and liver. Elevation of FFA and very-low-density-lipoprotein (VLDL) in plasma causes fat accumulation in myocytes: intramyocellular lipid increases within 5 hours of the infusion of intralipid (64). Hyperglycemia expands the cytoplasmic pool of long-chain acyl-CoA through elevating malonyl-CoA concentration and the consequent suppression of CPT-1 (38). Fatty acids affect several important cellular events: they regulate gene transcription, uncouple oxidative phosphorylation, stimulate generation of ROS and activate signaling cascades involving the nuclear factor- κ B (NF κ B) transcription factor (38, 44). Elevated FFA are also associated with the reduction of insulin-stimulated IRS-1 phosphorylation and IRS-1-associated PI3-kinase activity (65). The triglyceride content of muscle is inversely related to insulin sensitivity (66).

Insulin resistance and diabetes have a major effect on the transport of metabolic fuels between tissues by lipoprotein particles. Insulin resistance may result in dyslipidemia in persons with normal glucose tolerance as well as in those with IGT and T2D (67, 68). However, diabetic dyslipidemia usually does not involve high low-density lipoprotein (LDL) concentrations. In T2D the prevalence of increased LDL-cholesterol is not greater than in non-diabetic population. On the other

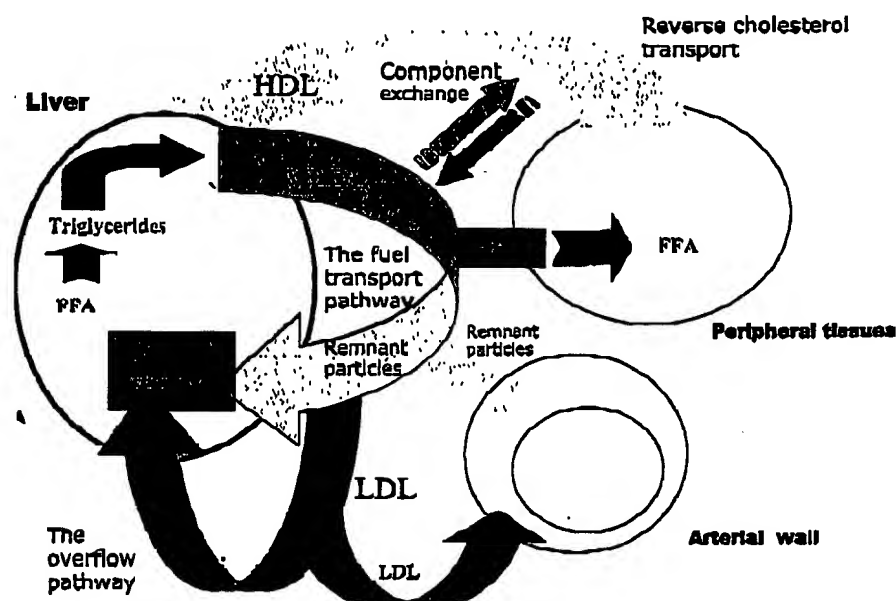


Figure 3 The central role of the lipoprotein fuel transport pathway in the fuel metabolism. Free fatty acids (FFA) are transported from the liver as triglycerides incorporated into the very-low-density lipoprotein (VLDL) particles. Lipoprotein lipase (LPL) hydrolyzes VLDL triglycerides at the periphery yielding FFA again. During the process, VLDL decreases in size, generating remnant particles. The remnants are atherogenic. A proportion of remnants transform further, forming LDL. The fuel transport pathway is a high-turnover path, which handles large number of particles. The low-density lipoprotein (LDL)

metabolism (the overflow pathway) is, in relative terms, a low turnover path. Note that there is component exchange between triglyceride-rich particles in the fuel transport pathway and the high-density lipoprotein (HDL), which participate in the reverse cholesterol transport. Cholesterol esters and apoproteins are transferred from HDL to triglyceride-rich particles in exchange for triglycerides. For clarity, chylomicron metabolism has been omitted from the Figure. Size and thickness of the arrows are not proportional to particle numbers.

hand, the low HDL concentration and high concentration of triglycerides in serum are about twice as prevalent in T2D as they are in non-diabetic individuals (3).

Triglycerides are distributed to tissues through the VLDL-remnant particles pathway, also called the fuel transport pathway (69–71). In this pathway, triglyceride-rich VLDLs, and also chylomicrons (when present), undergo lipolysis by the LPL, yielding remnant particles (Figure 3). This high-turnover pathway operates at about one tenth of the concentration of LDL in plasma. The particles in the fuel transport pathway exchange apoproteins, cholesterol esters and triglycerides with HDL at different stages of maturation. Remnant particles generated as a result of transfer of fatty acids from lipoprotein triglycerides to tissues by the LPL are atherogenic (72). In obesity, metabolic syndrome and diabetes the fuel transport pathway is overloaded due either to the excess production of VLDL or the low LPL activity. The outcome is an increase in the concentration of triglyceride-rich particles in plasma (however, increased flux through the fuel transport pathway may generate increased numbers of atherogenic remnants with little change in their plasma concentration). In addition, changes in the activity of the fuel transport pathway resulting in hypertriglyceridemia promote formation of smaller and denser, more atherogenic LDL particles (73).

It is unfortunate that, in spite of the metabolic importance of the fuel transport pathway, the only routinely applied measurement of its activity – plasma triglycerides – only crudely assesses several populations of triglyceride-rich lipoproteins present there. Thus, it is not entirely surprising that it has been difficult to unequivocally associate triglyceride concentration with cardiovascular risk. Recently introduced methods which measure triglyceride-rich particles provide a better insight into the operation of the fuel transport pathway, but they are not yet part of the routine laboratory practice (74, 75).

Hyperglycemia and Oxidative Stress

The excess of glucose and glucose metabolites in the extracellular fluid and in cells is the main factor determining the development of the vascular complications of diabetes. Hyperglycemia leads to the formation of glucose adducts with proteins, the AGE (40–42). AGE bind to their membrane receptor (RAGE) (76), and subsequently generate mediators such as TNF- α , IL-1- β , IL-6 (77) and vascular cell adhesion molecule-1 (VCAM-1) (78, 79). There is substantial evidence that AGE contribute to the development of atherosclerosis (80, 81). They were found in atheroma-like lesions (81), and the treatment with the soluble domain of RAGE completely suppressed atherosclerosis in apoE-deficient (streptozotocin) diabetic mice (82). Also, AGE elicit inflammatory response (83), and activate NF- κ B (84). Interestingly, inflammatory response was also elicited by dietary AGE: in a study involving 13 patients, serum C-reactive protein (CRP) concentration increased by 35% on high-AGE diet (85).

Another aspect of glucotoxicity, also associated with AGE formation, is the contribution of glucose to oxidative processes. Glucose may undergo autooxidation yielding ROS and intracellular precursors of AGE (46). Also, hyperglycemia alters the redox state by increasing the NADH/NAD⁺ ratio and decreasing NADPH/NADP. This in turn causes an increase in the flux through the polyol and hexosamine pathways. The high rate of ROS generation and/or low levels of antioxidants create oxidative stress (42, 45), which damages molecules and activates a number of signalling pathways. ROS activate PKC and NF- κ B (86). Hyperglycemia itself activates Ras-MAPK cascade and NF- κ B pathway (87). PKC and NF- κ B can also be activated by FFA (38). Importantly, normalizing mitochondrial ROS prevent glucose-induced activation of PKC, formation of AGE and activation of NF- κ B (88). Such data led to the development of an attractive hypothesis, which suggests that ROS production by the mitochondrial electron transport chain is the unifying mechanism of diabetic complications (44). Accordingly, hyperglycemia, by affecting the amount of proton donors within the cell, would increase electrochemical potential difference across the inner mitochondrial membrane (89) and thus lead to an increased production of superoxide and the activation of signaling pathways, imparting insulin resistance and damaging insulin secretion.

Inflammation and Hypercoagulable State in Diabetes and Cardiovascular Disease

Inflammation includes a range of phenomena such as cell-cell attraction, cell adhesion and cell activation. The main purpose of inflammatory reaction is to attract leukocytes and soluble mediators of immunity to the sites of infection (90). In atherosclerosis, inflammatory phenomena include adhesion of monocytes to endothelial surface, transmigration of cellular elements and lipids, and their deposition and activation in the arterial intima. The key role in inflammation is played by NF- κ B, which affects the inflammatory response and apoptosis through gene activation, and also influences adhesion molecules, endothelium-dependent vasodilatation and, through the transcription of tissue factor, thrombotic phenomena (91).

Low-grade inflammation is present in obesity, metabolic syndrome and diabetes (92–94). In obese persons, and particularly in those who are insulin resistant, the expression of TNF and IL-6 increases (95). Particularly interesting is that the deterioration of carbohydrate intolerance appears to accelerate on the background of low-grade inflammation, leading to the higher rate of transition to diabetes. In WOSCOPS, a trial of lipid-lowering treatment using pravastatin, the CRP concentration predicted the development of diabetes at 5 years (odds ratio (OR) 1.30) (96). In individuals whose CRP concentration was in the highest quintile, OR for the development of T2D was as high as 3.07. CRP also predicted the development of diabetes in the Women's Health Study (97). In the Atherosclerosis in

Communities Study (ARIC) study, involving 12,330 men and women followed up for 7 years, the white cell count and fibrinogen concentration also predicted transition to diabetes, with the highest quartile OR being 1.9 and 1.2, respectively (98).

Pre-diabetes and diabetes are also characterized by a hypercoagulable state. The concentration of fibrinogen, factor VII, von Willebrand factor (vWF) and the markers of decreased fibrinolysis such as plasminogen activator inhibitor-1 (PAI-1) antigen, or tissue-type plasminogen activator (tPA) antigen are all affected. The Framingham Offspring Study, demonstrated associations between fasting insulin concentration and PAI-1 antigen, tPA antigen, factor VII antigen, vWF antigen fibrinogen and viscosity in men and women with normal glucose tolerance. This extended to glucose intolerance: among those with IGT or IFG, PAI-1 and tPA antigens were associated with hyperinsulinemia (99). In the Insulin Resistance Atherosclerosis Study (100), increased rate of conversion to T2D was associated with increased CRP as well as PAI-1 and fibrinogen (the latter of borderline significance).

Low-grade inflammation is also present in cardiovascular disease. There is large body of evidence demonstrating that the small increase in the CRP concentration predicts cardiovascular events (for review see ref. 101). This predictive ability is independent of the concentration of total cholesterol and the total cholesterol to HDL-cholesterol ratio (71, 102, 103).

To put all the pieces of this complex puzzle together, it seems that the development of low-grade inflammation is enabled by the changed pattern of fuel (carbohydrate and fat) metabolism, which generates excess of 'toxic' metabolites such as glucose and FFA. The chain of events would lead from higher load of 'toxic' metabolites to changes in the redox state, consequent oxidative stress and ROS-mediated effects on signaling cascades. The latter would stimulate inflammatory response but also, because of multifunctional nature of signaling cascades, would further affect insulin action and enhance insulin resistance. The relationships between obesity, diabetes and atherosclerosis are illustrated in Figure 4.

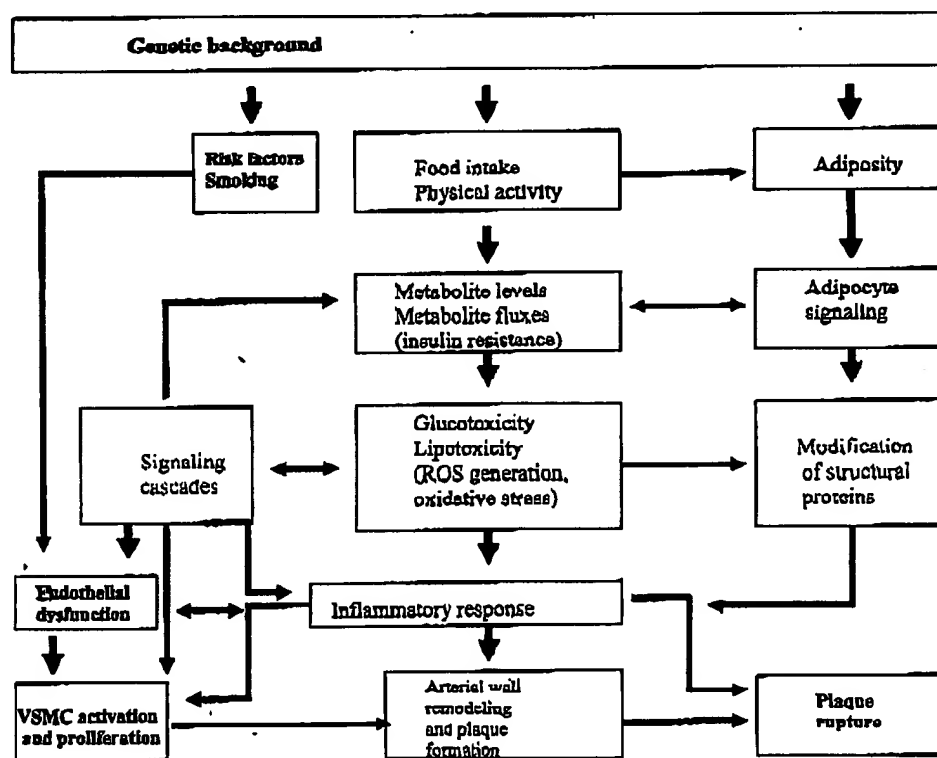


Figure 4 Relationships between obesity, diabetes and atherosclerosis. Blue panels: Increased food intake and/or decreased physical activity, aided by adipocyte signaling, change metabolite flux through the pathways of carbohydrate and fat metabolism. This generates excess of glucose and fatty acid derivatives resulting in metabolite toxicity (glucotoxicity and lipotoxicity), in part caused by the generation of reactive oxygen species (ROS). Subsequent changes include modification of structural proteins and interference with cell signaling systems (green panels). Please note the bi-directional interactions between metabolites and signaling sys-

tems. Black panels: Atherogenesis is accelerated by signals generated by the changed fuel metabolism as well as by external risk factors independent of energy metabolism, such as cigarette smoking. The risk-factor-induced endothelial dysfunction initiates cross-talk between endothelium, vascular smooth muscle cells (VSMC) and macrophages. Red panels: Inflammatory response develops as a result of dysfunctional fuel metabolism and impaired endothelial function, and is a major contributor to the formation of the atherosclerotic plaque and its rupture.

Treatment of Diabetes and the Prevention of Long-Term Complications

Increasing awareness of the relationships between obesity, diabetes and cardiovascular disease, all to an extent mediated by changes in the fuel metabolism, influences the approach to the treatment of diabetes. Perhaps the single most important conceptual change in the last decade has been the broadening of approach to diabetes from that focused exclusively on the control of glycemia to the recognition of the importance of the parallel management of cardiovascular risk factors.

The maintenance of good glycaemic control has been long-recognized as fundamental for the care of diabetes (104). Two major trials, Diabetes Control and Complications Trial (DCCT) and UK Prospective Diabetes Study (UKPDS) have confirmed the long-held view that microvascular complications are associated with the level of glycemia. The DCCT (105), which involved T1D patients, and the UKPDS (106, 107) in T2D individuals, demonstrated that maintaining good diabetic control decreases the incidence of diabetic complications (108). However, the results of both trials seem to indicate that the level of glycemia is not a major determinant of atherosclerotic disease. The UKPDS showed a relatively small, 16% decrease in the incidence of myocardial infarction (MI) ($p = 0.052$) with HbA_{1c} decreasing from a mean of 7.9 to 7.0% (108). Still, a correlation was observed between HbA_{1c} and the risk of cardiovascular death (108). Recently, the follow-up to the DCCT, the Epidemiology of Diabetes Interventions and Complications Trial (EDIC), demonstrated that the rate of increase of intima-media thickness after 6 years was lower in patients who were intensively treated during DCCT (109). The increasing thickness was also associated with age, baseline systolic blood pressure, smoking, LDL to HDL-cholesterol ratio, urinary albumin excretion and the mean glycated hemoglobin value observed during DCCT.

Treatment of cardiovascular risk factors improves cardiovascular outcomes in diabetes. Also, the treatment of hypertension in diabetes with ACE-inhibitors and angiotensin receptor antagonists decreases progression of diabetic nephropathy (110) in the UKPDS, each 10 mm Hg decrease in mean systolic blood pressure was associated with a 12% reduction of complications related to diabetes, an 11% reduction in MI, a 13% reduction in microvascular complications, and a 15% decrease in diabetes mortality (27). Further, there were risk reductions in the group assigned to tight blood pressure control (144/82 mm Hg) compared with that assigned to less tight control (154/87 mm Hg). There was a 32% reduction in deaths related to diabetes, 44% in stroke and 37% in microvascular endpoints (111).

Lipid-lowering trials demonstrate that the benefit of lowering lipids using HMG-CoA reductase inhibitors (statins) in diabetes are the same, if not higher, than in non-diabetic populations (112). Therefore, the target values for risk factor management are stricter in the diabetic patients than in non-diabetic individuals. According to the American Diabetes Association (ADA)

(27) and the JNC7 Report (110) the recommended treatment goal for diabetic patients is the blood pressure below 120/80 mm Hg, while the general target remains below 140/90 mm Hg. The recent recommendation of the ATP III of the National Cholesterol Education Program considered diabetes a 'CHD risk equivalent', automatically conferring a high coronary heart disease (CHD) risk status on individuals with this disease (21). This translates into the need for a more intensive management: for instance the initiation of lifestyle measures in diabetes is recommended at the lower LDL level (above 99 mg/dl; 2.6 mmol/l) than in non-diabetic individuals with multiple CHD risk factors (above 129 mg/dl; 3.4 mmol/l) (see ref. 113 for more detailed discussion).

Apart from clinical studies that focus on a single risk factor, there is also emerging evidence that multifactorial intervention, extending beyond maintenance of glycemic control, is particularly effective in the prevention of the long-term complications. The recent example of such intervention in T2D is the Steno-2 study conducted in Denmark, which involved 160 patients with T2D and microalbuminuria (114). This randomized, controlled trial compared standard clinical management with an intensive target-driven management of hyperglycemia, hypertension, dyslipidemia and microalbuminuria, and behavior modification including smoking cessation and exercise program. The patients were treated with ACE inhibitors, vitamin supplements, aspirin, metformin and gliclazide, and insulin when required. Hypertension was treated with ACE-inhibitors or angiotensin II receptor antagonists, thiazides, calcium channel blockers and β -blockers. Dyslipidemia was managed using statins, fibrates or the combination of the two. The patients were managed by a team of doctor, nurse and dietitian, with a 3-monthly consultation schedule throughout the study. The analysis of microvascular endpoints was conducted after 4 years and macrovascular ones after 7.8 years. The primary endpoints were death from cardiovascular causes, non-fatal MI, coronary artery bypass graft, angioplasty, non-fatal stroke, non-traumatic amputation and vascular surgery. The intensive care group achieved greater reduction in glycated hemoglobin, total cholesterol and triglyceride concentrations, and blood pressure and urinary albumin excretion. Most importantly, there was an impressive decrease in the risk of cardiovascular disease (OR = 0.47), nephropathy (OR = 0.39), retinopathy (OR = 0.42) and autonomic neuropathy (OR = 0.37).

Implications for Laboratory Medicine

The increasingly recognized common denominators between obesity, diabetes and cardiovascular disease need to be reflected in the laboratory support for diabetes care. Diagnosis of glucose intolerance and diabetes, and monitoring of treatment of diabetes mellitus, depend entirely on the laboratory tests. The spectrum of tests employed in routine diabetes care

has remained relatively narrow. Comprehensive guidelines on the laboratory investigations in diabetes have been published recently by the National Academy of Clinical Biochemistry and the ADA (115, 116).

While the measurement of plasma glucose remains the only method recommended for the diagnosis of diabetes and glucose intolerance, glycated hemoglobin testing is the key for the monitoring of long-term control. The diagnosis of diabetes and glucose intolerance (117, 118) and the use and standardization of HbA_{1c} measurements (107, 119, 120) are discussed in detail elsewhere in this issue. Point-of-care testing (POCT) remains important not only as a time-efficient method of measuring glucose in acute situations but also as an optimal monitoring tool for patients at home (121). Here, there is a need for noninvasive miniaturized appliances to increase patients' comfort and their compliance with treatment (122, 123). Fast-turnover POCT measurements carried out in diabetic clinics provide important instant feedback to patients.

However, it is the tests relevant to the assessment of risk of long-term complications, and in particular the presence of, and the preventive treatments for, cardiovascular disease, that have gained importance in the management of diabetes. The range of tests suitable to monitor the progress of microvascular complications is exceedingly narrow: in a routine practice it is limited to the assessment of renal function and to the measurement of microalbuminuria (124, 125). Where the assessment of the risk of cardiovascular disease is concerned, the risk factor profile currently used in the non-diabetic populations applies. The conventional test profile used for this purpose is all quite rudimentary: in the standard risk assessment, the rationale for which is rooted in the epidemiological data, only two laboratory variables are used: total cholesterol and HDL-cholesterol, while calculated LDL-cholesterol is the parameter of choice for instituting and monitoring lipid-lowering treatment (for review see 21, 71).

The measurement of serum triglyceride concentration is important because it is one of the markers of the metabolic syndrome, and also a factor which contributes to the low HDL-concentration. Triglyceride concentration is presently the only routinely available measurement of the activity of the lipoprotein fuel transport pathway. More specific measurements of the triglyceride-rich lipoproteins would provide better insight into the operation of this pathway in physiological and pathological conditions. Microalbuminuria is also a marker of cardiovascular risk (125) and should be assessed together with lipoprotein variables in diabetic patients. Finally, several new cardiovascular risk markers have been identified in the recent years (71, 126, 127). Out of these, CRP (71, 102, 103), fibrinogen (128, 129), and homocysteine (130–132) attracted most attention. The statement on the use of the new cardiovascular risk markers has been recently published in the USA (133).

To summarize, this article has discussed common mechanisms which underpin obesity, diabetes and cardiovascular disease. Awareness of these commonali-

ties now affects our approach to the treatment of diabetes. It is also highly relevant to laboratory medicine: laboratory support for diabetes care needs to be planned as a package which, along with tests traditionally required for diagnosis of diabetes and monitoring of glycemic control, should include measurements relevant to the assessment of the risk, and the effectiveness of treatment, of the microvascular complications and cardiovascular disease. Continuous refinement of this test profile poses an important challenge to laboratory medicine.

Acknowledgements

The author thanks Professor J. Baynes for his advice and criticism, and Miss Jacky Gardiner for excellent secretarial assistance.

References

1. Diamond J. The double puzzle of diabetes. *Nature* 2003; 423:599–602.
2. Bell GI, Polonsky KS. Diabetes mellitus and genetically programmed defects in beta-cell function. *Nature* 2001; 414:788–91.
3. Mooradian A. Cardiovascular disease in type 2 diabetes mellitus: current management guidelines. *Arch Intern Med* 2003; 163:33–40.
4. Savage PJ. Cardiovascular complications of diabetes mellitus. *Ann Intern Med* 1996; 124:123–6.
5. Knowler WC, Barrett-Connor E, Fowler SE, Hamman RF, Lachin JM, Walker EA, et al. Reduction in the incidence of type 2 diabetes with lifestyle intervention or metformin. *N Engl J Med* 2002; 346:393–403.
6. King H, Aubert RE, Herman WH. Global burden of diabetes 1995–2025: prevalence, numerical estimates, and projections. *Diabetes Care* 1998; 21:1414–31.
7. Steinberger J, Daniels SR. Obesity, insulin resistance, diabetes and cardiovascular risk in children: an American Heart Association Scientific Statement from the Atherosclerosis, Hypertension, and Obesity in the Young Committee (Council on Cardiovascular Disease in the Young) and the Diabetes Committee (Council on Nutrition, Physical Activity, and Metabolism). *Circulation* 2003; 107:1448–53.
8. King H, Aubert RE, Herman WH. Global burden of diabetes, 1995–2025: prevalence, numerical estimates, and projections. *Diabetes Care* 1998; 21:1414–31.
9. Zimmet P, Alberti KGMM, Shaw J. Global and societal implications of the diabetes epidemic. *Nature* 2001; 414:782–7.
10. Campbell I. The obesity epidemic: can we turn the tide? *Heart* 2003; 89 (Suppl II):II22–4.
11. Gloyn AL, McCarthy MI. The genetics of type 2 diabetes. *Best Pract Res Clin Endocrinol Metab* 2001; 15:286–308.
12. Koberling J, Tillil H. Empirical risk figures for first-degree relatives of non-insulin dependent diabetics. In: Koberling J, Tattersall R, editors. *The genetics of diabetes mellitus*. London: Academic Press, 1982:201–9.
13. Horikawa Y, Oda N, Cox NJ, Li X, Orho-Melander M, Hara M, et al. Genetic variation in the gene encoding calpain-10 is associated with type 2 diabetes mellitus. *Nat Genet* 2000; 26:163–75.
14. Semenkovich CF, Heinecke JW. The mystery of diabetes and atherosclerosis: time for a new plot. *Diabetes* 1997; 46: 327–34.

15. Kahn BB, Flier JS. Obesity and insulin resistance. *J Clin Invest* 2000; 108:473-81.
16. Vollenweider P. Insulin resistant states and insulin signaling. *Clin Chem Lab Med* 2003; 41:1107-19.
17. The Expert Committee on the Diagnosis and Classification of Diabetes Mellitus. Report of the Expert Committee on the Diagnosis and Classification of Diabetes Mellitus. *Diabetes Care* 2003; 26:S4-S20.
18. Hubert HB, Feinleib M, McNamara PM, Castelli WP. Obesity as an independent risk factor for cardiovascular disease: a 26-year follow-up of participants in the Framingham Heart Study. *Circulation* 1983; 67:968-77.
19. Must A, Spadano J, Coakley EH, Field AE, Colditz G, Dietz WH. The disease burden associated with overweight and obesity. *J Am Med Assoc* 1999; 282:1623-29.
20. Alberti KG, Zimmet PZ. Definition, diagnosis and classification of diabetes mellitus and its complications. Part 1: diagnosis and classification of diabetes mellitus. Provisional report of a WHO consultation. *Diabet Med* 1998; 15:539-53.
21. Expert Panel on Detection, Evaluation and Treatment of High Blood Cholesterol in Adults. Executive Summary of the Third Report of the National Cholesterol Education Program (NCEP) Expert Panel on Detection, Evaluation and Treatment of High Blood Cholesterol in Adults (Adult Treatment Panel III). *J Am Med Assoc* 2001; 285:2486-97.
22. Dominiczak MH. Metabolic syndrome. *Curr Opin Lipidol* 2003; 14:329-32.
23. Meigs JB. The metabolic syndrome. *Br Med J* 2003; 327:61-2.
24. Modan M, Halkin H, Almog S, Lusky A, Eshkol A, Shefi M, et al. Hyperinsulinemia: a link between hypertension, obesity and glucose intolerance. *J Clin Invest* 1985; 75:809-17.
25. Ferrannini E, Haffner SM, Stern MP. Essential hypertension: an insulin-resistant state. *J Cardiovasc Pharmacol* 1990; 15:918-925.
26. Hanson RL, Imperatore G, Bennett PH, Knowler WC. Components of the 'metabolic syndrome' and incidence of type 2 diabetes. *Diabetes* 2002; 51:3120-7.
27. American Diabetes Association. Treatment of hypertension in adults with diabetes. *Diabetes Care* 2003; 26(Suppl 1):S80-S82. (ADA).
28. Haffner SM, Lehto S, Ronnemaa T, Pyörälä K, Laakso M. Mortality from coronary heart disease in diabetic subjects with type 2 diabetes and in non diabetic subjects with and without prior myocardial infarction. *N Engl J Med* 1998; 339:229-34.
29. Evans JMM, Wang J, Morris AD. Comparison of cardiovascular risk between patients with type 2 diabetes and those who had had a myocardial infarction: cross sectional and cohort studies. *Br Med J* 2002; 324:939-42.
30. Stern MP. Diabetes and cardiovascular disease: the 'common soil' hypothesis. *Diabetes* 1995; 44:369-74.
31. Astrup A, Finer N. Redefining type 2 diabetes: 'diabesity' or 'obesity dependent diabetes mellitus'? *Obes Rev* 2000; 1:57-9.
32. Schmidt MI, Duncan BB. Diabesity: an inflammatory metabolic condition. *Clin Chem Lab Med* 2003; 41:1120-30.
33. Mann JI. Diet and risk of coronary heart disease and type 2 diabetes. *Lancet* 2002; 356:783-9.
34. Tuomilehto J, Lindstrom J, Eriksson JG, Valle TT, Haanala H, Ilanne-Parikka P, et al. Prevention of type 2 diabetes mellitus by changes in lifestyle among subjects with impaired glucose tolerance. *N Engl J Med* 2001; 344:1343-50.
35. Dominiczak MH. Glucose homeostasis and fuel metabolism. In: Baynes J, Dominiczak MH, editors. *Medical biochemistry*. London: Mosby, 1999:243-66.
36. Unger RH. Lipotoxicity in the pathogenesis of obesity-dependent NIDDM. *Diabetes* 1995; 44:863-70.
37. Unger RH. Lipotoxic diseases. *Annu Rev Med* 2002; 53:319-36.
38. McGarry D. Dysregulation of fatty acid metabolism in the etiology of type 2 diabetes. *Diabetes* 2002; 51:7-18.
39. Gerich JE. Contributions of insulin-resistance and insulin-secretory defects to the pathogenesis of type 2 diabetes mellitus. *Mayo Clinic Proceedings* 2003; 78:447-58.
40. Baynes JW. Role of oxidative stress in development of complications in diabetes. *Diabetes* 1991; 40:405-12.
41. Brownlee M. Advanced protein glycosylation in diabetes and aging. *Ann Rev Med* 1996; 46:223-34.
42. Baynes JW, Thorpe SR. Role of oxidative stress in diabetic complications: a new perspective on an old paradigm. *Diabetes* 1999; 48:1-9.
43. Miyata T, Ishikawa T, van Ypersele de Strihou C. Carbonyl stress and diabetic complications. *Clin Chem Lab Med* 2003; 41:1150-8.
44. Brownlee M. Biochemistry and molecular cell biology of diabetic complications. *Nature* 2001; 414:813-20.
45. Piconi L, Quagliariello L, Ceriello A. Oxidative stress in diabetes. *Clin Chem Lab Med* 2003; 41:1144-9.
46. Wolff SP, Dean RT. Glucose autooxidation and protein modification: the potential role of 'autooxidative glycosylation' in diabetes mellitus. *Biochem J* 1987; 245:243-50.
47. Ross R. The pathogenesis of atherosclerosis: a perspective for the 1990s. *Nature* 1993; 362:801-9.
48. Ross R. Atherosclerosis - an inflammatory disease. *N Engl J Med* 1999; 340:116-26.
49. Gersony RD, Fuster V. Atherogenesis. In: Rifai N, Warnick GR, Dominiczak MH, editors. *Handbook of lipoprotein testing*, 2nd ed. Washington DC: AACC Press, 2000:31-46.
50. Palmer RMJ, Ferrige AG, Moncada S. Nitric oxide release accounts for the biological activity of endothelium-derived relaxing factor. *Nature* 1987; 327:524-6.
51. Sattler AR, Kahn CR. Insulin signalling and the regulation of glucose and lipid metabolism. *Nature* 2001; 414:799-806.
52. Evans JL, Goldfine ID, Maddux BA, Grodsky GM. Are oxidative stress-activated signaling pathways mediators of insulin resistance and β -cell dysfunction? *Diabetes* 2003; 52:1-8.
53. Cline GW, Petersen KF, Krssak M, Shen J, Hundal RS, Trajanoski Z, et al. Impaired glucose transport as a cause of decreased insulin-stimulated muscle glycogen synthesis in type 2 diabetes. *N Engl J Med* 1999; 341:240-6.
54. More S, Passan JE. An adipocentric view of signaling and intracellular trafficking. *Diabetes Metab Res Rev* 2002; 18:345-56.
55. Straub S, Sharp GWG. Glucose-stimulated signaling pathways in biphasic insulin secretion. *Diabetes Metab Res Rev* 2002; 18:451-63.
56. Hermann C, Assmus B, Urbich C, Zeiher AM, Dimmeler S. Insulin-mediated stimulation of protein kinase Akt: a potent survival signaling cascade for endothelial cells. *Atheroscler Thromb Vasc Biol* 2000; 20:402-16.
57. Ghilardi N, Ziegler S, Wiestner A, Stoffel R, Helm MH, Skoda RC. Defective STAT signaling by the leptin receptor in diabetic mice. *Proc Natl Acad Sci USA* 1996; 93:6231-5.
58. Tschritter O, Fritzsche A, Thamer C, Haap M, Shirkavand F, Rahe S, et al. Plasma adiponectin concentrations predict insulin sensitivity of both glucose and lipid metabolism. *Diabetes* 2003; 52:239-43.
59. Zhang M, Kumar S, Barnett A, Eggo M. Tumour necrosis factor- α exerts dual effects on human adipose leptin

- synthesis and release. *Mol Cell Endocrinol* 2000; 159: 79-88.
60. Saladin R, De Vos P, Guerre-Millo M, Leturque A, Girard J, Staels B, et al. Transient increase in obese gene expression after food intake or insulin administration. *Nature* 1995; 377:527-9.
 61. Hardie L, Gullhot N, Trayhurn P. Regulation of leptin production in cultured mature white adipocytes. *Horm Metab Res* 1996; 28:685-9.
 62. Lindsay RS, Funahashi T, Hanson RL, Matsuzawa Y, Tanaka S, Tataranni PA, et al. Adiponectin and development of type 2 diabetes in the Pima Indian population. *Lancet* 2002; 360:57-8.
 63. Hotamielgil GS, Peraldi P, Budavari A, Ellis R, White MF, Spiegelman BM. IRS-1-mediated inhibition of insulin receptor tyrosine kinase activity in TNF- α - and obesity-induced insulin resistance. *Science* 1996; 271:665-8.
 64. Boden G, Chen X, Roemer J, Berton M. Effects of a 48-h fast infusion on insulin secretion and glucose utilization. *Diabetes* 1986; 44:1239-42.
 65. Marcucci M, Griffin M, Estrada P, Barucci N, Cline G, Shulman G. Elevations in free fatty acids induce insulin resistance via inhibition of IRS-1-associated PI-3-kinase activity in vivo. *Diabetes* 1999; 4 (Suppl):284A.
 66. Pan DA, Lilloja S, Kriketos AD, Milner MR, Baur LA, Bogardus C, et al. Skeletal muscle triglyceride levels are inversely related to insulin action. *Diabetes* 1997; 46:983-8.
 67. Leake M, Barrett-Connor E. Asymptomatic hyperglycemia is associated with lipid and lipoprotein changes favoring atherosclerosis. *Arteriosclerosis* 1989; 9:665-72.
 68. Garg A, Helderman JH, Koffler M, Ayuso R, Rosenstock J, Reagin P. Relationship between lipoprotein levels and in vivo insulin action in normal young white men. *Metabolism* 1988; 37:982-7.
 69. Dominiczak MH. Apolipoproteins and lipoproteins in human plasma. In: Rifal N, Warnick GR, Dominiczak MH, editors. *Handbook of lipoprotein testing*, 2nd ed. Washington DC: AACC Press, 2000:1-30.
 70. Dominiczak MH. Hyperlipidaemia and cardiovascular disease. *Curr Opin Lipidol* 2002; 13:343-5.
 71. Dominiczak MH. Risk factors for coronary disease: the time for a paradigm shift? *Clin Chem Lab Med* 2001; 39:907-19.
 72. Rapp JH, Leepine A, Hamilton RL, Colyvas N, Chaumeton AH, Tweedie-Hardman J, et al. Triglyceride-rich lipoproteins isolated by selected-affinity anti-apolipoprotein B immunosorption from human atherosclerotic plaque. *Arterioscler Thromb* 1994; 14:1767-74.
 73. Austin MA, King MD, Vranizan KM, Krauss RM. Atherogenic lipoprotein phenotype: A proposed genetic marker for coronary heart disease risk. *Circulation* 1990; 82:495-506.
 74. Leary ET, Wong T, Baker DJ, Cilla D, Zhong J, Warnick GR, et al. Evaluation of an immunoseparation method for quantitative measurement of remnant-like particle-cholesterol in serum and plasma. *Clin Chem* 1998; 44:2490-8.
 75. Cohn JS, Marooux C, Davignon J. Detection, quantification, and characterization of potentially atherogenic triglyceride-rich remnant lipoproteins. *Arterioscler Thromb Vasc Biol* 1999; 19:2474-86.
 76. Schmidt AM, Vianna M, Gerlach M, Brett J, Ryan J, Kao J, et al. Isolation and characterization of two binding proteins for advanced glycosylation end products from bovine lung which are present on the endothelial cell surface. *J Biol Chem* 1992; 267:14987-97.
 77. Vlassara H, Brownlee M, Manogue KR, Dinarello CA, Pasaglan A. Cachectin/TNF and IL-1 induced by glucose-modified proteins: role in normal tissue remodeling. *Science* 1988; 240:1546-8.
 78. Vlassara H, Fuh H, Donnelly T, Cybulsky M. Advanced glycation endproducts promote adhesion molecule (VCAM-1, ICAM-1) expression and atheroma formation in normal rabbits. *Mol Med* 1995; 1:447-56.
 79. Schmidt AM, Hori O, Chen Jing X, Li J F, Crandall J, Zhang J, et al. Advanced glycation endproducts interacting with their endothelial receptor induce expression of vascular cell adhesion molecule-1 (VCAM-1) in cultured human endothelial cells and in mice: a potential mechanism for the accelerated vasculopathy of diabetes. *J Clin Invest* 1995; 96:1395-403.
 80. Dominiczak MH. Atherosclerosis. In: Colaco CALS, editor. *The glycation hypothesis of atherosclerosis*. Austin, TX: Landes Bioscience, 1997:1-28.
 81. Nakamura Y, Horii Y, Nishino T, Shiiki H, Sakaguchi Y, Kagoshima T, et al. Immunohistochemical localization of advanced glycosylation endproducts in coronary atheroma and cardiac tissue in diabetes mellitus. *Am J Pathol* 1993; 143:1649-56.
 82. Bucciarelli LG, Wendt T, Qu Wu, Lu Yan, Lalla E, Rong Ling Ling, et al. RAGE blockade stabilizes established atherosclerosis in diabetic apolipoprotein E-null mice. *Circulation* 2002; 16:2827-35.
 83. Schmidt AM, Yan SD, Yan SF, Stern DM. The multiligand receptor RAGE as a progression factor amplifying immune and inflammatory responses. *J Clin Invest* 2001; 108:949-55.
 84. Bierhaus A, Schliekofer S, Schwaninger M, Andrassy M, Humpert PM, Chen J, et al. Diabetes-associated sustained activation of the transcription factor nuclear factor-kappaB. *Diabetes* 2001; 50:2792-808.
 85. Vlassara H, Cai W, Crandall J, Goldberg T, Oberstein R, Dardaine V, et al. Inflammatory mediators are induced by dietary glycoxidants, a major risk factor for diabetic angiopathy. *Proc Natl Acad Sci USA* 2002; 99:15699-801.
 86. Du X, Matsumura T, Szabo C, Edelstein D, Brownlee M. Hyperglycemia-induced superoxide activates PKC, the hexosamine pathway, AGE formation, and NF κ B via poly (ADP-ribose) polymerase inhibition of GAPDH. *Diabetes* 2002; 51(Suppl 2):A175.
 87. Schliekofer S, Andrassy M, Chen J, Rudofsky R, Schneider J, Wendt T, et al. Acute hyperglycemia causes intracellular formation of CML and activation of ras, p42/44 MAPK and nuclear factor kappaB in PBMCs. *Diabetes* 2003; 52:621-33.
 88. Nishikawa T, Edelstein D, Du XL, Yamagishi S, Matsumura T, Kaneda Y, et al. Normalizing mitochondrial superoxide production blocks three pathways of hyperglycaemic damage. *Nature* 2000; 404:787-90.
 89. Korshunov SS, Skulachev VP, Starkov AA. High protein potential activates a mechanism of production of reactive oxygen species in mitochondria. *FEBS Lett* 1997; 416: 15-8.
 90. Roitt I, Brostoff J, Male D. *Immunology*. London: Mosby, 1998:1-11.
 91. Barnes PJ, Karin M. Nuclear factor-kappaB: a pivotal transcription factor in chronic inflammatory diseases. *N Eng J Med* 1997; 336:1066-71.
 92. Festa A, D'Agostino Jr R, Howard G, Mykkanen L, Tracy RP, Haffner SM. Chronic subclinical inflammation as part of the insulin resistance syndrome: The Insulin Resistance Atherosclerosis Study (IRAS). *Circulation* 2000; 102:42-7.
 93. Yudkin JS, Stehouwer CD, Emels JJ, Coppack SW. C-reactive protein in healthy subjects: associations with obesity, insulin resistance, and endothelial dysfunction: a potential role for cytokines originating from adipose tissue? *Arterioscler Thromb Vasc Biol* 1999; 19:972-8.

94. Ford ES. Body mass index, diabetes, and C-reactive protein among US adults. *Diabetes Care* 1999; 22:1971-7.
95. Kern PA, Ranganathan G, Li Chung-Ling, Ranganathan G. Adipose TNF and IL-6 expression in human obesity-associated insulin resistance. *Diabetes* 2000; 49(Suppl. 1):A24.
96. Freeman DJ, Norrie J, Caslake MJ, Gaw A, Ford I, Lowe GD, et al. C-reactive protein is an independent predictor of risk for the development of diabetes in the West of Scotland Coronary Prevention Study. *Diabetes* 2002; 51:1596-600.
97. Pradhan AD, Manson JE, Rifai N, Buring JE, Ridker PM. C-reactive protein, interleukin 6, and risk of developing type 2 diabetes mellitus. *J Am Med Assoc* 2001; 286:327-34.
98. Schmidt MI, Duncan BB, Sharrett AR, Lindberg G, Savage PJ, Offenbacher S, et al. Markers of inflammation and prediction of diabetes mellitus in adults (Atherosclerosis Risk in Communities Study): a cohort study. *Lancet* 1999; 353:1649-52.
99. Meigs JB, Mittleman MA, Nathan DM, Tofler GH, Singer DE, Murphy-Sheehy PM, et al. Hyperinsulinemia, hyperglycemia, and impaired hemostasis. The Framingham Offspring Study. *J Am Med Assoc* 2000; 283:221-8.
100. Feeta A, D'Agostino Jr R, Tracy RP, Haffner SM. Elevated levels of acute-phase proteins and plasminogen activator inhibitor-1 predict the development of type 2 diabetes. The Insulin Resistance Atherosclerosis Study. *Diabetes* 2002; 51:1131-7.
101. Whicher J, Biasucci L, Rifai N. Inflammation, the acute phase response and atherosclerosis. *Clin Chem Lab Med* 1999; 37:495-503.
102. Ridker PM, Buring JE, Shih J, Matias M, Hennekens CH. Prospective study of C-reactive protein and the risk of future cardiovascular events among healthy women. *Circulation* 1998; 98:731-3.
103. Ridker PM, Hennekens CH, Buring JE, Rifai N. C-reactive protein and other markers of inflammation in the prediction of cardiovascular disease in women. *N Engl J Med* 2000; 342:836-43.
104. Liebi A. Challenges in optimal metabolic control of diabetes. *Diabetes Metab Res Rev* 2002; 18:S36-S41.
105. The Diabetes Control and Complications Trial (DCCT) Research Group. The effect of intensive treatment of diabetes on the development and progression of long-term complications in insulin-dependent diabetes mellitus. *N Engl J Med* 1993; 329:977-86.
106. UK Prospective Diabetes Study (UKPDS) Group. Intensive blood glucose control with sulphonylureas or insulin compared with conventional treatment and risk of complications in patients with type 2 diabetes (UKPDS 33). *Lancet* 1998; 352:837-53.
107. Manley S. Haemoglobin A_{1c} - a marker for complications of type 2 diabetes: the experience from the UK Prospective Diabetes Study (UKPDS). *Clin Chem Lab Med* 2003; 41:1182-90.
108. Stratton IM, Adler AI, Neil HA, Matthews DR, Manley SE, Cull CA, et al. Association of glycaemia with macrovascular and microvascular complications of type 2 diabetes (UKPDS 36): prospective observational study. *Br Med J* 2000; 321:405-12.
109. The Diabetes Control and Complications Trial/Epidemiology of Diabetes Interventions and Complications Research Group. Intensive therapy and carotid intima-media thickness in type 1 diabetes mellitus. *N Engl J Med* 2003; 348:2294-303.
110. Chobanian AV, Bakris GL, Black HR, Cushman WC, Green LA, Izzo JL, et al. The Seventh Report of the Joint National Committee on Prevention, Detection, Evaluation, and Treatment of High Blood Pressure. The JNC 7 Report. *J Am Med Assoc* 2003; 289:2560-72.
111. UK Prospective Diabetes Study Group. Tight blood pressure control and risk of macrovascular and microvascular complications in type 2 diabetes: UKPDS 38. *Br Med J* 1998; 317:703-12.
112. Pyorala K, Pedersen TR, Kjekshus J, Faergeman O, Olsson AG, Thorgeirsson G. Cholesterol lowering with simvastatin improves prognosis of diabetic patients with coronary heart disease: a subgroup analysis of the Scandinavian Simvastatin Survival Study (4S). *Diabetes Care* 1997; 20:614-20.
113. Battisti WP, Palmisano J, Keane WF. Dyslipidemia in patients with type 2 diabetes. The relationship of lipids, kidney disease, and cardiovascular disease. *Clin Chem Lab Med* 2003; 41:1174-81.
114. Gaede P, Vedel P, Larsen N, Jensen GV, Parving HH, Pedersen O. Multifactorial intervention and cardiovascular disease in patients with type 2 diabetes. *N Engl J Med* 2003; 346:383-93.
115. Sacks DB, Bruns DE, Goldstein DE, Maclaren NK, McDonald JM, Parrott M. Guidelines and recommendations for laboratory analysis in the diagnosis and management of diabetes mellitus. *Diabetes Care* 2003; 25:750-86.
116. Sacks DB, Bruns DE, Goldstein DE, Maclaren NK, McDonald JM, Parrott M. Guidelines and recommendations for laboratory analysis in the diagnosis and management of diabetes mellitus. *Clin Chem* 2002; 48:436-72.
117. Kernohan AFB, Parry CG, Small M. Clinical impact of the new criteria for the diagnosis of diabetes mellitus. *Clin Chem Lab Med* 2003; 41:1239-45.
118. Jørgensen LGM, Brandslund I, Petersen PH, de Fine Olivarius N, Stahl M. The effect of the new ADA and WHO guidelines on the number of diagnosed cases of diabetes mellitus. *Clin Chem Lab Med* 2003; 41:1246-50.
119. Little RR. Glycated hemoglobin standardization - National Glycohemoglobin Standardization Program (NGSP) perspective. *Clin Chem Lab Med* 2003; 41:1291-8.
120. John WG. Haemoglobin A_{1c}: analysis and standardization. *Clin Chem Lab Med* 2003; 41:1259-65.
121. Price CP. Point-of-care testing in diabetes mellitus. *Clin Chem Lab Med* 2003; 41:1213-9.
122. Mastrorotaro J. The MiniMed continuous glucose monitoring system (CGMS). *J Pediatr Endocrinol Metab* 1999; 12 (Suppl 3):S761-8.
123. Garg SK, Potts RO, Ackerman NR, Ferri SJ, Tamada JA, Chase HR. Correlation of fingerstick blood glucose measurements with GlucoWatch biographer glucose results in young subjects with type 1 diabetes. *Diabetes Care* 1999; 22:1708-14.
124. Parving H-H. Renoprotection in diabetes: genetic and non-genetic risk factors and treatment. *Diabetologia* 1998; 41:745-60.
125. Neil A, Hawkins M, Potok M, Thorogood M, Cohen D, Mann J. A prospective population-based study of microalbuminuria as a predictor of mortality in NIDDM. *Diabetes Care* 1993; 16:996-1003.
126. Ridker PM. Evaluating novel cardiovascular risk factors: can we better predict heart attacks? *Ann Intern Med* 1999; 130:933-7.
127. Harjai KJ. Potential new cardiovascular risk factors: left ventricular hypertrophy, homocysteine, lipoprotein(a), triglycerides, oxidative stress, and fibrinogen. *Ann Intern Med* 1999; 131:376-86.
128. Yamell JW, Baker IA, Sweetnam PM, Bainton D, O'Brien JR, Whitehead PJ, et al. Fibrinogen, viscosity, and white

- blood cell count are major risk factors for Ischemic heart disease. The Caerphilly and Speedwell collaborative heart disease studies. *Circulation* 1991; 83:836-44.
129. Stec JJ, Silbershatz H, Toiler GH, Matheney TH, Sutherland P, Lipinska I, *et al.* Association of fibrinogen with cardiovascular risk factors and cardiovascular disease the Framingham Offspring Population. *Circulation* 2000; 102:1634-8.
 130. Hofmann MA, Kohl B, Zumbach MS, Borcea V, Bierhaus A, Henkels M, *et al.* Hyperhomocyst(e)inemia and endothelial dysfunction in IDDM. *Diabetes Care* 1998; 21:841-8.
 131. Stehouwer CDA. Heterogeneity of the association between plasma homocysteine and atherothrombotic disease: insights from studies of vascular structure and function. *Clin Chem Lab Med* 2001; 39:705-9.
 132. Yeromenko Y, Lavie L, Levy Y. Homocysteine and cardiovascular risk in patients with diabetes mellitus. *Nutr Metab Cardiovasc Dis* 2001; 11:108-10.
 133. Pearson TA, Mensah GA, Alexander RW, Anderson JL, Cannon RO III, Criqui M, *et al.* Markers of inflammation and cardiovascular disease: application to clinical and public health practice: a statement for healthcare professionals from the Centers for Disease Control and Prevention and the American Heart Association [AHA/CDC Scientific Statement]. *Circulation* 2003; 107:499-511.

Corresponding author: Dr. M. H. Dominiczak, Department of Biochemistry, Gartnavel General Hospital, 1053 Great Western Road, Glasgow G12 0YN, UK
 Phone: +44 0141 211 2788, Fax: +44 0141 211 3452,
 E-mail: m.h.dominiczak@clinmed.gla.ac.uk,
 mhd1b@clinmed.gla.ac.uk

PREVALENCE OF IMPAIRED GLUCOSE TOLERANCE AMONG CHILDREN AND ADOLESCENTS WITH MARKED OBESITY

RANJANA SINHA, M.D., GENE FISCH, Ph.D., BARBARA TEAGUE, R.N., WILLIAM V. TAMBORLANE, M.D.,
BRUNA BANYAS, R.N., KARIN ALLEN, R.N., MARY SAVOYE, R.D., VERA RIEGER, M.D., SARA TAKSALI, M.P.H.,
GINA BARBETTA, R.D., ROBERT S. SHERWIN, M.D., AND SONIA CAPRIO, M.D.

ABSTRACT

Background Childhood obesity, epidemic in the United States, has been accompanied by an increase in the prevalence of type 2 diabetes among children and adolescents. We determined the prevalence of impaired glucose tolerance in a multiethnic cohort of 167 obese children and adolescents.

Methods All subjects underwent a two-hour oral glucose-tolerance test (1.75 mg of glucose per kilogram of body weight), and glucose, insulin, and C-peptide levels were measured. Fasting levels of proinsulin were obtained, and the ratio of proinsulin to insulin was calculated. Insulin resistance was estimated by homeostatic model assessment, and beta-cell function was estimated by calculating the ratio between the changes in the insulin level and the glucose level during the first 30 minutes after the ingestion of glucose.

Results Impaired glucose tolerance was detected in 25 percent of the 55 obese children (4 to 10 years of age) and 21 percent of the 112 obese adolescents (11 to 18 years of age); silent type 2 diabetes was identified in 4 percent of the obese adolescents. Insulin and C-peptide levels were markedly elevated after the glucose-tolerance test in subjects with impaired glucose tolerance but not in adolescents with diabetes, who had a reduced ratio of the 30-minute change in the insulin level to the 30-minute change in the glucose level. After the body-mass index had been controlled for, insulin resistance was greater in the affected cohort and was the best predictor of impaired glucose tolerance.

Conclusions Impaired glucose tolerance is highly prevalent among children and adolescents with severe obesity, irrespective of ethnic group. Impaired oral glucose tolerance was associated with insulin resistance while beta-cell function was still relatively preserved. Overt type 2 diabetes was linked to beta-cell failure. (N Engl J Med 2002;346:802-10.)

Copyright © 2002 Massachusetts Medical Society.

THE epidemic of childhood obesity in the United States has been accompanied by a marked increase in the frequency of type 2 diabetes.^{1,2} In adults, type 2 diabetes develops over a long period, and most, if not all, patients initially have impaired glucose tolerance, which is an intermediate stage in the natural history of type 2 diabetes³ and predicts the risk of the development of

diabetes⁴ and cardiovascular disease.⁵ With appropriate changes in lifestyle, progression from impaired glucose tolerance to frank diabetes can be delayed or prevented.^{6,7} Thus, great emphasis has recently been placed on the early detection of glucose intolerance in adults.

Although severe obesity has a prominent role in the pathogenesis of type 2 diabetes in children and adolescents,¹ it is unknown whether it is a risk factor for impaired glucose tolerance. We undertook a study to determine the prevalence of glucose intolerance in a multiethnic cohort of obese children and adolescents. Abnormal beta-cell function, as manifested by the release of large amounts of proinsulin relative to insulin levels, is clearly present in patients with overt type 2 diabetes.^{8,9} Disproportionate hyperproinsulinemia is thought to represent an impending failure of insulin secretion in adults.⁸ The earlier an increase in the ratio of proinsulin to insulin occurs in the prediabetic phase, the more likely it is that abnormal processing of insulin by beta cells is fundamental to the pathogenesis of diabetes. We therefore examined the intracellular processing of proinsulin to determine whether alterations are present early in the development of glucose intolerance in obese children and adolescents.

METHODS

Study Population

We recruited 55 children (4 to 10 years of age) and 112 adolescents (11 to 18 years of age) who had been referred to the Yale Pediatric Obesity Clinic between 1999 and 2001. Body weight was measured with a digital scale to the nearest 0.1 kg, and height was measured in triplicate with a wall-mounted stadiometer. The body-mass index — the weight in kilograms divided by the square of the height in meters — was calculated. All subjects had a body-mass index that was higher than the 95th percentile for age and sex and were thus classified as obese.¹⁰ Approximately 58 percent of the subjects were non-Hispanic white, 23 percent were non-Hispanic black, and 19 percent were Hispanic (Table 1). A detailed medical and family history was obtained from all subjects, and a physical examination was performed, including staging of puberty on the basis of breast development in girls and genital development in boys according to the criteria of Tanner¹¹ (stage 1 indicates preadolescent charac-

From the Departments of Pediatrics (R.S., W.V.T., V.R., S.T., G.B., S.C.) and Internal Medicine (R.S.S.), the Children's General Clinical Research Center (G.E., B.T., B.B., K.A., M.S.), and the Division of Biostatistics, Department of Epidemiology and Public Health (G.E.), Yale University School of Medicine, New Haven, Conn. Address reprint requests to Dr. Caprio at the Department of Pediatrics, Yale University School of Medicine, 333 Cedar St., P.O. Box 208064, New Haven, CT 06520, or at sonia.caprio@yale.edu.

IMPAIRED GLUCOSE TOLERANCE IN OBESE CHILDREN AND ADOLESCENTS

TABLE 1. CLINICAL CHARACTERISTICS ACCORDING TO SEX AND AGE GROUP.*

CHARACTERISTIC	CHILDREN (N=55)		ADOLESCENTS (N=112)	
	MALE (N=17)	FEMALE (N=38)	MALE (N=54)	FEMALE (N=58)
Race or ethnic group (no.)				
Non-Hispanic white	12	23	26	37
Non-Hispanic black	3	9	12	14
Hispanic	2	7	16	7
Age (yr)	8±0.3	7±0.3	14±0.3	14±0.2
Range	6-10	4-10	11-17	11-18
Weight (kg)	62±15	54±8	104±4	104±0.2
Height (cm)	138±3	133±2	166±1	162±1
Body-mass index	22±8	20±1	37±1	34±1

*Plus-minus values are means ±SE.

teristics, and stage 5 indicates adult characteristics). All subjects were otherwise in good health and had normal thyroid function; none were taking any medications. A total of 23 of the adolescent girls (approximately 40 percent) had hirsutism, oligomenorrhea, acne, and increased levels of total testosterone, suggesting the presence of the polycystic ovary syndrome. The study was approved by the Institutional Review Board of the Yale University School of Medicine. Written informed consent was obtained from the parents and oral consent from the children and adolescents.

Oral Glucose-Tolerance Test

All subjects followed a weight-maintenance diet consisting of at least 250 g of carbohydrates per day for seven days before the study, as confirmed by the fact that body weight remained stable (measured to the nearest 0.5 kg). Subjects were studied in the Children's Clinical Research Center at the Yale University School of Medicine at 8 a.m. after a 12-hour overnight fast. After the local application of a topical anesthetic cream containing 2.5 percent lidocaine and 2.5 percent prilocaine (Emla, Astra Zeneca, Wilmington, Del.), one antecubital intravenous catheter was inserted for blood sampling, and its patency was maintained by slow infusion of normal saline. Each child then rested while watching a videotape for 30 minutes. Two baseline samples were then obtained for measurements of plasma glucose, insulin, C peptide, proinsulin, and lipids. Thereafter, flavored glucose (Orangedex, Custom Laboratories, Baltimore) in a dose of 1.75 g per kilogram of body weight (up to a maximum of 75 g) was given orally, and blood samples were obtained every 30 minutes for 120 minutes for the measurement of plasma glucose, insulin, and C peptide. Impaired glucose tolerance was defined, according to the American Diabetes Association guidelines, as a fasting plasma glucose level of less than 126 mg per deciliter and a two-hour plasma glucose level of 140 to 200 mg per deciliter; type 2 diabetes was defined as a fasting glucose level of 126 mg per deciliter or higher or a two-hour plasma glucose level of more than 200 mg per deciliter.¹³

Although the oral glucose-tolerance test is the most sensitive method for detecting early diabetes, it can result in misclassification.¹³ To determine the reproducibility of the results, we repeated the test three months later in four obese children with normal glucose tolerance and in six obese children and adolescents with impaired glucose tolerance.

Biochemical Analysis

The plasma glucose level was determined with a glucose analyzer (Beckman Instruments, Brea, Calif.), and the plasma lipid

levels were determined by the Yale Core Lipid Laboratory with an AutoAnalyzer (model 747-200, Roche-Hitachi, Indianapolis). Plasma insulin was measured with a radioimmunoassay made by Linco (St. Charles, Mo.), which has less than 1 percent cross-reactivity with C-peptide and proinsulin. Plasma C-peptide levels were determined with an assay made by Diagnostic Product (Los Angeles), and total proinsulin with another radioimmunoassay kit (Linco), which has no cross-reactivity with insulin and a detection limit of 0.15 pmol. The intraassay variation was 11 percent for insulin, 13 percent for C peptide, and 9 percent for proinsulin, and the interassay variation was 13 percent for insulin, 12 percent for C peptide, and 11 percent for proinsulin.

Calculations

To assess beta-cell function, we used the insulinogenic index, calculated as the ratio of the increment in the plasma insulin level to that in the plasma glucose level during the first 30 minutes after the ingestion of glucose. We found that in children and adolescents, the insulinogenic index correlates well with the early insulin response obtained during a hyperglycemic-clamp study ($r=0.68$, $P<0.001$). A low insulinogenic index predicts the development of diabetes in adults.¹⁴⁻¹⁷ Insulin resistance was determined by homeostatic model assessment¹⁸ and calculated as the product of the fasting plasma insulin level (in microunits per milliliter) and the fasting plasma glucose level (in millimoles per liter), divided by 22.5. Lower insulin-resistance values indicate a higher insulin sensitivity, whereas higher values indicate a lower insulin sensitivity. The estimate obtained with homeostatic model assessment (the insulin-resistance index) correlated well ($r=-0.71$, $P<0.001$) with measures of insulin resistance obtained from obese and nonobese children and adolescents with the use of the euglycemic-hyperinsulinemic clamp technique; a similar correlation has been reported in adults.^{18,19}

Statistical Analysis

All values are expressed as means ±SE. Variables that were not normally distributed (insulin level, insulin-resistance index, proinsulin level, and two-hour plasma insulin level) were log-transformed for analysis. However, for clarity of interpretation, results are expressed as untransformed values. Differences in the means of continuous variables were tested by two-tailed *t*-tests. Nonparametric statistics were applied in the analyses of data that had a skewed distribution. An analysis of covariance was used to compare the plasma levels of glucose, insulin, C peptide, and proinsulin and the insulin-resistance index of subjects with normal glucose tolerance with the values for those with impaired glucose tolerance, with age and body-mass index as covariates. Multiple logistic-regression analysis was used to evaluate the model with the use of two goodness-of-fit tests (Proc Logistic procedure, SAS software, release 6.10, SAS Institute, Cary, N.C.)²⁰ and to determine the relative risks of impaired glucose tolerance among obese children and adolescents. The dependent variable in multiple logistic-regression analyses was the plasma glucose level at 120 minutes. The independent variables entered in the several models generated were age, body-mass index, fasting insulin and proinsulin levels, two-hour plasma insulin level, the insulin-resistance index, and the insulinogenic index.

RESULTS

Prevalence of Impaired Glucose Tolerance and Silent Type 2 Diabetes

A total of 25 percent of the children and 21 percent of the adolescents had impaired glucose tolerance (Table 2). Silent diabetes was diagnosed in four adolescents (4 percent). Among the children and adolescents with impaired glucose tolerance, 51 percent were non-

Hispanic white, 30 percent were non-Hispanic black, and 19 percent were Hispanic. Four adolescents — two black and two Hispanic — had diabetes. Fourteen girls with apparent cases of the polycystic ovary syndrome had normal glucose tolerance, six had impaired glucose tolerance, and two had diabetes. A total of 30 percent of the combined group of those with impaired glucose tolerance and those with frank diabetes had a parental history of type 2 diabetes; the rate was 25 percent among those with normal glucose tolerance ($P=0.54$).

More children with impaired glucose tolerance were girls, whereas the numbers of boys and girls were similar in the groups of adolescents with impaired glucose tolerance. The body-mass index was higher among adolescents with impaired glucose tolerance or diabetes than among those with normal glucose tolerance.

Reproducibility of the Oral Glucose-Tolerance Test

The mean plasma glucose levels at two hours during the first oral glucose-tolerance test (108 ± 7 mg per deciliter for subjects with normal glucose tolerance and 152 ± 3 mg per deciliter for those with impaired glucose tolerance) were similar to those obtained during the second oral glucose-tolerance test in subjects studied to determine the reproducibility of the results

(107 ± 12 mg per deciliter for subjects with normal glucose tolerance and 146 ± 3 mg per deciliter for those with impaired glucose tolerance). Thus, the diagnosis was confirmed during the second test in all six subjects with impaired glucose tolerance who were evaluated. Three non-Hispanic black girls were followed for two to five years, during which time the oral glucose-tolerance test was repeated several times. Subject 1 had impaired glucose tolerance at 6 years of age, which persisted until 11 years of age, when diabetes developed. Subject 2 had normal glucose tolerance at 8 years of age, which then progressed to impaired glucose tolerance at 12 years of age and remained impaired thereafter. Subject 3 had impaired glucose tolerance at six years of age, and frank diabetes developed at eight years of age.

Glucose, Insulin, and C-Peptide Responses to an Oral Glucose Challenge

Fasting plasma glucose levels were similar in the children irrespective of whether their glucose tolerance was normal or impaired (Fig. 1). In contrast, the adolescents with impaired glucose tolerance had higher fasting plasma glucose levels (90 ± 1 mg per deciliter [5.0 ± 0.06 mmol per liter]) than those with normal glucose tolerance (82 ± 1 mg per deciliter [4.6 ± 0.06

TABLE 2. CLINICAL AND METABOLIC PHENOTYPE OF OBESE CHILDREN AND ADOLESCENTS WITH NORMAL GLUCOSE TOLERANCE, IMPAIRED GLUCOSE TOLERANCE, OR TYPE 2 DIABETES.*

VARIABLE	CHILDREN (N=55)			ADOLESCENTS (N=112)				
	NORMAL GLUCOSE TOLERANCE (N=41)	IMPAIRED GLUCOSE TOLERANCE (N=14)	P VALUE	NORMAL GLUCOSE TOLERANCE (N=85)	IMPAIRED GLUCOSE TOLERANCE (N=28)	P VALUE	TYPE 2 DIABETES (N=4)	P VALUE
Race or ethnic group (no.)								
Non-Hispanic white	25	9		53	10		0	
Non-Hispanic black	8	4		17	7		2	
Hispanic	8	1		15	6		2	
Sex (no.)								
Male	15	2		40	12		2	
Female	26	12		45	11		2	
Age (yr)								
Range	7.5±0.3 4-10	8±0.5 5-10		14±1 11-18	15±0.4 13-18		16±1 11-18	
Body-mass index	30±1	32±1	<0.05	37±0.9	41±1	<0.001	41±5	<0.001
Fasting insulin level (μU/ml)	20±5	34±5	<0.001	30±2	66±7	<0.001	60±10	<0.001
Fasting C-peptide level (ng/ml)	2.6±0.3	3.2±0.2	<0.001	3.6±0.1	4.7±0.3	<0.001	4.5±1	<0.001
Insulin-resistance index†	5±0.6	7.2±1	<0.001	6.3±0.4	13±7	<0.001	14±3	<0.001

*Plus-minus values are means ±SE. All P values are for the comparison with the group with normal glucose tolerance. To convert values for insulin to picomoles per liter, multiply by 6; to convert values for C-peptide to nanomoles per liter, multiply by 0.331.

†The insulin-resistance index was determined by homeostatic model assessment and calculated as the product of the fasting plasma insulin level (in microunits per milliliter) and the fasting plasma glucose level (in millimoles per liter), divided by 22.5. Lower insulin-resistance values indicate a higher insulin sensitivity, whereas higher insulin-resistance values indicate a lower insulin sensitivity.

IMPAIRED GLUCOSE TOLERANCE IN OBESE CHILDREN AND ADOLESCENTS

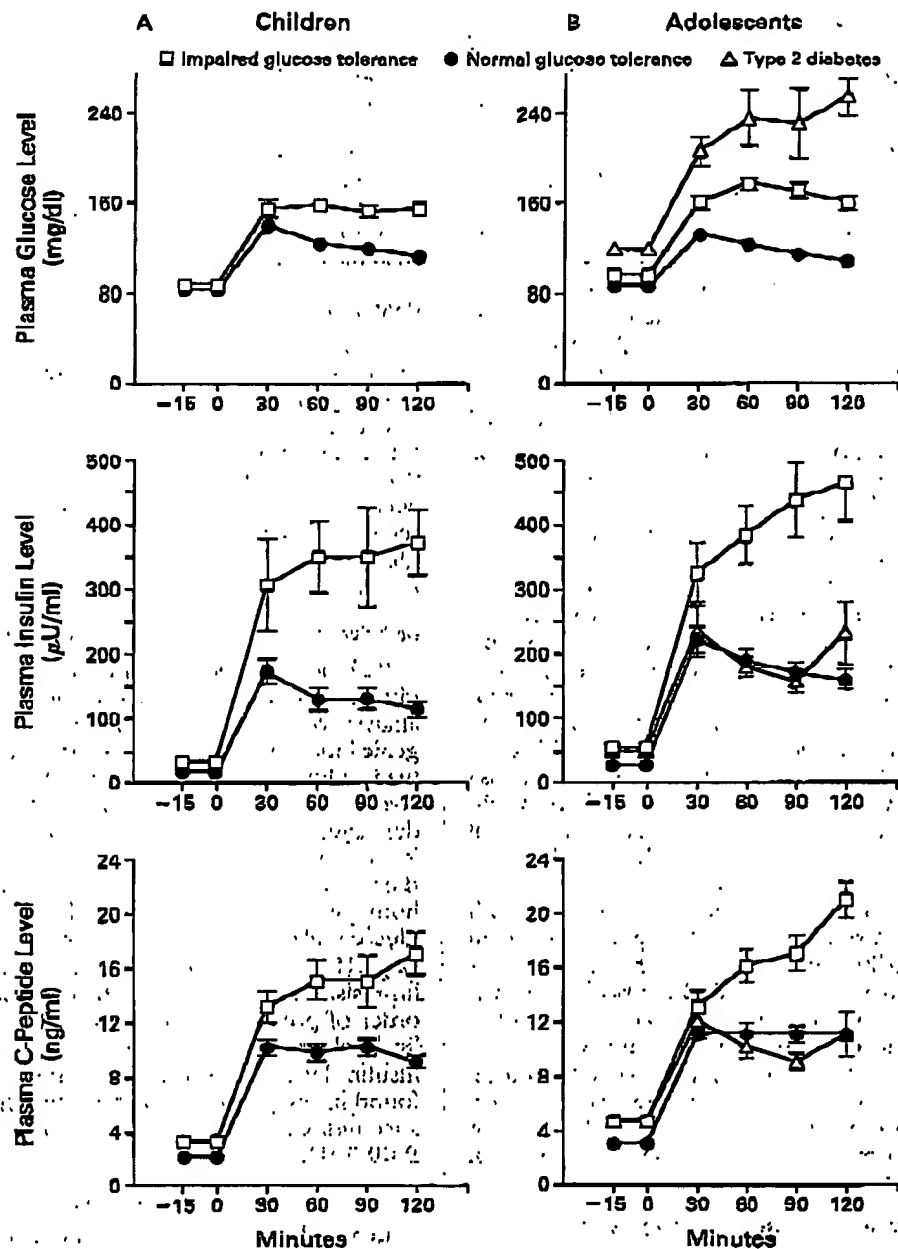


Figure 1. Mean (\pm SE) Plasma Glucose, Insulin, and C-Peptide Responses during the Oral Glucose-Tolerance Test in Obese Children (Panel A) and Adolescents (Panel B) with Normal Glucose Tolerance, Impaired Glucose Tolerance, or Type 2 Diabetes Mellitus.

Glucose (1.75 mg per kilogram) was administered at time 0. To convert values for glucose to millimoles per liter, multiply by 0.05551; to convert values for insulin to picomoles per liter, multiply by 6; to convert values for C peptide to nanomoles per liter, multiply by 0.331.

mmol per liter], $P=0.03$), and adolescents with type 2 diabetes had the highest fasting plasma glucose levels (118 ± 6 mg per deciliter [6.6 ± 0.33 mmol per liter], $P<0.001$). After the oral glucose-tolerance test, plasma glucose levels were higher in both children and adolescents with impaired glucose tolerance than in those with normal glucose tolerance and highest in subjects with frank diabetes ($P<0.001$). Fasting plasma insulin and C-peptide levels (Table 2) were higher in both children and adolescents with impaired glucose tolerance or diabetes than in subjects with normal glucose tolerance, even after adjustment for differences in the body-mass index. Similarly, the plasma insulin and C-peptide responses to oral glucose-tolerance testing were dramatically elevated in children and adolescents with impaired glucose tolerance as compared with the responses in those with normal glucose tolerance. In contrast, adolescents with silent diabetes had insulin and C-peptide responses similar to the responses in those with normal glucose tolerance.

Fasting Insulin and Proinsulin

Fasting proinsulin levels were nearly twice as high in children and adolescents with impaired glucose tolerance and diabetes as in those with normal glucose tolerance ($P<0.002$) (Fig. 2). The mean plasma proinsulin level was 1.6 ± 0.02 ng per milliliter in children with normal glucose tolerance, as compared with 2.6 ± 0.02 ng per milliliter in those with impaired glucose tolerance ($P=0.002$). The mean ratio of proinsulin to insulin was 0.11 ± 0.005 in children with normal glucose tolerance and 0.17 ± 0.01 in those with abnormal glucose tolerance. The fasting plasma proinsulin level was 2.4 ± 0.01 ng per milliliter in adolescents with normal glucose tolerance, 4.5 ± 0.06 ng per milliliter in those with impaired glucose tolerance, and 6.2 ± 0.12 in those with diabetes ($P=0.002$ for both comparisons with the adolescents with normal glucose tolerance). The ratio of proinsulin to insulin was 0.16 ± 0.002 in adolescents with normal glucose tolerance, 0.17 ± 0.02 in those with impaired glucose tolerance, and 0.23 ± 0.06 in those with diabetes ($P=0.30$ for both comparisons with the adolescents with normal glucose tolerance).

Early-Phase Insulin Secretion and Insulin Resistance

Impaired glucose tolerance in children was not associated with significant differences in the early changes in the glucose level, the insulin level, or the insulinogenic index (Fig. 3). In contrast, among adolescents with impaired glucose tolerance, there were changes in the plasma glucose level at 30 minutes that were significantly greater than those that occurred in adolescents with normal glucose tolerance, although these changes were not associated with a significant increase in plasma insulin levels. Consequently, the cal-

culated insulinogenic index was slightly but not significantly lower than that among adolescents with normal glucose tolerance ($P=0.09$). On the other hand, a significant reduction in the insulinogenic index was clearly observed among the adolescents with type 2 diabetes. After adjustment for differences in age and body-mass index, the subjects with glucose intolerance or diabetes had a significantly higher insulin-resistance index than did those with normal glucose tolerance ($P<0.001$) (Table 2).

Cardiovascular Risk Factors

Fasting lipid and lipoprotein profiles were similar in all groups, except that the fasting triglyceride levels were higher among the adolescents with impaired glucose tolerance than among those with normal glucose tolerance (150 ± 20 vs. 115 ± 7 mg per deciliter [1.7 ± 0.2 vs. 1.3 ± 0.08 mmol per liter], $P=0.05$). No differences in systolic and diastolic blood pressure were observed between children or adolescents with normal glucose tolerance and those with impaired glucose tolerance.

Risk Factors Associated with Impaired Glucose Tolerance

Risk factors associated with the presence of impaired glucose tolerance included in the logistic-regression analysis were the body-mass index, age, the insulinogenic index (as a categorical variable), the fasting plasma insulin and proinsulin levels, the two-hour insulin levels, and the insulin-resistance index. Body-mass index, age, and the insulinogenic index did not significantly predict impaired glucose tolerance. However, the insulin-resistance index strongly predicted the two-hour glucose level, with an odds ratio for impaired glucose tolerance of 1.27 (95 percent confidence interval, 1.15 to 1.40) per increment of 0.24 in the insulin-resistance index ($P<0.001$); other predictors, in order of predictive power, were the fasting proinsulin level, the two-hour insulin level, and the fasting insulin level. A positive, continuous relation was found in the entire cohort between the insulin-resistance index and the two-hour glucose level ($r=0.42$, $P<0.001$).

DISCUSSION

In a multiethnic cohort of obese children and adolescents, we found a high prevalence of impaired glucose tolerance. Previously undiagnosed type 2 diabetes was detected only among the adolescents (4 percent), and all four subjects with diabetes were members of minorities. Children and adolescents with impaired glucose tolerance included both white and minority children. The risk factors associated with impaired glucose tolerance included insulin resistance, marked hyperinsulinemia both after fasting and after a glucose challenge, and hyperproinsulinemia after fasting.

IMPAIRED GLUCOSE TOLERANCE IN OBESE CHILDREN AND ADOLESCENTS

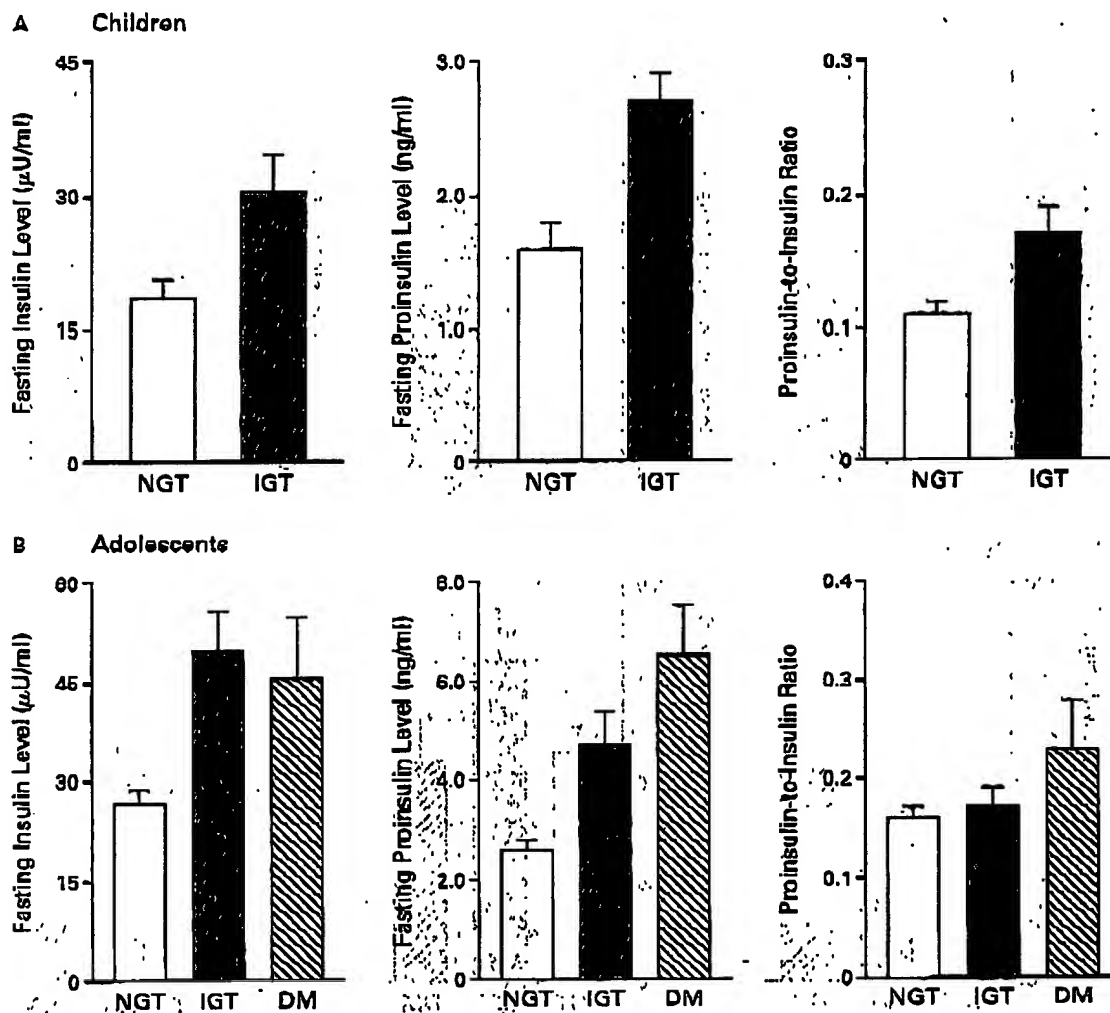


Figure 2. Mean (\pm SE) Fasting Insulin and Proinsulin Levels and Proinsulin-to-Insulin Ratio in Obese Children (Panel A) and Adolescents (Panel B) with Normal Glucose Tolerance (NGT), Impaired Glucose Tolerance (IGT), or Type 2 Diabetes Mellitus (DM). To convert values for insulin to picomoles per liter, multiply by 6; to convert values for proinsulin to picomoles per liter, multiply by 0.00939.

Like Arslanian et al.,²¹ we also found impaired glucose tolerance in some obese adolescents with the polycystic ovary syndrome. On the other hand, our study did not confirm that a family history of type 2 diabetes is a risk factor for impaired glucose tolerance, perhaps because we studied a group of high-risk obese children and adolescents. Although children and adolescents with mildly impaired glucose tolerance provide a unique model that can help us identify the early events that lead to diabetes without the confounding effects of aging and hyperglycemia, there is little information

available about risk factors associated with impaired glucose tolerance in young persons. Our data indicate that insulin resistance is a strong predictor of the two-hour plasma glucose levels in obese children and adolescents. Thus, it may play an important part in the transition from normal to impaired glucose tolerance.

The degree of obesity was not found to be a significant risk factor, possibly because the majority of our subjects were severely obese. The effects of obesity on the deterioration of glucose tolerance are most likely mediated by its metabolic complications — particular-

The New England Journal of Medicine

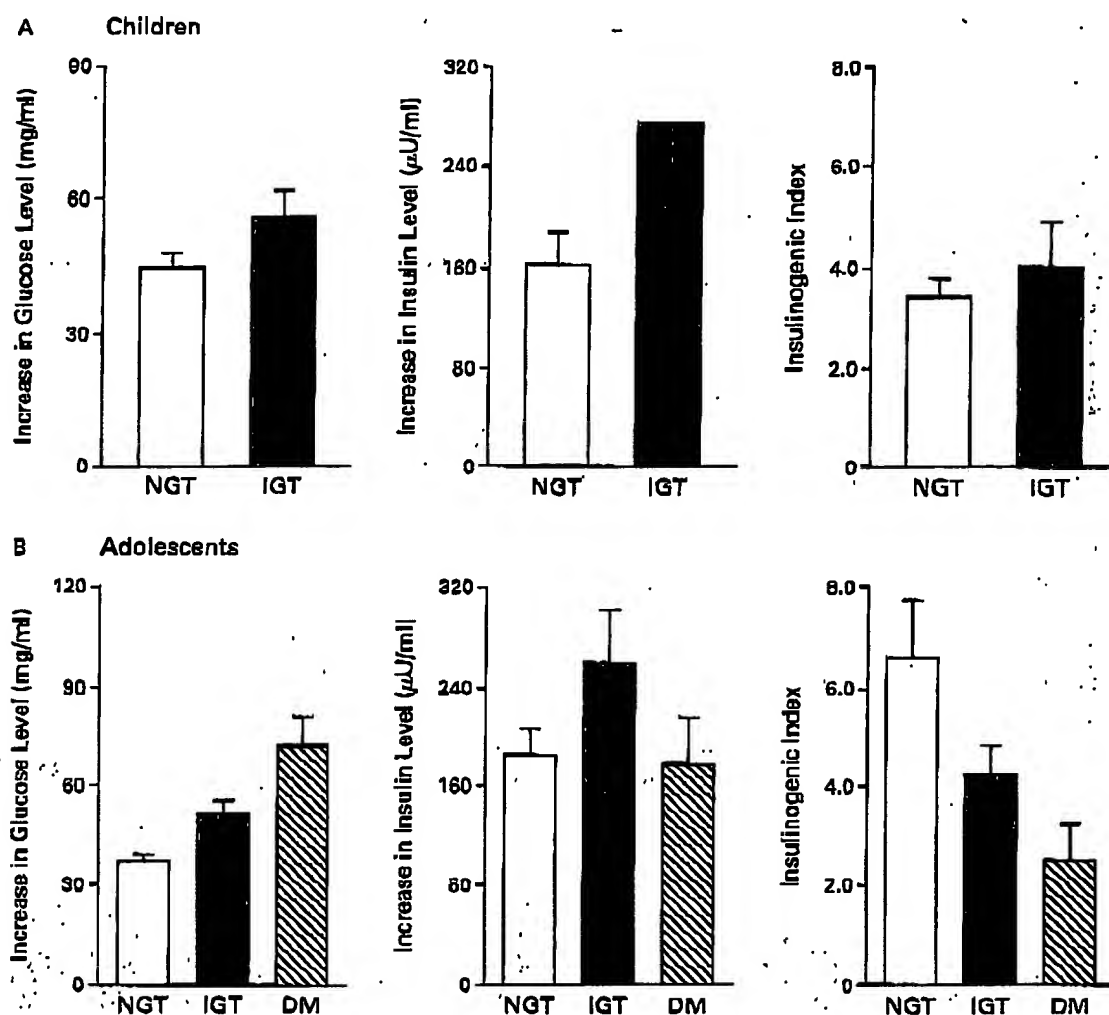


Figure 3. Mean (\pm SE) Changes from Base Line to 30 Minutes in Plasma Glucose and Insulin Levels and the Ratio of the Change in Insulin to the Change in Glucose (the Insulinogenic Index) in Obese Children and Adolescents with Normal Glucose Tolerance (NGT), Impaired Glucose Tolerance (IGT), or Type 2 Diabetes Mellitus (DM).

To convert values for glucose to millimoles per liter, multiply by 0.05551; to convert values for insulin to picomoles per liter, multiply by 8.

ly insulin resistance and hyperinsulinemia. Similar findings have been reported among adult Pima Indians²² and Mexican-American adults.²³ Although longitudinal studies are required to determine the sequence of events involved in the transitions from normal to impaired glucose tolerance and from glucose intolerance to diabetes, our study suggests that the onset of impaired glucose tolerance in obese children and adolescents is clearly associated with the development of severe insulin resistance while normal beta-cell function is still relatively preserved. In the presence of overt diabetes, insulin secretion declines, as demonstrated by

the lower insulin levels during the oral glucose-tolerance test in the adolescents with type 2 diabetes.

The loss of the first phase of insulin secretion has important pathogenic consequences, since it plays a key part in priming insulin action in target tissues that are responsible for normal glucose homeostasis.^{24,25} As a marker of early beta-cell response, we used the insulinogenic index, which was partially preserved in the adolescents with impaired glucose tolerance, whereas it was significantly reduced in the presence of frank diabetes. To further evaluate beta-cell function early in the prediabetic stage in obese children,

IMPAIRED GLUCOSE TOLERANCE IN OBESE CHILDREN AND ADOLESCENTS

we measured proinsulin levels and calculated the ratios of proinsulin to insulin. Disproportionate hyperproinsulinemia is a clear marker of beta-cell dysfunction in overt type 2 diabetes.^{8,9,26} In Japanese-American men,²⁷ Mexicans,²⁸ and elderly white persons,²⁹ increased proinsulin levels have been found to predict the development of type 2 diabetes. In this study, fasting proinsulin levels were increased in children with impaired glucose tolerance, but their proinsulin-to-insulin ratios did not differ significantly from the ratios among those with normal glucose tolerance. Thus, in the very early stages of glucose intolerance in children and adolescents, despite the increased demand for beta-cell secretion, the hyperproinsulinemia is proportional to the hyperinsulinemia. The vigorous hyperinsulinemic response to glucose found in the prediabetic stage in obese children and adolescents may reflect an up-regulation of beta-cell function caused by chronic severe insulin resistance. Such a degree of hyperinsulinemia is not present in adults with impaired glucose tolerance.³⁰ It is conceivable that advanced age, together with changes in the size and mass of beta cells, the accumulation of amyloid in the islets, or both may contribute to the phenotypic expression of impaired insulin secretion that is found in some adults with impaired glucose tolerance.^{9,22}

The oral glucose-tolerance test is a labor-intensive method for studying carbohydrate metabolism. Unquestionably, the fasting plasma glucose level is easier and faster to measure, and its measurement is more acceptable to patients than an oral glucose-tolerance test. In our cohort of obese children and adolescents with impaired glucose tolerance, the prevalence of impaired fasting glucose levels (more than 110 mg per deciliter or 6 mmol per liter) was extremely low (less than 0.08 percent), whereas all four adolescents with diabetes had impaired fasting glucose levels. This suggests that fasting hyperglycemia is indicative of a more advanced stage of clinical diabetes, and the determination of its presence represents a very insensitive method for detecting impaired glucose tolerance. Similar findings on the low prevalence of impaired fasting glucose levels in adolescents have recently been reported by Fagot-Compagna et al.³¹ Our study suggests that the oral glucose-tolerance test can reliably establish a diagnosis of impaired glucose tolerance, since the intraperson variation was low in obese children and adolescents. This test may be required for the early detection of impaired glucose tolerance as well as of silent type 2 diabetes in patients with severe childhood obesity.

In summary, this cross-sectional study suggests that insulin resistance, initially associated with hyperinsulinemia and hyperproinsulinemia, is the most important risk factor linked to the development of impaired glucose tolerance in severe childhood obesity. In the

presence of established diabetes, beta-cell failure becomes fully manifest.

Supported by grants (R01 HD-28016 [to Dr. Caprio], R01 HD 40787 [to Dr. Caprio], K24HD01464 [to Dr. Caprio], MO1 RR 00125, and MO1 RR 06022) from the National Institutes of Health.

We are indebted to all the children and adolescents who participated in the study; to Aida Grozman and Andrea Belous for technical assistance in measuring all hormones; and to Nancy Canetti for assistance in the preparation of the manuscript.

REFERENCES

1. Rosenbloom AL, Joe JR, Young RS, Winter NE. Emerging epidemic of type 2 diabetes in youth. *Diabetes Care* 1999;22:345-54.
2. Dabelea D, Pettit DJ, Jones KL, Arslanian SA. Type 2 diabetes mellitus in minority children and adolescents: an emerging problem. *Endocrinol Metab Clin North Am* 1999;28:709-29.
3. Polonsky KS, Sturis J, Bell GI. Non-insulin-dependent diabetes mellitus — a genetically programmed failure of the beta cell to compensate for insulin resistance. *N Engl J Med* 1996;334:777-83.
4. Edelstein SL, Knowler WC, Bain RP, et al. Predictors of progression from impaired glucose tolerance to NIDDM: an analysis of six prospective studies. *Diabetes* 1997;46:701-10.
5. Haffner SM, Stern ME, Hazuda HP, Mitchell BD, Patterson JK. Cardiovascular risk factors in confirmed prediabetic individuals: does the clock for coronary heart disease start ticking before the onset of clinical diabetes? *JAMA* 1990;263:2893-9.
6. Tuomilehto J, Knowler WC, Zimmet P. Primary prevention of non-insulin-dependent diabetes mellitus. *Diabetes Metab Rev* 1992;8:339-53.
7. Tuomilehto J, Lindström J, Eriksson JG, et al. Prevention of type 2 diabetes mellitus by changes in lifestyle among subjects with impaired glucose tolerance. *N Engl J Med* 2001;344:1343-50.
8. Porte D, Kahn SE. β -Cell dysfunction and failure in type 2 diabetes: potential mechanisms. *Diabetes* 2001;50(Suppl 1):S160-S163.
9. *Idem*. Hyperproinsulinemia and amyloid in NIDDM: clues to etiology of islet β -cell dysfunction? *Diabetes* 1989;38:1333-6.
10. Hammer LD, Kraemer HC, Wilson DM, Rimer PL, Dornbusch SM. Standardized percentile curves of body-mass index for children and adolescents. *Am J Dis Child* 1991;145:259-63.
11. Tanner JM. *Growth at adolescence*. 2nd ed. Oxford, England: Blackwell Scientific, 1962.
12. The Expert Committee on the Diagnosis and Classification of Diabetes Mellitus. Report of the Expert Committee on the Diagnosis and Classification of Diabetes Mellitus. *Diabetes Care* 1999;22(Suppl 1):S5-S19.
13. Phillips DIW, Clark PM, Hales CM, Osmond C. Understanding oral glucose tolerance: comparison of glucose or insulin measurements during the oral glucose tolerance test with specific measurements of insulin resistance and insulin secretion. *Diabet Med* 1998;11:286-92.
14. Eftedal S, Luft R, Wejnagel A. Aspects of the pathogenesis of type 2 diabetes. *Endocr Rev* 1984;5:595-610.
15. Kosaka K, Hagura K, Kuzuya T. Insulin responses in equivocal and definite diabetes, with special reference to subjects who had mild glucose intolerance but later developed definite diabetes. *Diabetes* 1977;26:944-52.
16. Kadawaki T, Miyake Y, Hagura K, et al. Risk factors for worsening to diabetes in subjects with impaired glucose tolerance. *Diabetologia* 1984;26:44-9.
17. Haffner SM, Miettinen H, Gaskill SP, Stern ME. Decreased insulin secretion and increased insulin resistance are independently related to the 7-year risk of NIDDM in Mexican-Americans. *Diabetes* 1995;44:1386-91.
18. Matthews DR, Hosker JP, Rudenski AS, Naylor BA, Treacher DF, Turner RC. Homeostasis model assessment: insulin resistance and β -cell function from fasting plasma glucose and insulin concentrations in man. *Diabetologia* 1985;28:412-9.
19. Bonora E, Kiechl S, Willkitz J, et al. Prevalence of insulin resistance in metabolic disorders: the St. Leonhard Study. *Diabetes* 1998;47:1643-9.
20. Stokes ME, Davis CS, Koch GG. Categorical data analysis using the SAS system. Cary, N.C.: SAS Institute, 1995:163-214.
21. Arslanian SA, Lewy VD, Danadian K. Glucose intolerance in obese adolescents with polycystic ovary syndrome: roles of insulin resistance and β -cell dysfunction and risk of cardiovascular disease. *J Clin Endocrinol Metab* 2001;86:66-71.
22. Saad MF, Knowler WC, Pettit DJ, Nelson RG, Mott DM, Bennett

The New England Journal of Medicine

PH. The natural history of impaired glucose tolerance in the Pima Indians. *N Engl J Med* 1988;319:1600-6.

23. Haffner SM, Miettinen H, Gaskill SP, Stern MP. Decreased insulin action and insulin secretion predict the development of impaired glucose tolerance. *Diabetologia* 1996;39:1201-7.

24. Gerich JB. The genetic basis of type 2 diabetes mellitus: impaired insulin secretion versus impaired insulin sensitivity. *Endocr Rev* 1998;19:491-503.

25. DeFronzo R. Pathogenesis of type 2 diabetes: metabolic and molecular implications for identifying diabetes genes. *Diabetes Rev* 1997;5:277-269.

26. Ward WK, LaCava EC, Paquette TL, Beard JC, Wallum BJ, Porte D Jr. Disproportionate elevation of immunoreactive proinsulin in type 2 (non-insulin-dependent) diabetes mellitus and in experimental insulin resistance. *Diabetologia* 1987;30:698-703.

27. Kohn SB, Leonetti DL, Pigeon RL, Boyko EJ, Bergstrom RW, Fujimoto WY. Proinsulin as a marker for the development of NIDDM in Japanese-American men. *Diabetes* 1995;44:173-9.

28. Haffner SM, Gonzalez C, Mykkanen L, Stern M. Total immunoreac-

tive proinsulin, immunoreactive insulin, and specific insulin in relation to conversion to NIDDM: the Mexico City Diabetes Study. *Diabetologia* 1997;40:830-7.

29. Mykkanen L, Haffner SM, Kuusisto T, Pyörälä K, Hales CN, Laakso M. Serum proinsulin levels are disproportionately increased in elderly pre-diabetic subjects. *Diabetologia* 1995;38:1176-82.

30. Razavi GM, Chen YDI, Hollenbeck CB, Sheu WH, Ostrega D, Polonsky KS. Plasma insulin, C-peptide, and proinsulin concentrations in obese and nonobese individuals with varying degrees of glucose tolerance. *J Clin Endocrinol Metab* 1993;76:44-8.

31. Pagot-Campagna A, Saadine J, Flegal KM, Beckles GL. Diabetes, impaired fasting glucose and elevated HbA1c in US adolescents: the Third National Health and Nutrition Examination Survey. *Diabetes Care* 2001; 24:Suppl 5:S184-S187.

Copyright © 2002 Massachusetts Medical Society.

FULL TEXT OF ALL JOURNAL ARTICLES ON THE WORLD WIDE WEB

Access to the complete text of the *Journal* on the Internet is free to all subscribers. To use this Web site, subscribers should go to the *Journal's* home page (<http://www.nejm.org>) and register by entering their names and subscriber numbers as they appear on their mailing labels. After this one-time registration, subscribers can use their passwords to log on for electronic access to the entire *Journal* from any computer that is connected to the Internet. Features include a library of all issues since January 1993 and abstracts since January 1975, a full-text search capacity, and a personal archive for saving articles and search results of interest. All articles can be printed in a format that is virtually identical to that of the typeset pages. Beginning six months after publication the full text of all original articles and special articles is available free to nonsubscribers who have completed a brief registration.

**This Page is Inserted by IFW Indexing and Scanning
Operations and is not part of the Official Record**

BEST AVAILABLE IMAGES

Defective images within this document are accurate representations of the original documents submitted by the applicant.

Defects in the images include but are not limited to the items checked:

- ☒ **BLACK BORDERS**
- ☒ **IMAGE CUT OFF AT TOP, BOTTOM OR SIDES**
- ☐ **FADED TEXT OR DRAWING**
- ☐ **BLURRED OR ILLEGIBLE TEXT OR DRAWING**
- ☐ **SKEWED/SLANTED IMAGES**
- ☒ **COLOR OR BLACK AND WHITE PHOTOGRAPHS**
- ☐ **GRAY SCALE DOCUMENTS**
- ☒ **LINES OR MARKS ON ORIGINAL DOCUMENT**
- ☐ **REFERENCE(S) OR EXHIBIT(S) SUBMITTED ARE POOR QUALITY**
- ☐ **OTHER:** _____

IMAGES ARE BEST AVAILABLE COPY.

As rescanning these documents will not correct the image problems checked, please do not report these problems to the IFW Image Problem Mailbox.